MITOTIC KINASES IN MEIOSIS

Olga Davydenko

A DISSERTATION

in

Biology

Presented to the Faculties of the University of Pennsylvania

in

Partial Fulfillment of the Requirements for the

Degree of Doctor of Philosophy

2013

Supervisor of Dissertation

_____

Michael A. Lampson, Ph.D.
Associate Professor of Biology

Graduate Group Chairperson

_____

Doris Wagner, Ph.D.
Professor of Biology

Dissertation Committee

Mark Goulian, Ph.D., Professor of Biology
Greg M. Guild, Ph.D., Professor of Biology and Department Chair
Tatyana Svitkina, Ph.D., Associate Professor of Biology
Francis Luca, Ph.D., Associate Professor of Cell Biology

DEDICATION

To my biggest fans – my parents and Richie

ACKNOWLEDGMENT

This work would not have been possible without the help and encouragement of many people. First, I would like to thank my advisor, Michael Lampson for giving me a chance to be part of his research group and to work in his lab. I thank him for being an excellent mentor, for knowing when to help me find the answers, and when to step back and let me figure them out on my own. Where my experience and knowledge were lacking, his were exhaustive; when I needed confidence in my work or myself, I could always count on his help and support. He taught me how to be a scientist, not just the skills and knowledge required to do research, but also how to be inquisitive and thorough. It has really been an honor and a pleasure working with him. I have also been extremely lucky to work closely with Richard Schultz. He has been an invaluable source in tackling the questions of my research, but also in planning my future career. I am extremely grateful for all that I was able to learn from him. I also thank my dissertation committee Mark Goulian, Tatyana Svitkina, Francis Luca and Greg Guild, for their recommendations and suggestions that helped me to better understand and complete this work.

There are no words great enough to thank Karen Schindler, who I collaborated with on the AURKC project. Working with her during the earlier stages of my dissertation can be well described as “oocyte boot camp”. She taught me everything I needed to become independent in my research. In and out of the lab, Karen is an inspiration and a role model for me, as a female scientist.

I would like to thank the past and present members of the Lampson lab. Maomao, I am so lucky to have you as a friend, coworker and very soon a neighbor! You have been my unwavering supporter, the friendly face in the audience when I was nervous; it always made my day when we would both get the memo. I cannot thank you enough for being patient, honest, helpful, and overall awesome. And of course I must thank Evan for never failing to commiserate with me when things were not going well, and to celebrate with me when they did. And Ed, who answered all of my questions, no matter how much of my ignorance they exposed! I also want to thank Teresa, for all the help and training she provided, and for being a friend above all else. I really miss you! And of course, I want to offer a sincere thank you to the members of the Schultz lab, especially Paula, Ma and Sergey for providing a positive and encouraging work environment, a helping hand and an abundance of gestures which may seem small to them but had a bigger impact than they may know.

ABSTRACT

MITOTIC KINASES IN MEIOSIS

Olga Davydenko

Michael A. Lampson

The goal of the first meiotic division is the faithful segregation of homologous chromosomes to produce a gamete with proper ploidy. To achieve this, chromosomes must align at the metaphase plate of a bipolar meiotic spindle, biorient and separate equally at anaphase. Compared to mitosis, meiotic divisions are associated with extra challenges for the mitotic cell division machinery. First, meiotic spindles are acentrosomal, and bipolarity establishment is more complex than during mitosis. Second, homologous chromosomes must biorient and separate during meiosis I, unlike during most other cell divisions, which separate sister chromatids. Meiotic cells have adapted the mitotic enzymatic machinery to regulate these meiotic processes. This dissertation describes the uniquely meiotic properties of two mitotic master regulators, Aurora B kinase (AURKB) and Cyclin-dependent kinase 1 (CDK1). Chapter 2 addresses why mammalian oocytes have a germ-cell specific homolog of Aurora B kinase, Aurora C (AURKC). AURKB is required for chromosome biorientation and segregation during mitosis and meiosis, and most experimental evidence suggests that AURKC is not functionally different. To investigate the role of AURKC, the current study takes advantage of AURKC knock-out mouse oocytes and preimplantation embryos. Chapter 2 shows that the effect of lacking AURKC becomes more pronounced and deleterious as

meiosis and early embryonic divisions progress. I conclude that AURKC is likely required to compensate for the loss of AURKB protein, which is rapidly degraded during meiosis. Chapter 3 investigates CDK1 as the molecular clock responsible for the timing of kinetochore-microtubule attachments during meiosis I. Likely because of the prolonged spindle formation and bipolarity establishment in the acentrosomal mouse oocyte meiosis, kinetochore-microtubule attachments are delayed until late in metaphase I. This is unlike mitosis, where attachments are constantly made and broken. Chapter 3 answers the long-standing question of how attachments are timed. Using CDK1 inhibition and precocious activation techniques, I find that this kinase controls the timing of kinetochore-microtubule binding. The studies reported in this dissertation demonstrate the unique adaptations found in mitotic kinase AURKB and CDK1 functions to the unique requirements of meiotic divisions.

Table of Contents

LIST OF FIGURES

CHAPTER 1

Introduction: Meiosis-Specific Functions of Mitotic Kinases that Accommodate Unique Requirements of Meiotic Spindles

SUMMARY

The goal of meiosis is the faithful segregation of chromosomes to produce a euploid gamete. This process relies on a bipolar spindle, whose microtubules are able to bind kinetochores of the chromosomes and equally separate them at anaphase. Compared to mitosis, meiotic divisions are associated with extra challenges for the cell division machinery. In mitosis, spindle bipolarity is established through separation of two centrosomes, which nucleate microtubules and form the poles of the spindle. However most meiotic divisions are acentrosomal, which results in a more complicated route to spindle bipolarity and establishment of kinetochore-microtubule attachments. The first meiotic division also involves biorientation and segregation of homologous chromosome pairs instead of sister chromatids, like in mitosis. This results in a unique chromosomal configuration, which must be accommodated by the regulatory machinery. This introduction discusses the various adaptations of the existing mitotic machinery to accommodate the unique requirements of the meiotic spindles.

Unique features of meiotic spindles

The goal of meiosis is faithful segregation of homologous chromosomes to produce a haploid egg. During the two meiotic divisions, oocytes halve their genetic material in preparation for fertilization by first separating homologous chromosomes in meiosis I, then sister chromatids in meiosis II. These divisions must be executed properly to avoid fertilization of aneuploid eggs, which produce embryos with improper chromosomal numbers. To achieve faithful segregation at anaphase, the kinetochores of homologous chromosomes must capture microtubules (MTs) emanating from opposite poles of the bipolar spindle (bi-orientation). The two centrosomes of mammalian somatic cells confer an inherent bipolarity to their spindles. However, oocyte spindles in most species are acentrosomal and achieve bipolarity through a variety of centrosome-independent mechanisms (Dumont and Desai, 2012). Aside from their acentrosomal nature, oocyte spindles have evolved to accommodate unique chromosomal configurations not seen in somatic cells, namely the pairing, cohesion, alignment and segregation of homologous chromosome pairs (bivalents) instead of sister chromatids like in mitosis. Meiotic cells of various species adapted the existing mitotic kinase machinery to accommodate the unique requirements of meiotic spindles.

Roles of mitotic kinases in acentrosomal meiotic spindle assembly

Cyclin-dependent kinase 1 (CDK1) and acentrosomal spindles

As most meiotic cells are acentrosomal, their path to spindle bipolarity is more complex than that of mitotic cells. One mitotic master-regulator kinase that takes on

some meiosis-specific roles is the Cyclin-dependent kinase 1 (CDK1). It is one of the most important regulators of both mitotic and meiotic cell cycles, which controls M-phase resumption, anaphase progression and many other cellular processes. CDK1 must associate with cyclin proteins to become active, and its activity is thought to be limited by cyclin levels in the cell. While a variety of cyclin proteins can associate with CDK1 during various stages of the cell cycle, the cyclin B1 and B2 are the major M-phase cyclins (Satyanarayana and Kaldis, 2009). The CDK1-cyclin B complex also participates in the establishment of bipolarity of mitotic spindles. There CDK1 phosphorylates the Eg5 kinesin, which then localizes to spindle poles and promotes their separation at the G2/M transition setting up the bipolarity of the mitotic spindle (Lim et al., 2009; Meraldi and Nigg, 2002). This CDK1 function is likely conserved in meiosis. In the meiotic Xenopus egg extracts, where the Eg5 kinesin is required for spindle bipolarity, CDK1 phosphorylation of Eg5 incrases its binding of microtubules and Xenopus egg extract spindles (Blangy et al., 1995; Cahu et al., 2008; Walczak et al., 1998). However, there are also meiosis-specific roles of CDK1 that are required for acentrosomal spindle formation and bipolarity.

During the *Caenorhabditis elegans* (worm) oocyte mitosis, chromosome segregation and spindle formation are controlled by CDK1 (Cdc2) in complex with cyclin B1 or B3 (cyb-1, cyb-3), such that knockdown of Cdc2 or either of these cyclins disrupts spindle formation. However in meiosis, cyb-1 and cyb-3 seem to be non-essential for this function of Cdc2. Instead, knockdown of cyb-2 phenocopies the knockdown of Cdc2 and results in a complete failure to assemble bipolar spindles. This means that in *C. elegans*

oocytes, cyclin B2 (instead of cyclin B1 and B3 like in mitosis) in complex with CDK1 has a unique meiosis-specific role in spindle formation (Voet et al., 2009). This role of cyclin B2 in organizing a bipolar spindle was also observed in *Rana Japonica* (frog) oocytes using the antisense RNA approach. Knockdown of cyclin B2 resulted in monopolar spindles and abnormal polar body extrusion. Taken together with the spindle microtubule localization of this cyclin, these results indicate the requirement for cyclin B2 for oocyte spindle formation in this organism (Kotani et al., 2001).

CDK1 may regulate spindle bipolarity by modifying downstream targets that have known regulatory functions in acentrosomal spindle organization. Aurora A kinase and Polo-like kinase 1 (Plk1) are spindle-pole localizing proteins, whose activity is central to bipolar spindle formation in both mitotic and meiotic cells (Hoar et al., 2007; Marumoto et al., 2003; Mori et al., 2007; Petronczki et al., 2008; Terada et al., 2003). In *Xenopus laevis* (frog) Aurora A must be phosphorylated for it to be activated, and injection of cyclin B2 into oocytes is enough to activate Aurora A. In fact, Cdc2-cyclin B must be present and active for Aurora A activation in egg extracts (Maton et al., 2003). In starfish oocytes the Aurora kinase homolog ApAurora functions as both Aurora A and Aurora B kinases (Abe et al., 2010). There, the ApAurora and Plk1 activity profiles in cycling meiotic extracts are similar to that of CDK1, such that ApAurora and Plk1 activity is maximal or minimal when same is true for CDK1 activity. When CDK1 is inactivated using chemical inhibitors or phosphatases, ApAurora and Plk1 are inhibited also (Abe et al., 2010; Kishimoto, 2011; Okano-Uchida et al., 2003). These findings indicate that activation of these spindle formation regulators is dependent on the CDK1-cyclin B

activity (Abe et al., 2010; Kishimoto, 2011; Maton et al., 2003; Okano-Uchida et al., 2003). Although the direct effect of this CDK1-dependent activation on spindle formation has not been tested, we can predict its importance. Similarly, in *Drosophila Melanogaster* (fly) oocytes, which also exhibit acentrosomal meiotic spindles, a mutation in a conserved CDK1 subunit Cks30a, produces oocytes with disrupted bipolar spindle morphology and chromosome alignment. Because this mutation causes a mis-localization of spindle pole proteins Msps and D-TACC, which are important for spindle bipolarity, the meiotic CDK1 may function upstream of these two proteins on the path to bipolarity (Pearson et al., 2005). The relationship between CDK1 and spindle pole proteins Aurora A, Plk1, Msps and D-TACC in mammalian oocytes remains to be investigated.

Because the mammalian oocyte spindles are acentrosomal, they achieve bipolarity through progressive clustering of microtubule organizing centers (MTOCs) first into multipolar spindle intermediates, then finally into a bipolar spindle 3-4 hours after germinal vesicle breakdown (GVBD) (Schuh and Ellenberg, 2007). By this time in mid-metaphase I, chromosomes congress to the equator of the newly-formed bipolar spindle, however their kinetochores do not start stably binding microtubules until late in metaphase I, 6-8 hours after GVBD (Brunet et al., 1999; Gui and Homer, 2012; Kitajima et al., 2011). This delay in kinetochore-microtubule (K-MT) binding is unique to oocyte meiosis. In mitosis of somatic cells, K-MT attachment formation begins immediately after nuclear envelope breakdown (NEBD), and complete bi-orientation is achieved within minutes, compared to hours in meiosis I.

The attachment delay during meiosis I likely exists to prevent incorrect bi-orientation, which can result from stabilizing attachments while spindles are still multipolar (Fig. 1 A) (Kolano et al., 2012; Lane et al., 2012). Although it is unknown what dictates the timing of K-MT stabilization, the profile of CDK1 activity during meiosis suggests its involvement. In contrast to mitosis, where CDK1 activity rises sharply before NEBD then remains constant throughout M-phase (Gavet and Pines, 2010), in meiosis I of mammalian oocytes, CDK1 is activated slowly starting at GVBD and throughout metaphase I. Its activity reaches a maximum at ~6 hours after GVBD, concurrent with attachment stabilization (Fig. 1 A) (Choi et al., 1991; Gavin, 1994; Polanski et al., 1998). Based on this observation, it has been proposed that the gradual increase in CDK1 activity acts as a timing mechanism to regulate the timing of K-MT attachments. Chapter 2 of the dissertation addresses this question.

Another unusual feature of oocyte spindles is their asymmetric position. Unlike most mitotic spindles, which are centrally positioned and span the diameter of the cell, oocyte spindles are usually much smaller than the cell diameter (Fabritius et al., 2011). Because of their small size, the position and rotation of the spindles must be regulated to control the location of anaphase. In oocytes, spindles are parallel to the cell cortex during metaphase I, then rotate to a perpendicular position at anaphase I onset in order to expel half the chromosomes into the polar body. In *C. elegans* oocytes, this process depends on accumulation of microtubule motor dynein at spindle poles. Because CDK1 inhibition results in dynein accumulation at the spindle poles, CDK1 blocks spindle rotation until anaphase I likely by preventing dynein accumulation. Thus at anaphase I in *C. elegans*

oocytes, spindle rotation is initiated when dynein is accumulated at poles due to decreasing levels of CDK1 activity when cyclin B is degraded (Ellefson and McNally, 2011).

Aurora B kinase and acentrosomal spindles

Aurora B kinase is the catalytic member of the Chromosomal Passenger Complex (CPC), which also consists of the inner centromere protein INCENP, and targeting subunits survivin and borealin. During mitosis, the CPC localizes to centromeres at metaphase, where it regulates K-MT attachments and is required for proper chromosome bi-orientation; at anaphase it localizes to the spindle midzone, where it regulates cytokinesis (Ruchaud et al., 2007). The CPC also participates in the formation of bipolar spindles. RNAi depletion of various CPC components, which produces kinetochore-microtubule misattachments, also results in aberrant spindle poles. Therefore the CPC must contribute to the canonical centrosome-dependent spindle assembly, where microtubules are nucleated at spindle poles and are stabilized when they encounter kinetochores (Adams et al., 2001; Gassmann et al., 2004; Wadsworth and Khodjakov, 2004).

Studies done in the Xenopus meiotic egg extracts, where microtubules are nucleated in the vicinity of chromosomes and then sorted into an antiparallel arrays to produce a bipolar spindle (Dumont and Desai, 2012), show that the CPC also plays a crucial role in this acentrosomal process. When the function of the complex is disrupted via Aurora kinase B inhibition or dominant negative mutation, borealin knockout and other means, normal spindle formation in frog egg extracts is inhibited. Instead, short

bipolar or monopolar acentrosomal spindles form (Gadea and Ruderman, 2005; Ohi et al., 2004; Sampath et al., 2004; Shao et al., 2012). Several of these studies have identified the microtubule catastrophe kinesin MCAK as the target of Aurora kinase B. When MCAK is inhibited via Aurora B phosphorylation, microtubules nucleated at the chromosomes are stabilized and are able to assemble into a bipolar spindle. A similar role for CPC is observed in *C. elegans* oocytes, where an INCENP mutation disrupts the chromosome-driven spindle assembly. That study also highlights another meiosis-specific role for the CPC – the requirement for INCENP to stabilize the central spindle during metaphase I, in contrast to mitosis, where this INCENP function only becomes important when chromosomes separate at anaphase (Colombié et al., 2008). These examples demonstrate the involvement of Aurora B in acentrosomal spindle formation. These roles have to investigated in mammalian oocytes.

Kinetochore-microtubule attachments are not stabilized until late in meiosis I, as discussed above. Despite that, chromosomes are able to align at the metaphase plate by mid-metaphase I (Kitajima et al., 2011). It is thought that chromosomes are able to align in this attachment-independent way by traveling along microtubules via lateral K-MT interactions (Cai et al., 2009; Kapoor et al., 2006; Magidson et al., 2011). However, it is unknown how lateral interactions are converted into end-on attachments. A recent study done in fission yeast *Schizosaccharomyces pombe* hints that this process may by regulated by Aurora B (there, Ipl1) and Mps1 kinases. Mps1 is part of the spindle assembly checkpoint (SAC) in mitosis and meiosis – a pathway that inhibits anaphase until all kinetochores form stable K-MT attachments and biorient (Gillies et al., 2013;

Gilliland et al., 2007; Hached et al., 2011; Maciejowski et al., 2010; Musacchio and Salmon, 2007).

Using Ipl1 and Mps1 mutants that had a more severe phenotypes during yeast meiosis than mitosis, the role of these two kinases was assessed in the progressive events leading from meiosis initiation until spindle formation and chromosome biorientation. Spindle formation during yeast meiosis I presents special challenges to the regulatory machinery, as at the beginning of prophase I, kinetochores are attached to the spindle pole body (SPB), and must first be released before the spindle can form and they can biorient. When a meiosis-null Ipl1 allele is used, centromeres fail to release the SPB during prophase, which suggests that this process is Ipl1-dependent. The subsequent process of chromosome alignment that involves lateral sliding of kinetochores against spindle microtubules was found to involve Mps1. Chromosomes in yeast cells with a mutant Mps1 copy also failed to make the kind of rapid processive movements towards spindle poles that are characteristic of end-on attachments. These results indicate that Ipl1 (Aurora B) and Mps1 act sequentially to achieve biorientation during yeast meiosis I. Ipl1 is required to release centromere attachments to the SPB, then Mps1 enables lateral sliding of kinetochores against spindle MTs to achieve chromosome congression and subsequently converts lateral interactions into end-on ones prior to anaphase I (Meyer et al., 2013). This offers an insight into how lateral K-MT interactions can be converted into stable attachments, however this role of Mps1 needs to be investigated in other systems.

Meiosis-specific roles of mitotic kinases to accommodate separation of homologous chromosome pairs at meiosis I

Meiosis I cohesion regulation

In mitosis, sister chromatids are held together at the centromeres via a multiprotein cohesin ring complex. This association is important for bi-orientation, generation of interkinetochore tension and proper segregation of chromosomes. Only when centromeric cohesion is cleaved at anaphase sister chromatids can separate. To prevent cohesion from premature cleavage and allow bi-orientation, mitotic cells have developed a mechanism that protects centromeric cohesins during metaphase. There, Bub1 – a kinase member of the SAC – recruits Shugoshin protein to the centromeres, where it prevents cohesins from cleavage (Clift and Marston, 2011; Kitajima et al., 2004; Kitajima et al., 2005; Remeseiro and Losada, 2013; Tang et al., 2004). In contrast to mitosis, during meiosis I, homologous chromosome pairs are held together by the chiasmata at the recombination sites and cohesion is maintained between sister chromatid arms. After arm cohesion is lost at anaphase I, centromeric cohesion between sisters is protected until anaphase II. This chromosomal configuration means that cohesion must be maintained on chromosome arms during meiosis I, instead of only at centromeres, like in mitosis. While some meiotic cells employ the mitotic Bub1/Shugoshin pathway to protect chromosome cohesion (Bernard et al., 2001; Clift and Marston, 2011; Riedel et al., 2006), many have assigned meiotic cohesion protection roles to other mitotic players.

A key member of the spindle assembly checkpoint, BubR1, has adopted a meiosis-specific role in cohesion protection. In Drosophila oocytes and spermatids, a

point mutation in the kinase domain of the BubR1 conserved homolog Mad3 does not affect its SAC function, but results in chromosome nondisjunction during anaphase I, which is characteristic of a cohesion defect (Malmanche et al., 2007). These results indicate that Mad3/BubR1 has a meiosis-specific function, which is separate from its SAC function, in regulating chromosome arm cohesion during MI. The role of BubR1 in cohesion regulation in other organisms remains to be investigated.

CPC regulates cohesion, chromosome segregation during meiosis I

Aside from its other meiosis-specific roles already described here, the CPC has been recruited in many organisms to regulate cohesion during meiosis I. In Drosophila, a female-sterile INCENP mutant was found to cause premature chromosome separation in oocytes during MI. On closer investigation, the Drosophila Shugoshin protein MEI-S332, which is required for cohesion protection in mitosis and meiosis, was found to be phosphorylated by Aurora B and able to bind INCENP *in vitro*. When INCENP function or levels were perturbed, MEI-S322 localization and/or function were affected, then sister chromatid cohesion was prematurely lost at MI. Interestingly, when its Aurora B phosphorylation site is mutated, MEI-S322 is unable to localize to mitotic centromeres also, hinting at a possible role for the CPC in mitotic cohesion protection (Resnick et al., 2006). Similarly, in *Saccharomyces cerevisiae* (budding yeast) a meiosis-specific deletion of yeast Aurora B homolog Ipl1 resulted in premature chromosome separation during meiosis I. This was likely due to cohesion loss, which was demonstrated by the mislocalization from the centromeres of the cohesin subunit Rec8, similar to that seen in Bub1 and Sgo1 null mutants. To offer further insight into this mechanism, Ipl1 was

found to be required for centromeric localization of the Rts1/PP2A phosphatase, which dephosphorylates Rec8 thereby protecting it from cleavage (Yu and Koshland, 2007). These findings indicate that in budding yeast and Drosophila oocytes Ipl1 is required for cohesion protection during meiosis I.

Of the meiotic adaptations described here, those seen in *C. elegans* oocytes are perhaps the most unique. Most species described here have a single centromere per chromosome, which serves as a kinetochore building site that binds spindle microtubules and where cohesion is maintained throughout meiosis. *C. elegans* on the other hand, have holocentric chromosomes, which do not have designated centromeres. Instead the whole chromosomal surface can serve as a site for microtubule attachment and cohesion maintenance. This necessitates alternate mechanisms for cohesion protection in both mitosis and meiosis of this species. During mitosis, kinetochore proteins and cohesins localize along the whole length of holocentric chromosomes of the worm, and their functions are conserved (Oegema and Hyman, 2006). However during meiosis I, homologous chromosomes take on a completely different orientation. Each end of the *C. elegans* bivalent faces one of the spindle poles and serves as a site for kinetochore assembly (Fig. 1 B). The bivalents are held together by cohesin complexes distal to the chiasmata at the crossover sites, such that at anaphase I, cohesin complexes between the homologous chromosomes are cut, while those holding the sisters are protected, much like in monocentric meioses (Fig. 1 B) (Melters et al., 2012; Schvarzstein et al., 2010).

Like in many species described here, *C. elegans* oocytes rely on meiosis-specific Aurora B kinase (there, AIR-2) function in regulating cohesion. While most kinetochore

components in these oocytes assemble in cap-like structures on both ends of the bivalent facing spindle poles, AIR-2 does not co-localize with them during meiosis I. Instead, it is concentrated at the mid-bivalent region where homologous chromosomes are held together by cohesion (Fig. 1 B). When AIR-2 expression is disrupted using an RNAi approach, *C. elegans* oocytes progress through anaphase I without segregating their chromosomes. While chromosome biorientation is unaffected at metaphase I, the chromosomal mass stretches at anaphase, but fails to separate, instead collapsing back together at telophase. Furthermore, when AIR-2 is knocked down using RNAi, localization of the cohesin subunit Rec8 is affected, and it is found to be a direct AIR-2 substrate *in vitro* (Kaitna et al., 2002; Rogers et al., 2002). These findings indicate that Aurora B/AIR-2 phosphorylates Rec8, which leads to its cleavage at anaphase I of worm oocyte meiosis. This direct involvement of Aurora B kinase in cohesion cleavage in worm oocytes is the opposite of this kinase's function in yeast and Drosophila oocytes, where it is required for cohesion protection.

It was recently found that when kinetochore formation is disrupted in *C. elegans* oocytes, the ability of chromosomes to biorient is impaired, however chromosomes are able to segregate at anaphase I. These results indicate that during the acentrosomal *C. elegans* oocyte meiosis, chromosomes can separate at anaphase I independent of kinetochore-microtubule attachments, which in most mitotic and meiotic cells pull the chromosomes towards opposite poles of the spindle. Instead, in worm oocytes, homologous chromosomes are pushed apart by the microtubules that assemble at the spindle midzone, originating at the midbivalent region at anaphase I. It is thought that

the proteins that localize to the midbivalent ring are responsible for chromosome separation. One such protein is CLASP^{CLS-2} – a microtubule plus-end binding protein that regulates microtubule stability. Using a series of RNAi knockdowns, CLASP was found to be localized to the midbivalent region by BUB-1, whose localization in turn depends on AIR-2. Taken together, these findings indicate that in worm oocyte meiosis, AIR-2 regulates chromosome separation by recruiting BUB-1, which in turn recruits CLASP to stabilize microtubules at the spindle midzone and separate homologous chromosomes at anaphase I (Dumont et al., 2010). Analysis of the unique localization of AIR-2 during meiosis I of *C. elegans* oocytes highlights two roles of this kinase in anaphase chromosome separation. At the midbivalent region, AIR-2 is required for cohesion cleavage, which is immediately followed by chromosome separation that relies on the AIR-2-dependent growth of the spindle midzone microtubule network to push the chromosomes apart. While the CPC and Aurora B kinase regulate mitotic cytokinesis (Carmena et al., 2012), this function of AIR-2 in the worm is meiosis-specific.

Aurora B/C kinases in mammalian meiosis and early embryogenesis

Aurora kinases are conserved and essential regulators of chromosome segregation in all known mammalian mitotic and meiotic divisions. There are three Aurora kinases in mammals. Aurora A (AURKA) localizes to the spindle poles and is required for bipolarity establishment, while Aurora B (AURKB) is a part of the CPC, as described above. These kinases are expressed ubiquitously in mammalian tissues, while the third homolog Aurora C (AURKC) is mostly limited to germ cells (Gopalan et al., 1997; Tseng et al., 1998; Yanai et al., 1997). AURKC has a unique localization in meiotic cells,

where it is detected all over the chromatin, in contrast to AURKB, which is normally at centromeres. This difference in localization suggests that the two kinases may have distinct functions during meiosis I. However, their high sequence similarity as well as most experimental evidence suggest that AURKC, does not have a function that is distinct from AURKB (Fernández-Miranda et al., 2011; Sasai et al., 2004; Slattery et al., 2009). Despite that, AURKC must have a crucial role during meiosis and early embryogenesis, because it is conserved among all mammals, and mice lacking AURKC are sub-fertile (Kimmins et al., 2007). Chapter 2 of this dissertation addresses why both AURKB and AURKC are present in oocytes and preimplantation embryos.

Conclusions

While mitotic functions of such kinases as CDK1, Aurora B, Mps1, Bub1 and BubR1 are relatively well understood, our knowledge of their meiotic involvement is not as advanced. While we expect that many of their functions are conserved between the mitotic and meiotic divisions, we now know that they have also taken on a number of adaptations to help cells cope with the unique requirements of meiosis. The main challenges to the mitotic machinery are the acentrosomal meiotic spindle, and the conformational differences presented by the biorientation and separation of homologous chromosome pairs instead of sister chromatids. CDK1 and Aurora B kinase both participate in the regulation of acentrosomal spindle bipolarity as well as cohesion protection or cleavage in the context of meiotic chromosome bivalents. Many of the findings are reported in non-mammalian species, and their conservation to higher organisms remains to be investigated.

Figure 1

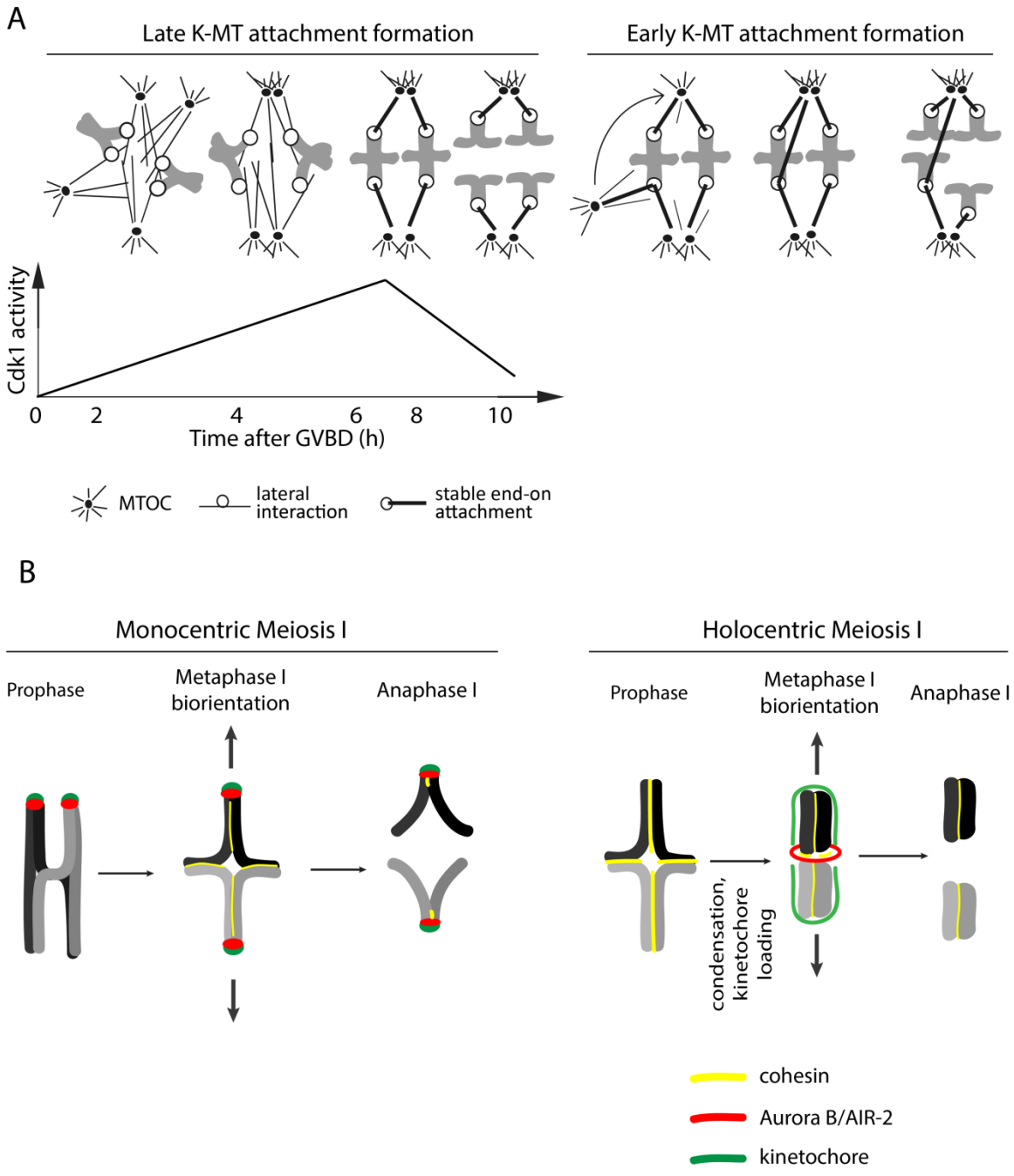
A
Late K-MT attachment formation
Early K-MT attachment formation
Cdk1 activity
0
2
4
6
8
10
Time after GVBD (h)
MTOC
lateral interaction
stable end-on attachment
B
Monocentric Meiosis I
Prophase
Metaphase I biorientation
Anaphase I
Holocentric Meiosis I
Prophase
Metaphase I biorientation
Anaphase I
condensation, kinetochore loading
cohesin
Aurora B/AIR-2
kinetochore

Figure 1. Chromosome biorientation and segregation in acentrosomal meiosis I.

Monocentric and holocentric meiosis I. (A) Diagrams illustrate stabilization of early and late K-MT attachments in oocyte meiosis. At 0-4 h after GVBD, MTOCs progressively cluster to form a bipolar spindle, while kinetochores only interact with MTs laterally (left diagram). CDK1 activity is progressively rising during this time, peaking ~6-8 h after GVBD. Plot is a representation of *in vitro* histone H1 kinase activity (Choi et al., 1991; Gavin, 1994; Polanski et al., 1998). Stable K-MT attachments are only established after MTOCs cluster into a bipolar spindle, leading to proper biorientation and chromosome segregation. If K-MT attachments are established earlier (right diagram), while the spindle is still multipolar and MTOC clustering is incomplete, improper attachments can form, leading to lagging chromosomes and missegregation at anaphase I. (B) Diagrams illustrate sites of kinetochore formation, Aurora B localization and chromosome cohesion in monocentric and holocentris meiosis I. In monocentric meiosis (left), chromosome biorientation is defined by the site of kinetochore localization (green) with Aurora B kinase (red) localizing to centromeres adjacent to kinetochores. At anaphase I, cohesion (yellow) is protected at centromeres, while it's cleaved along the arms. In holocentric meiosis (right), where no centromeres are present, when chromosomes condense during metaphase I, kinetochores form cup-shaped structures distal to the crossover sites. Aurora B/AIR-2 localizes at the mid-bivalent in a ring-shaped structure adjacent to cohesin complexes that hold the homologs together.

CHAPTER 2

Maternally-recruited Aurora C kinase is more stable than Aurora B to support mouse oocyte maturation and early development

The data in Chapter 2 have been published (Schindler et al., 2012)

SUMMARY

Aurora kinases are highly conserved, essential regulators of cell division. Two Aurora kinase isoforms, A and B (AURKA and AURKB), are expressed ubiquitously in mammals, whereas a third isoform, Aurora C (AURKC), is largely restricted to germ cells. Because AURKC is very similar to AURKB, based on sequence and functional analyses, why germ cells express AURKC is unclear. We report that *Aurkc*$^{-/-}$ females are sub-fertile, and that AURKB function declines as development progresses based on increasing severity of cytokinesis failure and arrested embryonic development. Furthermore, we find that neither *Aurkb* nor *Aurkc* is expressed after the 1-cell stage, and that AURKC is more stable during maturation than AURKB using fluorescently-tagged reporter proteins. In addition, *Aurkc* mRNA is recruited during maturation. Because maturation occurs in the absence of transcription, post-transcriptional regulation of *Aurkc* mRNA, coupled with the greater stability of AURKC protein, provides a means to ensure sufficient Aurora kinase activity, despite loss of AURKB, to support both meiotic and early embryonic cell divisions. These findings suggest a model for the presence of AURKC in oocytes: that AURKC compensates for loss of AURKB through differences in both message recruitment and protein stability.

INTRODUCTION

Aurora kinases are highly conserved cell-cycle regulators with essential roles in chromosome segregation. There are three Aurora kinases in mammals: Aurora kinases A and B (AURKA or B) are ubiquitously expressed and their functions have been extensively studied, whereas AURKC is largely limited to germ cells (Gopalan et al., 1997; Hu et al., 2000; Yanai et al., 1997); many human cancer cell lines express AURKC (Baldini et al., 2011) and some somatic tissues express AURKC at low levels (Price et al., 2009; Yan et al., 2005a; Yan et al., 2005b). It is not clear, however, why germ cells require a third AURK. Because isoforms can have different functions, it is tempting to speculate that AURKC exists because its mitotic counterparts simply cannot execute unique features of meiosis.

One unique feature of meiosis is the generation of haploid gametes from diploid precursor cells by a reductional chromosome segregation during meiosis I (MI) followed by an equational division at meiosis II (MII) without an intervening round of DNA replication. In oocytes, another unique feature is that meiosis is not a continuous process because there is a growth period during a prolonged arrest at prophase I, followed by a cell division cycle during oocyte maturation, and a second arrest at metaphase of MII, until fertilization, which triggers completion of MII. Furthermore, proteins in the oocyte must support the first mitotic cell cycles of the embryo prior to zygotic genome activation. Despite these obvious differences, several observations suggest that AURKC may not have a specialized function. AURKB and AURKC are highly similar in sequence (61% identical), and AURKC can functionally compensate for loss of AURKB

when ectopically expressed in somatic cells (Sasai et al., 2004; Slattery et al., 2009). Furthermore, embryos that lack AURKB can develop to but not beyond the blastocyst, as long as AURKC is present, consistent with the idea that AURKB and C have similar functions (Fernández-Miranda et al., 2011).

Given the sequence similarity and apparent redundant function, it is unclear why germ cells have a third AURK. Male mice lacking AURKC are sub-fertile because of post-meiotic defects including abnormally condensed chromatin and abnormally shaped acrosomes, but females were not examined (Kimmins et al., 2007). Mutations in human AURKC cause meiotic arrest and formation of tetraploid sperm (Ben Khelifa et al., 2011) suggesting an essential role in cytokinesis in male meiosis. Experiments in mouse oocytes using a chemical inhibitor of AURKB (ZM447439) do not address the function of AURKB because AURKC is also inhibited (Gautschi et al., 2008; Lane et al., 2010; Shuda et al., 2009; Swain et al., 2008; Vogt et al., 2008). Strategies using dominant negative versions of AURKC are also difficult to interpret, because the mutant may also compete with AURKB (Yang et al., 2010). Overexpression studies have similar limitations because both kinases interact with INCENP and these studies did not report expression levels of AURKB versus AURKC (Sharif et al., 2010). Therefore, no experiments to date have directly addressed why oocytes contain a third AURK.

A hint as to the need for oocytes to express AURKC comes from comparisons of AURKB and AURKC sequences. AURKB contains N-terminal destruction motifs that AURKC lacks. In mitotic cell cycles, these motifs regulate AURKB destruction by the anaphase-promoting complex/cyclosome (APC/C) at cytokinesis, prior to G1 of the

following cell cycle (Nguyen et al., 2005; Stewart and Fang, 2005). The CDH1 (FZR1 in mouse) regulator of the APC/C binds the KEN box (aa 4-9, in mouse) and both CDH1 and CDC20 bind the A box (aa 26-29, in mouse). AURKB also contains 4 putative D-boxes, which AURKC also contains, whose functions in regulating its stability are unclear(Nguyen et al., 2005; Stewart and Fang, 2005). Because there are two rounds of chromosome segregation without an intervening cell cycle in meiosis, if AURKB is degraded after MI (as it is during mitosis), there may be no opportunity to regenerate additional AURKB to support MII. Based on these sequence comparisons, we hypothesized that oocytes contain a third AURK because of differential regulation of AURKC protein levels relative to AURKB.

For the first time, we demonstrate that female mice lacking AURKC are sub-fertile due to an increasing in severity of phenotypes that begins with mild chromosome misalignment causing arrest at MI and continues during embryogenesis with cytokinesis failure. The progression of these phenotypes indicates a gradual loss of AURK activity during oocyte maturation and early development. Consistent with this model, we find that AURKB protein is less stable than AURKC during meiotic maturation. Moreover, we find that *Aurkc* message is recruited for translation during oocyte maturation to ensure sufficient AURK activity during meiosis and embryonic development. Expression of AURKB in *Aurkc*$^{-/-}$ oocytes and embryos rescues the meiotic and cytokinesis defects, respectively, consistent with the hypothesis that AURKB can compensate for the loss of AURKC. Taken together, we propose that AURKC is an example of an isoform of a

cell-cycle regulator that is recruited during meiotic maturation to support meiosis, fertilization and early embryonic cell division.

RESULTS

AURKC is required for normal oocyte maturation and embryo development

AURKC expression is largely limited to germ cells, yet a role during oocyte meiotic maturation is not clear. We re-derived cyropreserved *Aurkc*$^{+/-}$ embryos to generate mice lacking *Aurkc* (Kimmins et al., 2007) to determine the requirement of AURKC in female gametes. Oocytes from knockout mice do not express detectable *Aurkc* message or AURKC protein; the amount of *Aurkb* mRNA is unaffected in knockout mice (Fig. 8 A-B). The number of full-grown oocytes from superovulated, sexually mature female *Aurkc*$^{-/-}$ mice (34.6 +/- 3.8; n= 10) was not statistically different than the numbers from control littermates (44.67 +/- 6.2; n=9). Nevertheless, our breeding trials revealed that they were sub-fertile, averaging 2 fewer pups per litter (Fig. 2 A), but with a similar number of days between litters compared to control littermates (Fig. 9).

To determine if AURKC is required for oocyte meiotic maturation, we first matured oocytes to metaphase of MI and, after fixation and staining, examined chromosome alignment. Although the overall percentage of MI oocytes from knockout mice with chromosome misalignment was not strikingly different than wild-type controls we observed a greater variation from mouse-to-mouse in oocytes from knockout females

(Fig. 2 B). Next, we monitored the time of polar body emission and found that significantly more oocytes from AURKC knockout mice arrested in MI, as indicated by failure to extrude a polar body (Fig. 2 C). Furthermore, the oocytes that failed to extrude a polar body did not undergo cytokinesis whereas those oocytes that did extrude a polar body were delayed by 1 h entering anaphase I compared to controls (Fig. 2 D). These oocytes were then fixed and analyzed by immunocytochemistry, and a significant portion of those from *Aurkc*$^{-/-}$ mice displayed abnormal chromosome alignment regardless of whether they arrested at MI or progressed to MII (Fig. 2 D-F). We did not observe, however, any increase in aneuploidy incidence (1/35 aneuploid eggs in knockouts and 0/12 aneuploid eggs in controls). This finding is consistent with oocytes containing misaligned chromosomes arresting at metaphase of MI.

Because mice lacking *Aurkb* develop to the blastocyst stage (Fernández-Miranda et al., 2011), it is likely that AURKC also functions during early embryonic cell divisions. To test this hypothesis, we isolated 1-cell embryos from wild-type, heterozygous or knockout females that were mated to wild-type males and allowed the embryos to develop *in vitro*. Significantly fewer embryos from *Aurkc*$^{-/-}$ females cleaved to the 2-cell stage (Fig. 3 A). Moreover, we found that significant numbers of 1-cell embryos attempted and failed to complete cytokinesis (Fig. 3 B, C), and we frequently observed prolonged membrane ruffling or blebbing (Fig. 10). Cytokinesis failure is a well-established phenotype of AURKB inhibition or mutation (Giet and Glover, 2001; Hauf et al., 2003; Severson et al., 2000; Yabe et al., 2009), and we used this phenotype to compare AURKB function in MI vs. the 1-cell stage in oocytes and embryos from *Aurkc*$^{-}$

$^{/-}$ females. The cytokinesis failure phenotype is much more severe at the 1-cell stage, indicating that AURKB activity declines as development progresses (Fig. 3 D).

Consistent with a gradual decline in AURKB activity, development of embryos from *Aurkc*$^{-/-}$ mothers became progressively worse with extended culture periods. Sixty-four hours after mating, ~35% of the control embryos developed to the 8-cell embryonic stage compared to only ~15% of the embryos from the knockout mothers (Fig. 3 E). Some of the latter embryos were fragmented with many arrested at the 2-cell stage. At 113 h, when nearly 75% of control embryos developed to the blastocyst stage, only ~25% of embryos from the knockout mothers were blastocysts (Fig. 3 F). Those embryos from the knockout mothers that did develop to the blastocyst stage appeared indistinguishable from control embryos. At this time point most of the embryos that had lagged behind in development had fragmented. These findings indicate that the subfertility of *Aurkc*$^{-/-}$ females was due to perturbations that begin during meiotic maturation (chromosome misalignment and cell cycle arrest) and become more pronounced during embryonic development (failure in cytokinesis).

AURKC is more stable than AURKB

Mice lacking AURKB develop up to the blastocyst stage of embryonic development because AURKC is sufficient for supporting the early mitotic divisions (Fernández-Miranda et al., 2011). In contrast, AURKB function declines between MI and the 1–cell stage, as indicated by increasing cytokinesis failure (Fig. 3 D), and AURKB does not support development to the blastocyst stage (Fig. 3 E, F). AURKB is unstable during mitosis because it is targeted for ubiquitin-mediated proteolysis after M

phase during each round of the cell cycle (Nguyen et al., 2005; Stewart and Fang, 2005). AURKC, however, lacks destruction motifs that AURKB contains, suggesting that it could be more stable. Moreover, quantitative real time PCR demonstrated that although oocytes (meiotically incompetent and full-grown oocytes) and eggs (MII) contained both *Aurkb* and *Aurkc* mRNA, as previously described (Shuda et al., 2009; Swain et al., 2008; Yang et al., 2010), these messages declined by the 2-cell stage (Fig. 3 G-H). Taken together, these data support the model that the amount of AURKB declines during meiosis and early embryonic mitosis and cannot be resynthesized until the blastocyst stage, whereas the amount of AURKC is maintained during preimplantation development.

To test whether AURKB and AURKC are differentially stable, we used a live-cell imaging assay. We co-microinjected *Aurkb-mCherry* and *Aurkc-Gfp* cRNAs into GV oocytes, then inhibited translation by adding cycloheximide, and measured mCherry and GFP intensities over time as reporters for the abundance of AURKB and C. Because long-term incubation in cycloheximide inhibits major meiotic cell-cycle transitions (Downs, 1990; Golbus and Stein, 1976), we monitored the destruction of AURKB and C during three shorter intervals: from GV to MI (GV-MI), from MI to MII (MI-MII) and in activated eggs that are exiting the MII arrest. Although both AURKC-GFP and AURKB-mCherry are progressively degraded (Fig. 4 A-C), AURKC-GFP is more stable than AURKB-mCherry in each interval. Overall, ~30% of AURKC-GFP was degraded between the GV stage and the 2-cell embryonic stage compared to ~70% of AURKB-mCherry (Fig. 4 D). To confirm that degradation was not specific to the fluorophore, we

compared AURKB-GFP to AURKB-mCherry and found identical degradation kinetics (Fig. 11 A). As a photo-bleaching control, non-degradable cyclin B-GFP fluorescence was constant under identical conditions (Fig. 11 B). Taken together these results show that AURKB and AURKC gradually decline during meiotic maturation but AURKC is more stable.

There are conflicting reports regarding whether oocytes contain AURKB. Some studies have reported localization of endogenous AURKB and exogenous AURKB-GFP to centromeres and mid-bodies in mouse oocytes (Vogt et al., 2009) whereas others have failed to do so (Yang et al., 2010). This discrepancy may be due to differences in the abundance of AURKB in the different mouse strains used coupled with poor reagents for detection. *Aurkb* and *Aurkc* mRNA are detectable by quantitative real time PCR and immunocytochemistry on maturing oocytes and developing embryos showed that AURKC localized to metaphase chromatin, and was undetectable by the blastocyst stage (BL) (Fig. 12). Even though *Aurkc* message was virtually absent in the early embryonic stages (Fig. 3 G-H), the protein still remained in the embryo (Fig. 12). We failed to reliably detect AURKB protein with commercially available reagents, but given the presence of *Aurkb* message and that *Aurkc*$^{-/-}$ mice are viable, it is likely that oocytes and early embryos contain AURKB protein. Furthermore, immunocytochemistry of human oocytes also demonstrates that both AURKB and AURKC are present (Avo Santos et al., 2011).

AURKB degradation does not depend on its N-terminus

Because the N-terminus of AURKB contains destruction motifs (Fig. 5 A) that are recognized by the APC/C during mitosis, we asked if AURKB and/or AURKC degradation is proteasome-dependent. Treatment with the proteasome inhibitor MG132 reduced degradation of both AURKs (Figs. 5 B and 13). To test whether the N-terminal motifs in AURKB could explain the difference in kinetics of proteasome-dependent destruction between AURKB and C, we tested the effects of mutating the KEN and A-boxes and deleting the first 93 amino acids of AURKB-GFP. In both cases the degradation kinetics were not affected (Fig. 5 C-D and Fig. 14 A-B). Furthermore, a chimeric version of AURKC that contained the first 90 amino acids of AURKB was degraded with similar kinetics as wild-type AURKC (Fig. 14 C). Taken together, these data strongly suggest that the difference in degradation kinetics between AURKB and C, although proteasome-dependent, cannot be explained by the destruction motifs in AURKB's N-terminus.

Aurkc is a maternally-recruited message

AURKC protein appears to increase between MI and MII when immunofluorescent signals are compared (Fig. 12). Because oocyte meiotic maturation takes place in the absence of transcription, protein levels are regulated by mRNA recruitment and mRNA degradation; recruitment is regulated by cytoplasmic polyadenylation element (CPE) and *DazL* binding sequences in 3'UTRs (Chen et al., 2011; Richter, 2007). *Aurkc* contains a conserved CPE (UUUUAU) in its 3' UTR that is in close proximity (11 nucleotides) to its hexanucleotide polyadenylation sequence

(HEX) (Fig. 6 A) and three putative *DazL* binding sites ($U_{2\text{-}10}C/GU_{2\text{-}10}$), suggesting that the increase in AURKC protein is due to recruitment of *Aurkc* mRNA during meiotic maturation. The *Aurkb* 3'UTR, however, also contains a CPE adjacent to the HEX and a second CPE further 5' to the HEX. To test whether *Aurkb* and/or *Aurkc* mRNAs are recruited during meiotic maturation, we fused the 3' UTRs of these kinases to a firefly luciferase (Luc) reporter (Fig. 6 A). Following injection and assay for luciferase activity, we found that the 3' UTR of *Aurkc* recruited *Luc* mRNA ~10 fold following maturation (Fig. 6 B), compared to ~3 fold for the *Aurkb* 3'UTR. Recruitment of *Luc* mRNA significantly depended upon the CPE in *Aurkc* because it was reduced to ~2.5 fold when two nucleotides of the *Aurkc* CPE had been mutated (Fig. 6 A, B). These data indicate that AURKC protein levels increase during meiotic maturation because its message is recruited for translation in a CPE-dependent manner.

AURKB can compensate for loss of AURKC in vivo

Mitotic cells depleted for AURKB are rescued by ectopic expression of AURKC, suggesting that they can carry out the same functions . Our data indicate that AURKB protein levels decline during oocyte maturation and embryonic development (Figs. 2-5). To determine if AURKB is functionally equivalent to AURKC and if increasing the amount of AURK activity in knockout oocytes and embryos can compensate for loss of AURKC, we matured oocytes from *Aurkc*$^{-/-}$ mice that were microinjected with cRNA encoding *mCherry*, *Aurkc-mCherry* or *Aurkb-mCherry*; oocytes from wild-type mice injected with *mCherry* served as controls. Expression of either *Aurkc*- or *Aurkb-mCherry* rescued both the MI arrest phenotype in *Aurkc*$^{-/-}$ oocytes (Fig. 7 A) and the cytokinesis

phenotype in 1-cell embryos from *Aurkc*$^{-/-}$ mothers (Fig. 7 C). Furthermore, AURKB was no longer restricted to centromeres at MI in *Aurkc*$^{-/-}$ oocytes, as it was in wild-type cells, but it adopted a chromatin localization that is typical of AURKC (Fig. 7 B). Similarly, AURKB-GFP mimicked AURKC centromere localization in *Aurkc*$^{-/-}$ eggs, whereas AURKB was not detected at centromeres in wild-type MII eggs (Fig. 7 B). Our findings that AURKB rescued the *Aurkc*$^{-/-}$ polar body extrusion and 1-cell cytokinesis defects and adopted the subcellular localization of AURKC indicate that AURKB can compensate for the loss of AURKC during meiosis and support the model that AURKB activity declines during meiotic maturation and embryonic development.

DISCUSSION

Here we report, for the first time, that female mice lacking *Aurkc* are sub-fertile. Oocytes from knockout mice have a higher incidence of chromosome misalignment and arrest at MI, and 1-cell embryos often fail in cytokinesis (Figs. 2, 3). These phenotypes are hallmarks of cells that lack Aurora kinase activity (Giet and Glover, 2001; Hauf et al., 2003; Yabe et al., 2009) and worsen as development continues (Fig. 3 D). Interestingly, the phenotypic severity (both *in vivo* and *in vitro*) varies between mice (Figs. 2 F, 3 B, 15 B). These differences could be explained by the degree of compensation by AURKB. In some cases AURKB levels may fall below a threshold necessary to support maturation or embryo development, and therefore viability is compromised. It is unlikely that the 6 additional pseudogene copies of *Aurkc* (Hu et al., 2000) or putative N-terminal splice variants (Yan et al., 2005a) compensate for loss of AURKB because we did not detect

their presence in oocytes from knockout mice (Fig. 8 A) using a Taqman probe that is 97-100% identical in sequence to these regions nor did we detect AURKC protein by immunocytochemistry with an antibody that recognizes the C-terminus (Fig. 8 C). Our *in vitro* maturation and development data demonstrate that the requirement for AURKC *in vitro* appears more severe than its requirement *in vivo* (compare figs. 2 B-F, 3 A-F to fig. 2 A). This difference may be due to hormonal priming for the *in vitro* experiments versus natural matings in the *in vivo* fertility trials. Alternatively, the amount of AURKB may be less following culture *in vitro*, and therefore it is unable to compensate as well as *in vivo*. When we isolated *in vivo* developed blastocysts from hormonally primed mice, we found fewer in the knockout females compared to wild-type, favoring the first model (Fig. 15 A, B). Unfortunately testing the second model is technically not feasible due to limitations in our ability to quantify the amount of AURKB protein.

Our findings that AURKB and AURKC stability and recruitment differ during meiosis (Figs. 4, 5 C and 6 B) provide an explanation for the existence of AURKC in oocytes. AURKB is a critical regulator of mitotic cell division, but its protein is not stable during meiotic maturation, and it is not transcribed again until the blastocyst stage (Figs. 3 G, 4). In contrast, AURKC protein increases during meiotic maturation, which reflects both its stability and CPE-mediated recruitment of *Aurkc* mRNA (Figs. 11, 6B). Although AURKB degradation depends upon the proteasome and the N-terminus of AURKB contains destruction elements that AURKC lacks, the N-terminus does not appear to regulate AURKB stability during meiosis as it does in mitosis (Fig. 5). Because both exogenous proteins gradually decline during meiosis, both may be

regulated via their C-terminal D-boxes (Fig. 5 A), but AURKB degradation is more pronounced (Fig. 4 D).

The discovery of these regulatory mechanisms, combined with evidence that embryos can develop to the blastocyst stage in the absence of AURKB (Fernández-Miranda et al., 2011), suggests that oocytes express a third AURK to compensate for the inherent instability of AURKB. Notably, expression of a non-degradable AURKB in somatic cells leads to aneuploidy, indicating that its degradation is important for mitotic cell cycles (Nguyen et al., 2005). Consistent with others studies, our data support the hypothesis that AURKB and AURKC have similar functions (Fernández-Miranda et al., 2011; Sasai et al., 2004; Slattery et al., 2009). There may be subtle functional differences between AURKB and C, however, that are not revealed in our assays, and oocytes lacking both AURKB and AURKC will be a powerful tool for answering this question.

AURKC is an example of a cell-cycle regulator isoform that is recruited during meiotic maturation to support meiosis, fertilization and early embryonic cell division. Other examples include WEE1B kinase and IP_3 receptor, which contribute to exit from MII (Oh et al., 2011; Xu et al., 2003), and CDC6 and ORC6L, which allow DNA replication following fertilization (Anger et al., 2005; Murai et al., 2010). We propose that these recruited mRNAs comprise a strategy to switch from a program of oocyte growth without cell division, during the prolonged cell-cycle arrest, to meiotic and mitotic divisions without growth, i.e., early embryonic cleavage stages.

MATERIALS AND METHODS

Oocyte and Embryo Collection, Culture and Microinjection

For experiments in Figs. 2-5, fully-grown germinal vesicle (GV)-intact oocytes from equine chorionic gonadotropin-primed (44-48 h before collection) 6-wk-old female CF-1 mice (Harlan) (Figs. 2-5) or from the indicated *Aurkc* genotype (Figs. 6-7) were obtained as previously described. Meiotic resumption was inhibited by addition of 2.5 μM milrinone (Sigma) to the collection, culture or microinjection medium (Tsafriri et al., 1996). Oocytes were cultured in Chatot, Ziomek, and Bavister (CZB) medium in an atmosphere of 5% CO_2 in air at 37°C and were collected and microinjected in MEM/PVP (polyvinylpyrrolidone, 3 g/L) (Chatot et al., 1989). To inhibit the proteasome, MG132 (Sigma) was added to the culture medium to a final concentration of 20 μM. To activate MII eggs, the eggs were placed in $Ca^{2+/}Mg^{2+}$ free CZB plus 10 mM $SrCl_2$ and 5 mg/mL cytochalasin B (Sigma C2743) 18 h after maturation. After 3 h, the eggs were washed free of $SrCl_2$. Oocytes were microinjected with 250 ng/ul of *Aurkb/c* cRNAs as previously described. Injected oocytes were held for 2-12 h prior to induction of maturation. For maturation experiments, oocytes were washed and cultured in milrinone-free CZB medium.

In Figs. 3 and 7, primed mice of the indicated *Aurkc* genotype (Fig. 7) were administered human chorionic gonadotropin (hCG) and mated to B6D2F1/J males (Jackson Laboratories). In Fig. 7, 1-cell embryos were isolated 20 h post-hCG from the ampullae and cultured in KSOM + amino acids (Millipore) in an atmosphere of 5% CO_2 in air at 37°C. In Fig. 12, embryos of the indicated stage were collected as previously

described and immediately frozen (Ma and Schultz, 2008). All animal experiments were approved by the institutional animal use and care committee and were consistent with the National Institutes of Health (NIH) guidelines.

Generation and genotyping of Aurkc$^{-/-}$ mice

Generation of *Aurkc*$^{-/-}$ was described previously (Kimmins et al., 2007). Lexicon Pharmaceuticals transferred cryopreserved *Aurkc*$^{+/-}$ embryos into pseudopregnant females and the resulting pups were sent to the University of Pennsylvania for further breeding. For genotyping, the copy number of *Neo* was quantified by real time PCR per the manufacturer's protocol. Briefly, tails were digested in 400 µl of lysis buffer (125 mM NaCl, 40 mM Tris, pH 7.5, 50 mM EDTA, pH 8, 1% sarkosyl, 5 mM DTT, and 50 µM spermidine) with 6 µL of Proteinase K (Sigma #P4850) for 2 h at 65°C. After dilution of 1:30 in water, the lysates were boiled for 5 min to denature Proteinase K. Two µL of the diluted DNA was added to each reaction. Primers to detect *Neo* (F: 5' CTCCTGCCGAGAAAGTATCCA-3'; R: GGTCGAATGGGCAGGTAG-3') were used at a final concentration of 300 nM and primers to detect *Csk* (for sample normalization) (F 5'-CTGGCCATCCGGTACAGAAT-3'; R 5'-TGCAGAAGGGAAGGTCTTGCT-3') were used at a final concentration of 100 nM. The TAMRA-quenched *Neo* probe (ABI) was conjugated to 6FAM and used at a final concentration of 100 nM and the TAMRA-quenched *Csk* probe was conjugated to VIC and used at a final concentration of 100 nM. The comparative C_t method was used to calculate the *Neo* copy number.

Cloning, mutagenesis and in vitro synthesis of cRNA

Generation of H2B-mCherry and non-degradable cyclin B-GFP were described previously (Duncan et al., 2009; Schindler and Schultz, 2009). To generate *Aurkb* and *Aurkc*-GFP and -mCherry, mouse *Aurk* sequences were amplified and cloned into pIVT-GFP or –mCherry (Igarashi et al., 2007). Truncated AURKB and chimeric AURKB/C constructs were also generated by PCR and cloned into pIVT-GFP. The *Aurkb*-KEN/A box mutant was generated by site-directed mutagenesis using the QuikChange Multi-site Mutagenesis (Agilent Technologies) kit per manufacturer's instructions. The KEN box (aa 4-9) was changed to AAN and the A box (aa 26-29; QRVL) was changed to QAVA. The 3'UTRs of *Aurkb* and *Aurkc* were PCR-amplified from full-length clones obtained from Open Biosystems and cloned into pIVT containing firefly luciferase. *Renilla* luciferase was generated as described previously (Murai et al., 2010). The CPE (TTTTAT) in the 3'UTR of *Aurkc* was mutated to TTGGAT using QuikChange.

Linearized DNA for *in vitro* transcription was achieved by NdeI digest for all *Gfp*-and *mCherry*-containing constructs. EcoRI digestion was used for luciferase-containing constructs. After purification of the digests (Qiagen PCR Cleanup) complementary RNAs (cRNAs) were generated using the mMessage mMachine T7 kit (Ambion) according to the manufacturer's instructions. The cRNA was purified using the RNAeasy kit (Qiagen) and eluted in 30 μL of RNAse-free water.

Real-time PCR

Fifty oocytes or embryos at the indicated stage were isolated from CF-1 mice and frozen prior to processing. After thawing on ice, 2 ng of *Gfp* mRNA was added to each

sample. Next, total RNA from the mixtures were purified using the PicoPure RNA isolation kit (Arcturus) per manufacturer's protocol. After purification, cDNA was generated by reverse transcription using random hexamers and Superscript II as previously described (Anger et al., 2005). Taqman probes specific for *Aurkb* (Mm01718146_g1) and *Aurkc* (Mm03039428_g1) (Applied Biosystems) were used for gene expression detection and the comparative C_t method was used to determine the difference in expression levels between stages. Data was acquired using an ABI Prism 7000 (Applied Biosystems).

Luciferase assay

The cRNAs of firefly luciferase fused to the 3'UTR of *Aurkb* or *Aurkc* (200 ng/μL) and *Renilla* luciferase (25 ng/μL) were co-injected into GV-intact oocytes from CF-1 mice as described above and incubated *in vitro* for at least 2 h in milrinone-containing medium. After incubation, one-half of the injected oocytes were matured to MII for 17 h. The other half was maintained at the GV stage. After washing in PBS+ PVP, single oocytes were collected and lysed in Passive Lysis Buffer (12 μL/oocyte) for 15 min at room temperature with shaking followed by incubation on ice until processing with the Dual Luciferase reporter assay system (Promega). The manufacturer's instructions were followed except that 10 μL of sample and 50 μL of Luciferase Assay Reagent II and of Stop and Glo Reagent were used. Signal intensities were obtained using a Monolight 2010 luminometer (Analytical Luminescence Laboratory, San Diego, CA). Background fluorescence was subtracted by measuring signals in uninjected

oocytes and firefly luciferase activities were normalized to that of *Renilla* luciferase and expressed as the fold recruitment in MII eggs compared to GV oocytes.

Immunocytochemistry

Following meiotic maturation or embryo development to the indicated stage, oocytes and embryos were fixed in phosphate-buffered saline (PBS) containing 3.7% paraformaldehyde for 1 h at room temperature and transferred to blocking buffer (PBS + 0.3% BSA + 0.01% Tween-20) for storage overnight at 4°C. After 15 min of permeabilization in PBS containing 0.1% Triton X-100 and 0.3% BSA, cells were incubated in rabbit anti-AURKC antibody (Bethyl A400-023A; epitope BL1217) at 1:30 or a polyclonal anti-β-tubulin antibody conjugated to Alexa 488 (Cell Signaling 3623) at 1:75 in blocking buffer for 1 h at room temperature in a humidified chamber. After washing, secondary Alexa Fluor 594 anti-rabbit antibody (Invitrogen A11012) was diluted 1:200 in blocking solution and the samples incubated for 1 h at room temperature. After a final wash in blocking buffer containing Sytox Green (Invitrogen S7020; 1:5000), cells processed to detect AURKC were mounted in VectaShield (Vector Laboratories). Cells processed to detect the spindle were mounted in VectaShield containing 3 μg/mL propidium iodide. Ploidy analysis was acquired as described previously (Duncan et al., 2009; Stein and Schindler, 2011). Images were collected with a spinning disk confocal using a 100X 1.4 NA oil immersion objective and processed using Image J software (NIH) as previously described (Chiang et al., 2010a).

Live-cell imaging

To monitor destruction of the exogenous AURKs, GV oocytes were co-microinjected with the indicated cRNAs. Following injection, oocytes were maintained at the GV stage for 16-17 h (for the GV-MI time course), 10-11 h (for the MI-MII time course) or 1 h (for the MII activation time course) prior to maturation. To inhibit translation, oocytes were placed in 10 ng/μL cycloheximide (Sigma C7698) 1 h prior to live imaging. Similar, but not as robust as effect, was observed when cycloheximide was omitted. For live imaging, each oocyte or activated egg was transferred into an individual drop of CZB medium or $Ca^{2+/}Mg^{2+}$ free CZB containing $SrCl_2$ and cytochalasin B, respectively. All drops contained cycloheximide and were under oil in a FluoroDish (World Precision Instruments). DIC, GFP and mCherry image acquisition was started at 0 (GV-MI), 6 (MI-MII), and 18 h (MII activation) after maturation on a Leica DM6000 microscope with a 40X 1.25 NA oil immersion objective and a charge-coupled device camera (Orca-AG, Hamamatsu Photonics) controlled by Metamorph Software. The microscope stage was heated to 37°C and 5% CO_2 was maintained using a microenvironment chamber (PeCon) and an airstream incubator (ASI 400, Nevtek). Images of individual cells were acquired every 30-60 min during the indicated intervals. For each oocyte, fluorescence was calculated at each time point as a fraction of the fluorescence at the first time point.

To monitor meiotic timing and timing of 1-cell cleavage, oocytes and embryos from the indicated genotypes were matured in drops of CZB or KSOM +AA, respectively, under oil in a FluoroDish. DIC images were acquired every 10 min on the

microscope described above using a 20X 0.4 NA objective to monitor the timing of GVBD and polar body extrusion or every 5 min to capture cytokinesis in 1-cell embryos.

Fertility trials

Wild-type and knockout *Aurkc* female mice of sexual maturity (6 weeks) were continually mated to wild-type B6D2 (Jackson Laboratories) male mice of known fertility for 8 months. Cages were checked daily for the presence and number of pups.

Statistical Analysis

One-way ANOVA and Student's t-Test, as indicated in figure legends, were used to evaluate the differences between groups using Prism software (GraphPad Software). $P < 0.05$ was considered significant.

Figure 2

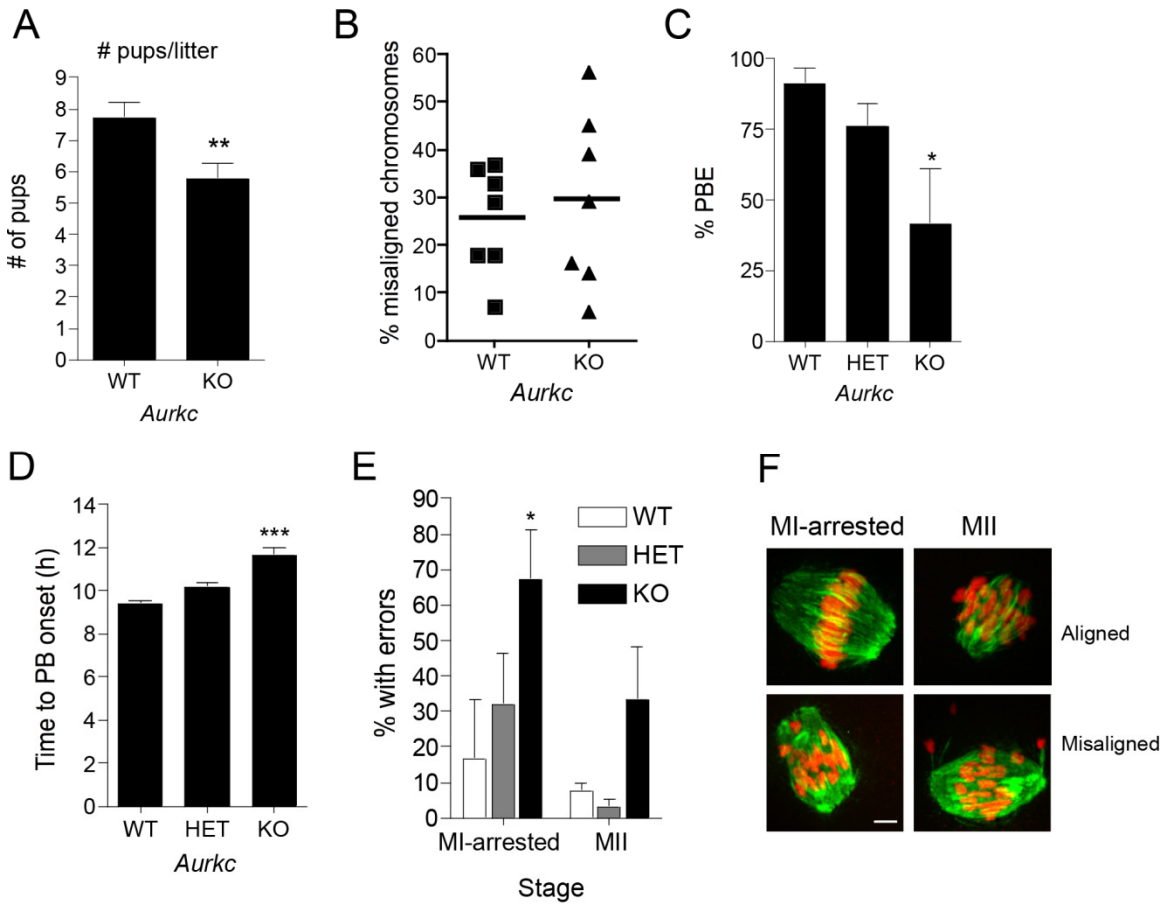

Figure 2. Loss of AURKC leads to meiotic abnormalities. (**A**) Results of fertility trials. The average number of pups born to females of the indicated genotype over an 8 month breeding trial is shown. (**B**) 20-45 GV-intact oocytes were isolated from mice of the indicated genotype and matured *in vitro* for 8 h prior to fixation at MI. Percent misalignment was plotted for each mouse analyzed. **(C-F)** GV-intact oocytes were isolated from mice of the indicated genotype and matured *in vitro* to determine incidence (B) and timing (C) of polar body extrusion (PBE). Cells were fixed when controls (WT)

had reached MII and processed for immunocytochemistry to detect chromosomes and spindles. The percentage of oocytes that contained abnormal chromosome configurations at either MI or MII was determined (E), and representative images are shown (F). Graphs represent mean (±SEM) from at least 30 oocytes from 3 independent experiments. Scale bars 5 μm. One-way ANOVA was used to analyze the data in B-D. * $p<0.05$; ***$p<0.001$; WT, wild-type; HET, heterozygous; KO, knockout.

Figure 3

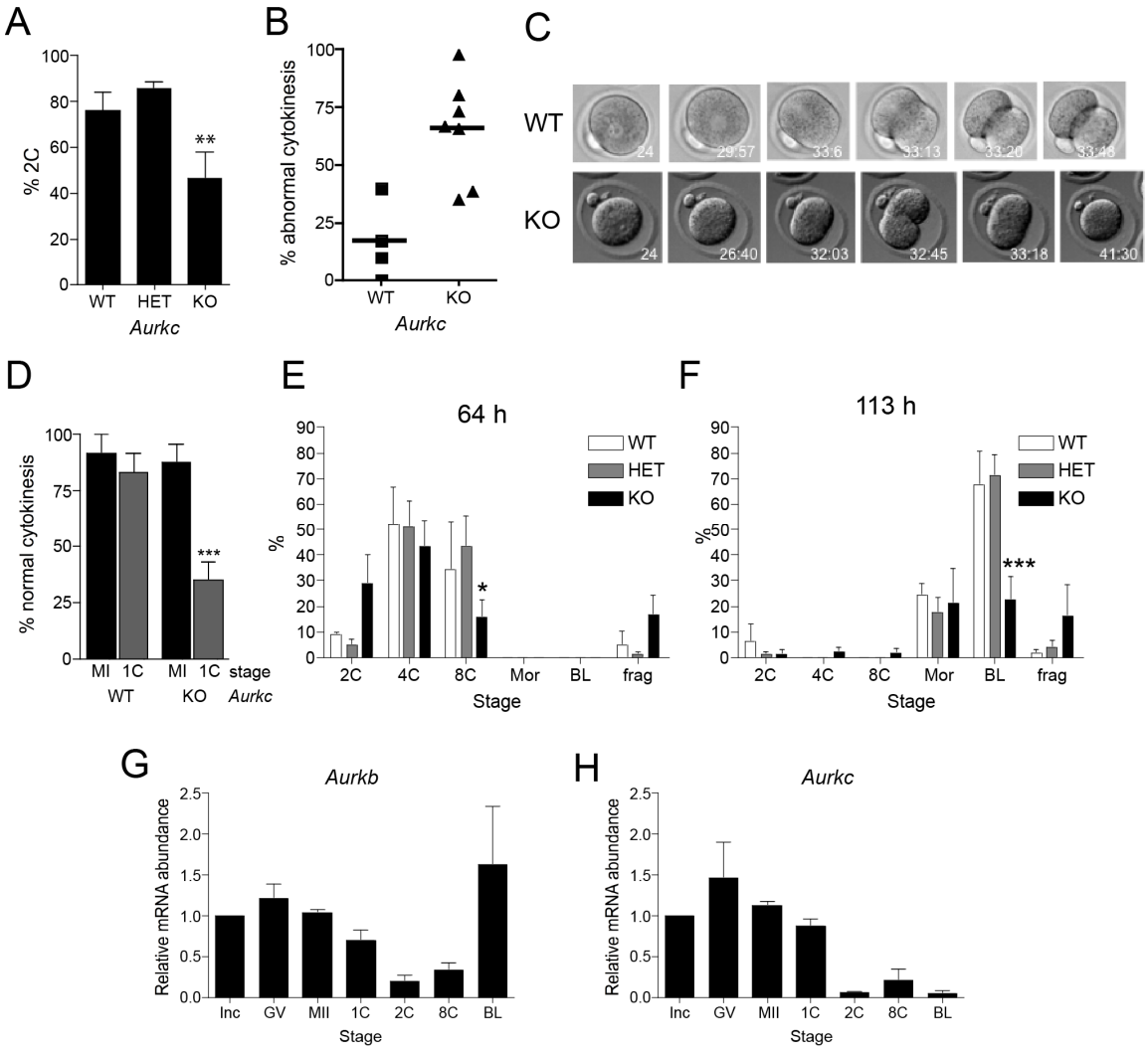
A
% 2C
WT HET KO
Aurkc
B
% abnormal cytokinesis
WT KO
Aurkc
C
WT
KO
24
29:57
33:6
33:13
33:20
33:48
24
26:40
32:03
32:45
33:18
41:30
D
% normal cytokinesis
MI 1C MI 1C stage
WT KO Aurkc
E
64 h
WT
HET
KO
%
2C 4C 8C Mor BL frag
Stage
F
113 h
WT
HET
KO
%
2C 4C 8C Mor BL frag
Stage
G
Aurkb
Relative mRNA abundance
Inc GV MII 1C 2C 8C BL
Stage
H
Aurkc
Relative mRNA abundance
Inc GV MII 1C 2C 8C BL
Stage

Figure 3. Embryonic development is compromised in *Aurkc-/-* mice. (A-F) Female mice of the indicated genotype were mated to wild-type males and 1-cell embryos were isolated and cultured *in vitro*. **(A)** The percent of 1-cell embryos that cleaved to the 2-cell embryonic stage. (B-D) Embryos were imaged live by DIC every 5-7 min. In B, the percent of embryos with abnormal cytokinesis was plotted for each mouse. C contains representative images of a WT embryo undergoing normal cytokinesis (top row) and a KO embryo failing cytokinesis (bottom row). The time stamp is hr: min after hCG injection. (D) The percentage of normal cytokinesis events from Figs. 2 C (MI) and 3 B (1C) were compared. **(E-F)** Embryo development was monitored at the indicated times after hCG and mating. These experiments were conducted 4 times with at least 2 mice per genotype each time, and the data are expressed as the mean ± SEM. (**G-H**) mRNA levels were measured by quantitative RT-PCR at the indicated stages. Data were normalized against a probe that detects exogenously added *Gfp* message. Mean (±SEM) from 3 independent experiments are shown. One-way ANOVA was used to analyze the data. * $p<0.05$; ** $p<0.01$; *** $p<0.001$; WT, wild-type; HET, heterozygous; KO, knockout; Inc, meiotically incompetent oocyte; GV, full grown GV-intact oocyte, MI, meiosis I; MII, meiosis II; 1C, 1-cell embryo; 2C, 2-cell embryo; 4C, 4-cell embryo; 8C, 8-cell embryo; frag, fragmented; Mor, morula; BL, blastocyst.

Figure 4

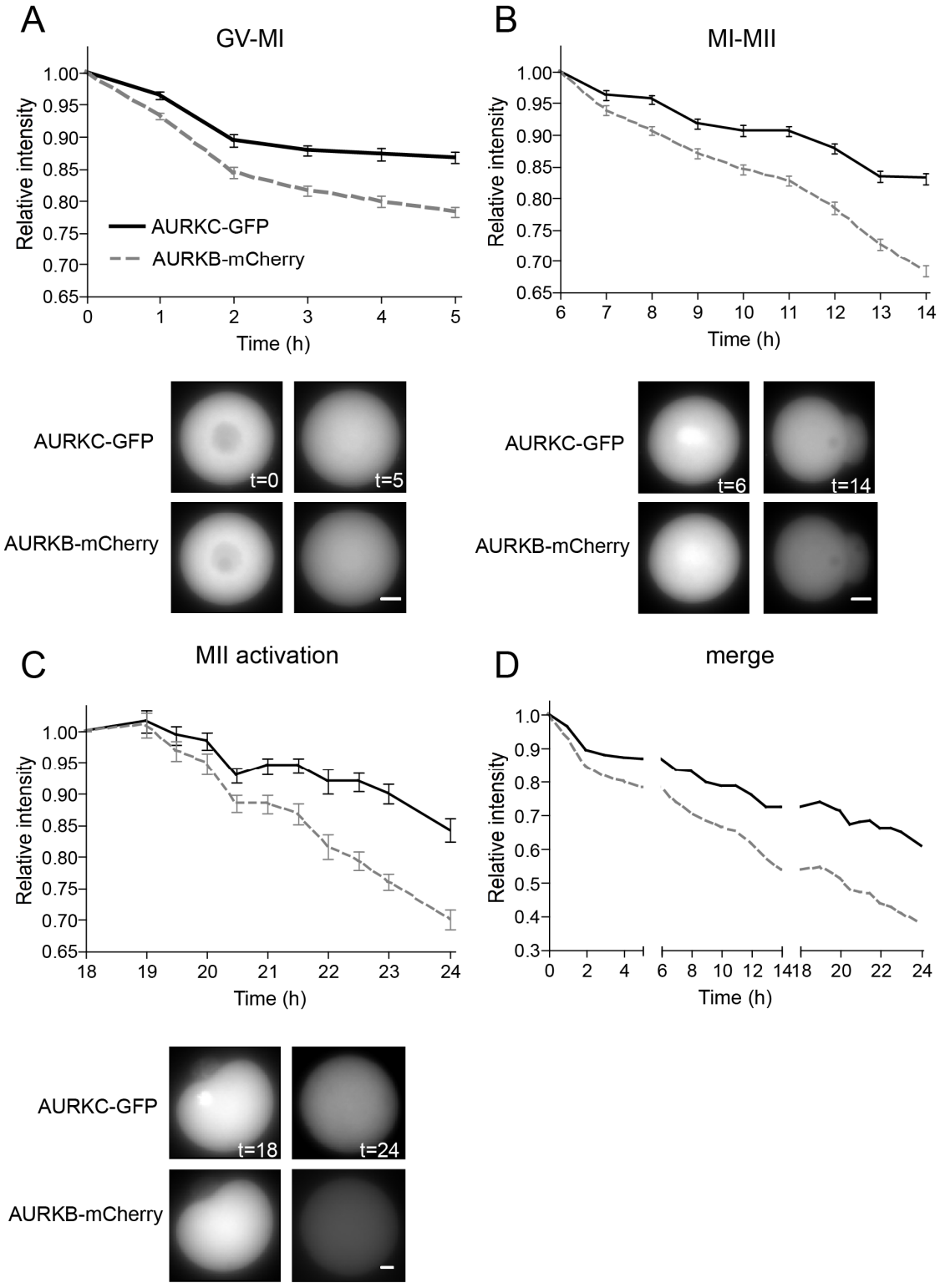
A
GV-MI
Relative intensity
1.00
0.95
0.90
0.85
0.80
0.75
0.70
0.65
AURKC-GFP
AURKB-mCherry
0
1
2
3
4
5
Time (h)
B
MI-MII
Relative intensity
6
7
8
9
10
11
12
13
14
Time (h)
AURKC-GFP
t=0
t=5
AURKB-mCherry
AURKC-GFP
t=6
t=14
AURKB-mCherry
C
MII activation
Relative intensity
18
19
20
21
22
23
24
Time (h)
D
merge
Relative intensity
1.0
0.9
0.8
0.7
0.6
0.5
0.4
0.3
0
2
4
6
8
10
12
14
18
20
22
24
Time (h)
AURKC-GFP
t=18
t=24
AURKB-mCherry

Figure 4. AURKC is more stable than AURKB during meiotic maturation. (A-C) GV-intact oocytes were co-injected with the indicated cRNAs and matured to the indicated stage. In each graph, the first time point is 1 h after cycloheximide addition, and fluorescent images were obtained at the indicated times. Below are representative images from each time course. Data represent mean (±SEM) from at least 30 oocytes from 2 independent experiments. Scale bars 5 μm. **(D)** Merge of the data from panels A-C. GV, Germinal vesicle; MI, meiosis I; MII, meiosis II.

Figure 5

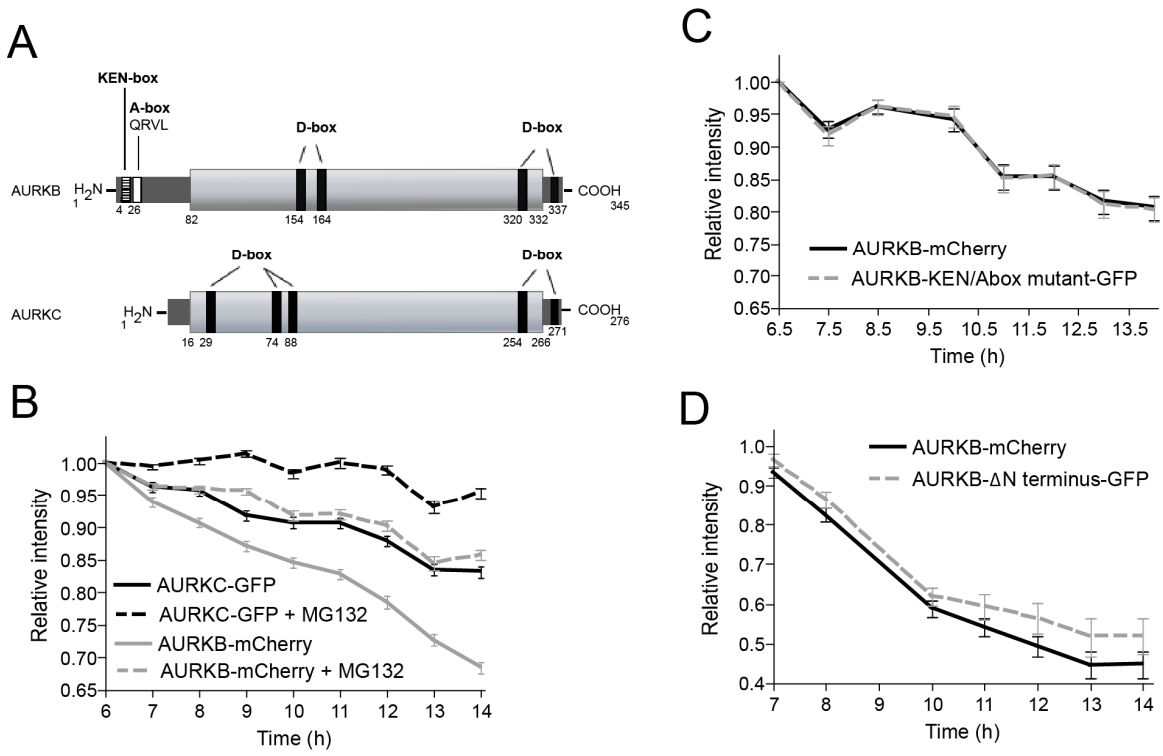

Figure 5. AURKB stability does not depend upon its N-terminus. (**A**) Schematic representation of AURKB and AURKC. KEN, A- and D-boxes are indicated, and the conserved regions are shaded in light gray. **(B-D)** GV-intact oocytes were co-injected with the indicated cRNAs and matured to the indicated stage. Cycloheximide was added 1 h prior to the first time point and fluorescent images were obtained at the indicated times. Data represent mean (±SEM) from at least 30 oocytes from 2 independent experiments. MG132 was added as indicated to inhibit the proteasome (B).

Figure 6

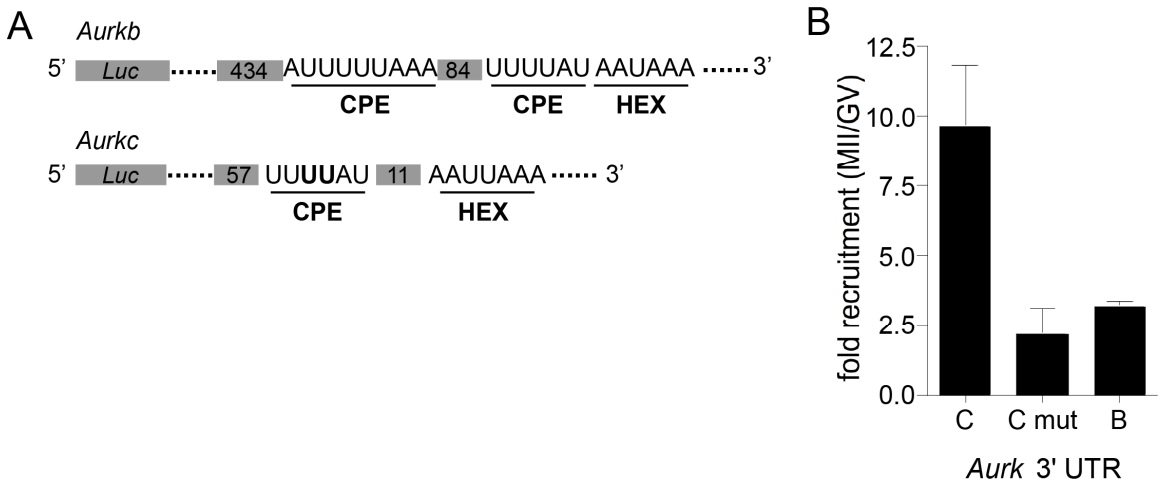

Figure 6. *Aurkc* is a maternally-recruited message. (**A**) Schematic representation of the Firefly luciferase (*Luc*) fusions to the *Aurkb* and *Aurkc* 3'UTRs. Putative CPE and hexonucleotide (HEX) motifs are underlined and the number of nucleotides between the motifs are indicated in the gray boxes. In *Aurkc*, the 2 nucleotides in the CPE that were mutated are in bold. Note that the lengths are not to scale. (**B**) GV-intact oocytes were co-injected with *Luc* fused to the indicated 3'UTR and *Renilla* luciferase as an injection volume control. Luminescence was measured and quantified as the fold difference in MII compared to GV. Data represent mean (±SEM) from 10 oocytes from 2 independent experiments. CPE, cytoplasmic polyadenylation element; mut, mutated.

Figure 7

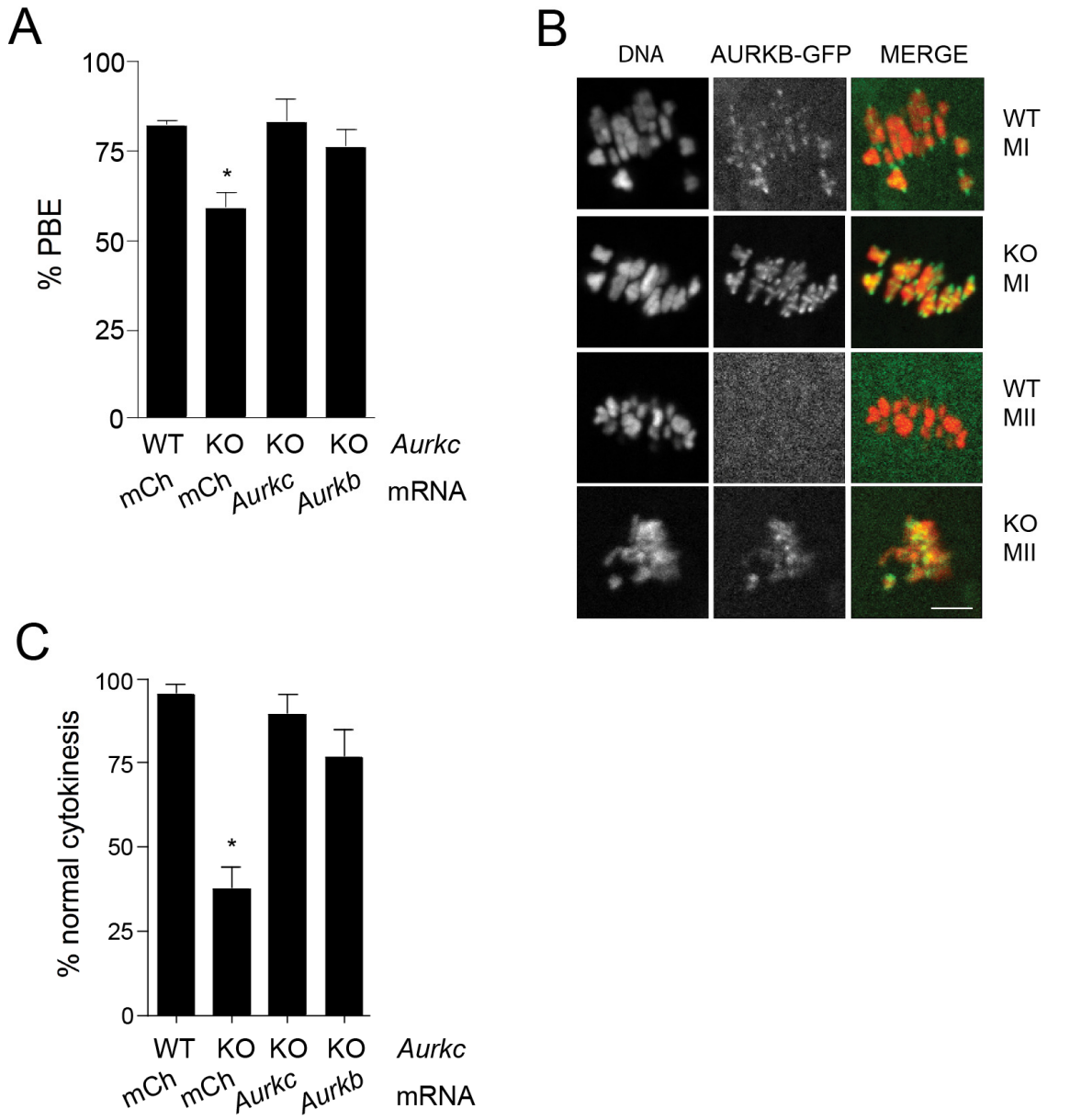
A
100
75
50
25
0
% PBE
*
WT
KO
KO
KO
Aurkc
mCh
mCh
Aurkc
Aurkb
mRNA
B
DNA
AURKB-GFP
MERGE
WT
MI
KO
MI
WT
MII
KO
MII
C
100
75
50
25
0
% normal cytokinesis
*
WT
KO
KO
KO
Aurkc
mCh
mCh
Aurkc
Aurkb
mRNA

Figure 7. Ectopic expression of AURKB in oocytes and embryos from *Aurkc* KO mice rescues their defects. (**A, C**) GV-intact oocytes or 1-cell embryos from a single mouse of the indicated genotype were subdivided and microinjected with the indicated cRNAs and matured to MII to determine incidence of PBE or developed to the 2-cell stage to monitor cytokinesis. These experiments were repeated 3 times with 2-4 knockout mice per experiment. (**B**) Wild-type or *Aurkc* KO oocytes were microinjected with *Aurkb-Gfp* cRNA, matured to MI and MII, and imaged live. Shown are representative images. Scale bars 5 μm. One-way ANOVA was used to analyze the data. * $p<0.05$; WT, wild-type; HET, heterozygous; KO, knockout; mCh, mCherry.

Figure 8

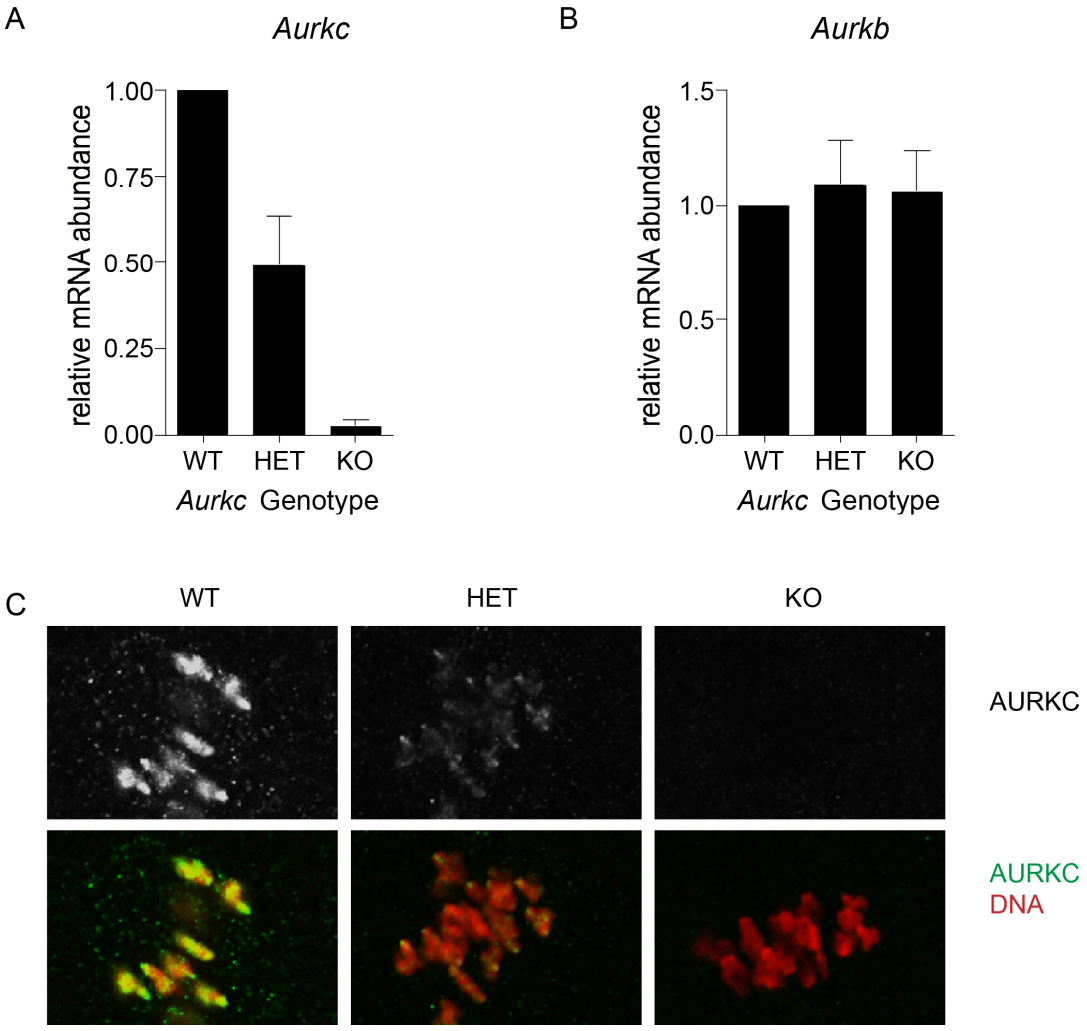

Figure 8. Abundance of *Aurkb* and *Aurkc* messages. (**A, B**) Fifty GV-intact oocytes from mice of the indicated genotypes were isolated, pooled and used for mRNA purification and generation of cDNA. Gene-specific Taqman probes were used to detect *Aurkc* (A) and *Aurkb* (B) messages. The abundance in the wild-type sample was set to 1. These experiments were repeated twice. (**C**) Oocytes from the indicated genotypes (crossed into the CF1 genetic background) were collected, matured to MI and processed with an anti-AURKC antibody. WT, wild-type; HET, heterozygous; KO, knockout.

Figure 9

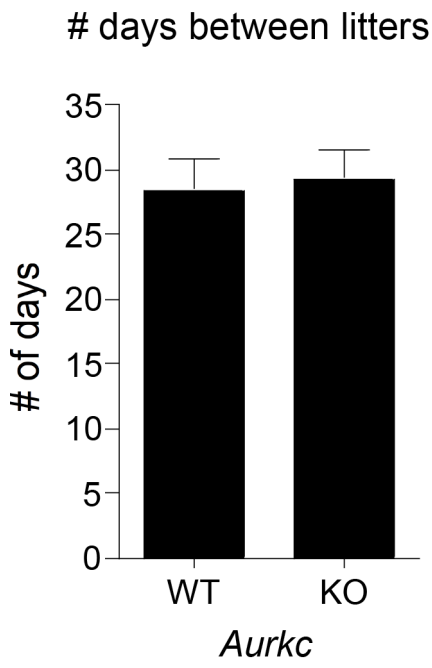

Figure 9. *Aurkc*-/- mice are subfertile. The average number of days between the birth of new litters for each female in the 8 month mating trial. The data are expressed as the mean +/- SEM. Student's t-Tests were used to analyze the data.

Figure 10

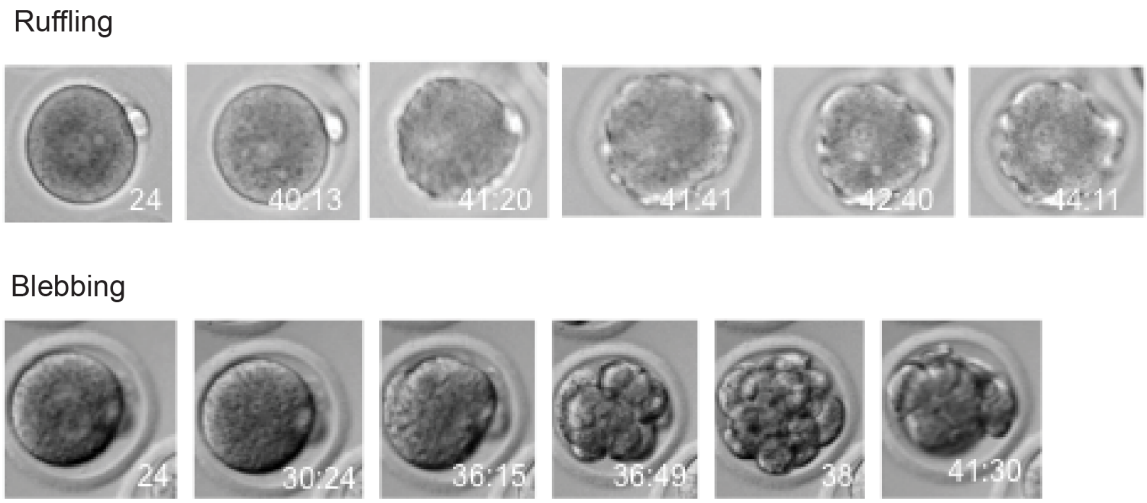

Figure 10. Examples of membrane ruffling and blebbing. Representative images of 1-cell embryos undergoing abnormal cytokinesis while being imaged live by DIC every 5-7 min. The time stamp is hr: min after hCG injection.

Figure 11

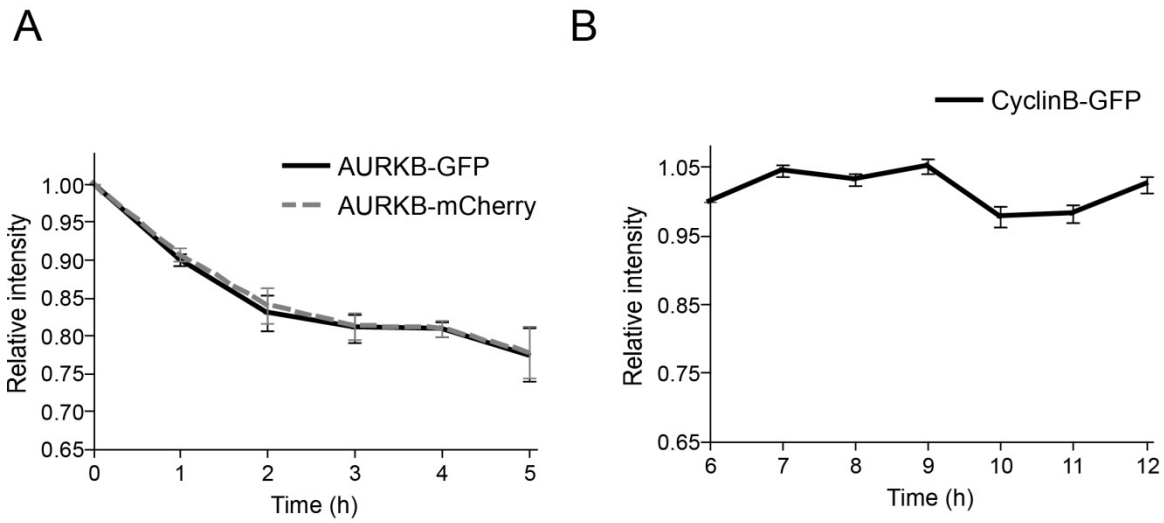

Figure 11. Destruction controls. (**A**) AURKB-GFP and AURKB-mCherry have the same destruction kinetics during meiotic maturation. (**B**) Non-degradable cyclinB-GFP signal does not diminish during a live imaging time course. GV-intact oocytes were injected with the indicated cRNAs and 1 h prior to the first time point cycloheximide was added. Fluorescent images were obtained at the indicated times. These time courses were conducted twice with at least 15 oocytes and the data are expressed as the mean ± SEM.

Figure 12

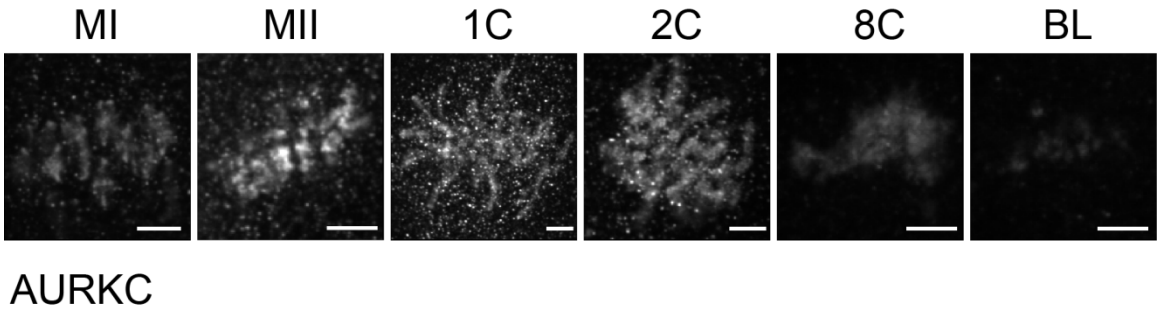

Figure 12. AURK C levels in mouse oocytes and embryos. GV oocytes or 1-cell embryos were collected and cultured *in vitro* and analyzed at the indicated stages by immunocytochemistry. Representative images are shown. Scale bars 5 μm. MI, meiosis I; MII, meiosis II; 1C, 1 cell embryo; 2C, 2 cell embryo; 8C, 8 cell embryo; BL, blastocyst.

Figure 13

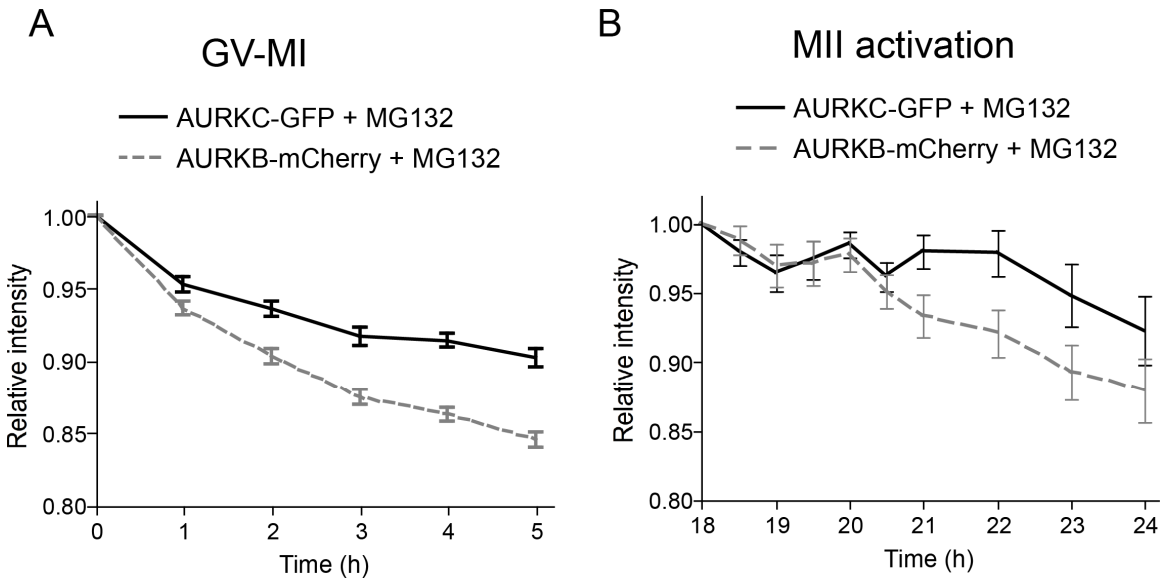

Figure 13. Destruction of AURKB and AURKC is proteosome dependent. GV-intact oocytes were co-injected with the indicated cRNAs and imaged at the indicated time intervals. Cycloheximide was added to the cells to stop translation 1 h prior to the first time point and MG132 was added to one-half of the cells to inhibit the proteosome. These time courses were conducted twice with at least 15 oocytes and the data are expressed as the mean ±SEM.

Figure 14

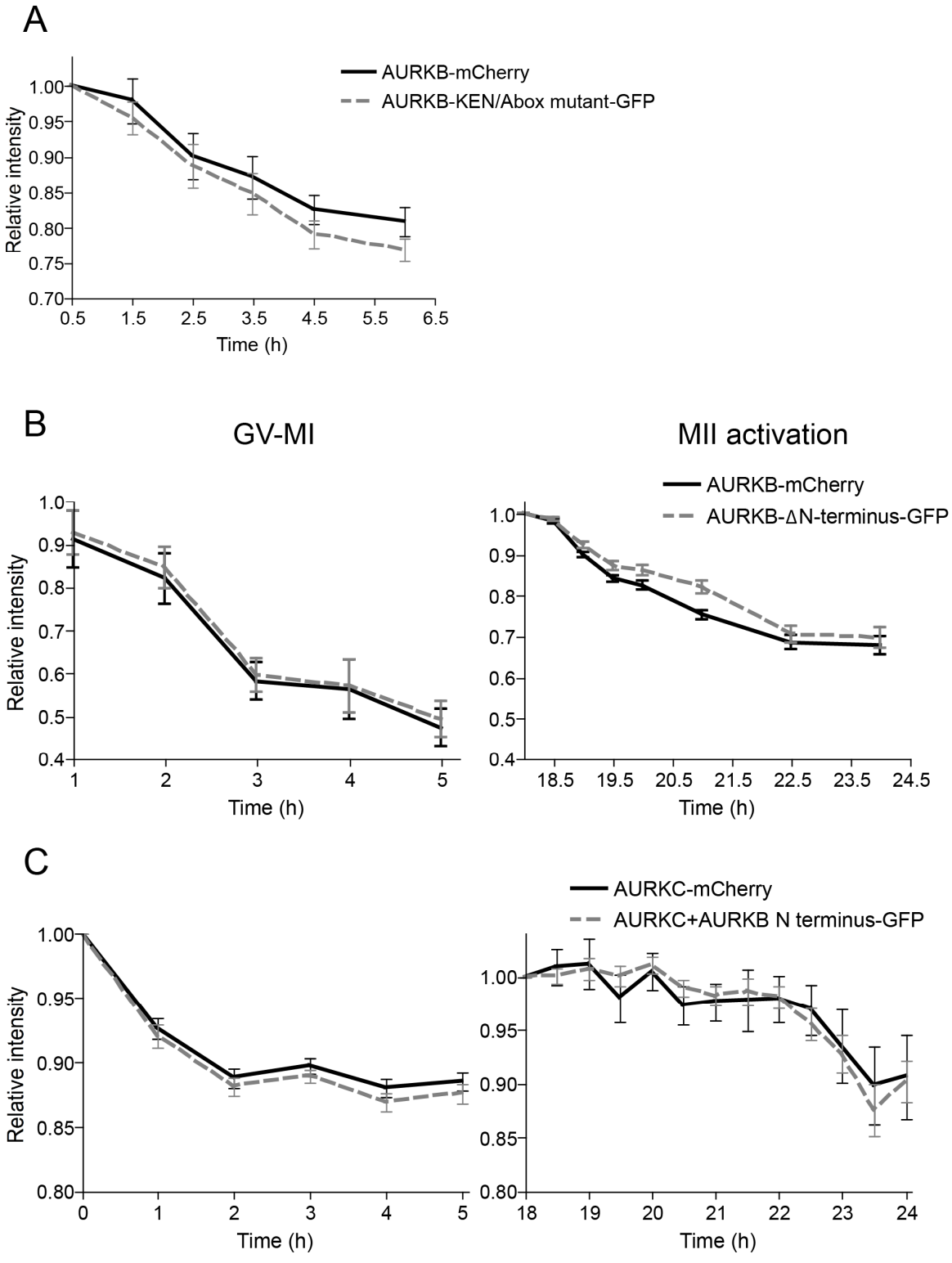
A
AURKB-mCherry
AURKB-KEN/Abox mutant-GFP
Relative intensity
Time (h)
B
GV-MI
MII activation
AURKB-mCherry
AURKB-ΔN-terminus-GFP
Relative intensity
Time (h)
C
AURKC-mCherry
AURKC+AURKB N terminus-GFP
Relative intensity
Time (h)

Figure 14. Stability of AURKB and AURKC mutants. (**A**) The stability of the KEN and A-box mutant AURKB-GFP is not different from the stability of wild-type AURKB-mCherry during meiotic maturation. (**B**) The stability of AURKB-GFP lacking the N-terminus is not different from the stability of wild-type AURKB-mCherry during meiotic maturation. (**C**) The stability of chimeric AURKC-GFP containing the N-terminus of AURKB does not differ from the stability of wild-type AURKC-mCherry. **(A-C)** GV-intact oocytes were co-injected with the indicated cRNAs and imaged at the indicated time intervals. Cycloheximide was added to the cells 1 h prior to the first time point. These time courses were conducted twice with at least 15 and the data are expressed as the mean ± SEM.

Figure 15

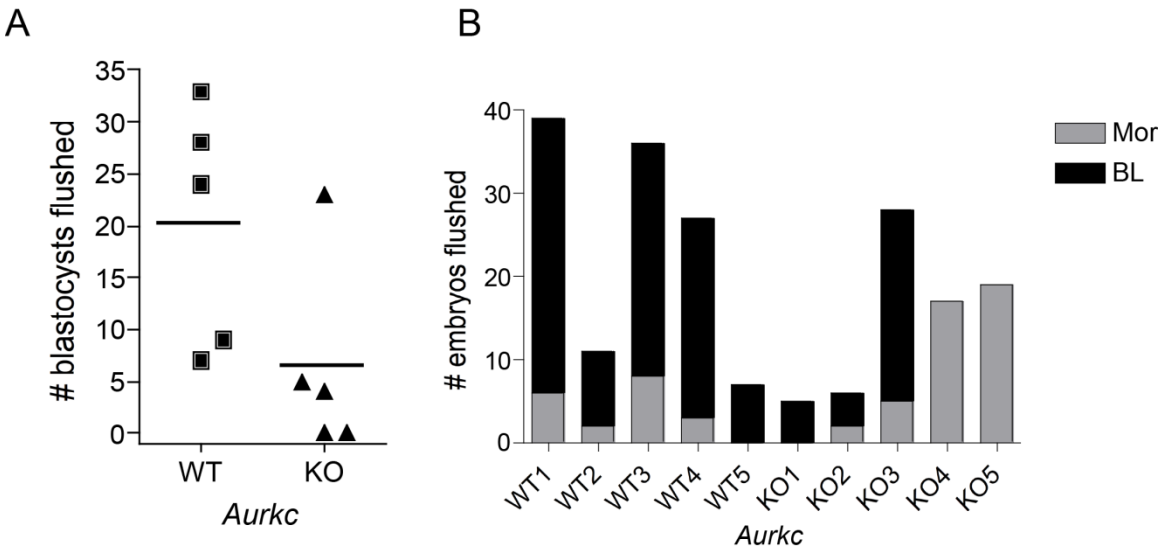

Figure 15. Number of embryos flushed from *Aurkc* WT and KO mice. (**A, B**) Female mice of the indicated genotype were hormonally primed and mated to wild-type males. Ninety-six hours after mating, embryos were flushed from uteri and counted. (**A**) The data is presented as the total number of blastocysts per mouse. The horizontal bar represents the mean. (**B**) The same data is presented as the total numbers of morulas and blastocysts per mouse. WT, wild-type; KO, knockout; Mor, morula; BL, blastocyst.

CHAPTER 3

Increased CDK1 activity determines the timing of kinetochore-microtubule attachments in meiosis I

The data in Chapter 3 are in press (Davydenko et al., 2013)

SUMMARY

Chromosome segregation during cell division depends on stable attachment of kinetochores to spindle microtubules. Mitotic spindle formation and kinetochore-microtubule (K-MT) capture typically occur within minutes of nuclear envelope breakdown. In contrast, during meiosis I in mammalian oocytes, formation of the acentrosomal bipolar spindle takes 3-4 hours, and stabilization of K-MT attachments is delayed an additional 3-4 hours. The mechanism responsible for this delay, which likely prevents stabilization of erroneous attachments during spindle formation, is unknown. Here we show that during meiosis I attachments are regulated by CDK1 activity, which gradually increases through prometaphase and metaphase I. Partial reduction of CDK1 activity delayed formation of stable attachments, whereas a premature increase in CDK1 activity led to precocious formation of stable attachments and eventually lagging chromosomes at anaphase I. These results indicate that the slow increase in CDK1 activity in meiosis I acts as a timing mechanism to allow stable K-MT attachments only after bipolar spindle formation, thus preventing attachment errors.

INTRODUCTION

The goal of the first meiotic division is proper segregation of homologous chromosomes to produce a euploid egg. To achieve faithful segregation at anaphase, the kinetochores of homologous chromosomes must capture microtubules (MTs) emanating from opposite poles of the bipolar spindle (bi-orientation). The two centrosomes of mammalian somatic cells confer an inherent bipolarity to the spindle, such that mitotic spindle formation and kinetochore-microtubule (K-MT) capture are relatively quick and typically occur within minutes of nuclear envelope breakdown. In contrast, the spindle of the mammalian oocyte is acentrosomal and achieves bipolarity through progressive merging of multiple microtubule organizing centers (MTOCs), first into multipolar intermediates and finally a bipolar spindle 3-4 hours following germinal vesicle breakdown (GVBD) (Schuh and Ellenberg, 2007). Although chromosomes congress to the equator of this newly formed bipolar spindle, microtubule fibers do not form stable end-on attachments to kinetochores until late in metaphase I (MI), 6-8 h after GVBD (Brunet et al., 1999; Gui and Homer, 2012; Kitajima et al., 2011).

The mechanism of the attachment delay in meiosis I is unknown, but it may increase the likelihood of bi-orientation by preventing stable attachments while spindles are multipolar and many MTOCs remain close to the chromosomes (Breuer et al., 2010; Kolano et al., 2012; Lane et al., 2012). In cancer cells with multiple centrosomes, attachments that form during a multipolar spindle intermediate can end up incorrect, leading to lagging chromosomes in anaphase and segregation errors (Ganem et al., 2009; Silkworth et al., 2009). A similar problem is likely to arise during meiosis I if

attachments are stabilized too soon, before spindle bipolarity is established. Preventing attachment errors may be especially important in oocytes, which can proceed to anaphase I in the presence of misaligned bivalents (Gui and Homer, 2012; Kolano et al., 2012; Lane et al., 2012) and have a high incidence of aneuploidy compared to untransformed somatic cells (Chiang et al., 2010b; Pan et al., 2008; Thompson and Compton, 2008).

Although it is unknown how K-MT attachments are delayed in oocytes, the profile of CDK1 activity during meiosis I suggests that this kinase may control the timing. In contrast to mitosis, where CDK1 activity increases rapidly before nuclear envelope breakdown and then remains constant until anaphase (Gavet and Pines, 2010), CDK1 activity slowly rises throughout prometaphase and metaphase I in oocytes and peaks ~6 h after GVBD, concurrent with stable attachment formation (Choi et al., 1991; Gavin, 1994; Polanski et al., 1998). Cyclin B protein progressively accumulates as CDK1 activity increases during meiosis I, which suggests that CDK1 activity is limited by cyclin B levels (Hampl and Eppig, 1995; Winston et al., 1997). Based on these observations we hypothesize that the gradual increase in cyclin B levels and CDK1 activity act as a timing mechanism to regulate the formation of stable K-MT attachments.

RESULTS

K-MT attachments are delayed in meiosis I

We first established a cold-stable microtubule assay to visualize K-MT fibers, which are preferentially stabilized at 4 °C while other MTs depolymerize (Rieder, 1981). To quantify K-MT interactions we scored individual kinetochores as stably end-on attached (contact with ends of cold-stable microtubules), unattached (no visible contact to microtubules), or lateral (contact with microtubule, but not end-on) (Fig. 16 A). Lateral interaction of kinetochores with microtubules typically precedes bi-orientation and attachment stabilization, as chromosomes travel along microtubules to congress to the spindle equator (Cai et al., 2009; Kapoor et al., 2006; Magidson et al., 2011). We found that during prometaphase I (2.5 h after GVBD), kinetochores primarily interact laterally with microtubules, whereas late in metaphase I (6.5 h after GVBD) ~70% of kinetochores are stably attached (Fig. 16 B). These results are consistent with previous findings (Brunet et al., 1999; Gui and Homer, 2012; Kitajima et al., 2011), and suggest that a timing mechanism controls formation of stable end-on attachments during meiosis I.

Aurora B/C kinases and tension regulate K-MT attachments during meiosis I

Because it is not known how the timing of K-MT interactions is regulated, we tested whether known regulators of K-MT stability function in meiosis I in oocytes. Aurora B kinase, well established as a key regulator, destabilizes attachments by phosphorylating kinetochore proteins responsible for MT binding (Lampson and Cheeseman, 2011). To test this function of Aurora B in meiosis I, oocytes were matured for 5.5 h after GVBD to allow normal spindle formation, then treated with 20 μM

ZM447439, an inhibitor of Aurora B and C; Aurora C is a highly similar meiotic isoform. This concentration is the lowest that produces a significant decrease in histone-H3 phosphorylation after a 1 h treatment. We find that Aurora B/C inhibition stabilizes attachments with nearly 100% of kinetochores connected to cold-stable microtubule fibers (Fig. 17 A, B). This result shows that during meiosis I Aurora kinase activity destabilizes K-MT attachments as in mitosis.

Another well-known mechanism contributing to attachment stability is the presence of tension due to binding of microtubules emanating from opposite spindle poles (Nicklas, 1997). Cohesin proteins hold chromosomes together such that tension is generated when microtubules pull on kinetochores (Oliveira and Nasmyth, 2010). To test whether tension contributes to stabilizing attachments in oocytes, we prematurely activated separase, the protease responsible for removing cohesins. Two mechanisms independently inhibit separase: phosphorylation by CDK1 and inhibitory binding by securin (Ciosk et al., 1998; Huang and Hatcher, 2005; Stemmann et al., 2001). Co-injection of cRNA encoding the AA-separase mutant, in which both residues phosphorylated by CDK1 are mutated, together with a securin morpholino abolishes tension at MI by prematurely destroying chromosome cohesion (Chiang et al., 2011). We find fewer cold-stable attachments in oocytes with separated chromatids, which lack tension, compared to controls with intact cohesion at MI (Fig. 17 C, D). In addition, in the absence of tension, more kinetochores interact with microtubules laterally as expected at an earlier stage in spindle formation (Fig. 17 C, insets).

One mechanism by which tension stabilizes attachments is by reducing phosphorylation of Aurora B substrates at kinetochores. To test this relationship between tension and Aurora B/C activity during meiosis I, we abolished cohesion while simultaneously inhibiting Aurora B and C. Under these conditions K-MTs were stabilized to a level similar to that of control oocytes late in MI (Fig. 17 E, F; Fig. 16 B). These results indicate that established regulators of K-MT attachments, tension and Aurora B/C, likely play a role during meiosis I.

Meiotic CDK1 activity controls the timing of stable K-MT attachments

Although tension and Aurora B/C kinases contribute to regulating attachments in meiosis I, it is not clear how they would explain the timing of stable attachments. To test whether CDK1 activity could act as a timing mechanism, we measured histone H1-kinase activity *in vitro* with oocytes matured from GV stage to anaphase I (Fig. 21 A and Fig. 18 A). Histone-H1 kinase activity increases gradually and plateaus 5-6 h after GVBD, when K-MT attachments are stabilized (Fig. 16 B). To test if high CDK1 activity is required to stabilize attachments, we cultured oocytes in low concentrations of the CDK1 inhibitor RO-3306 (0.5 and 2μM) and followed their progress to anaphase I. These concentrations were chosen to partially inhibit CDK1 activity, as indicated by increased time to GVBD (Fig. 18 B), whereas full inhibition would prevent GVBD. Time from GVBD to chromosome alignment was only slightly affected by this partial inhibition of CDK1. However following chromosome alignment, the inhibitor-treated cells arrested for more than 6 h before proceeding to anaphase I, compared to ~3 h in control oocytes (Fig. 18 B and Fig. 22). Anaphase I onset may be delayed in CDK1-inhibited cells due to a delay in

stabilizing K-MT attachments, which would keep the spindle assembly checkpoint active longer.

To directly test if partial CDK1 inhibition delays K-MT attachment, we assessed attachments using the cold-stable microtubule assay. Control oocytes increased their stable attachments from 44% at early MI (4.5 h after GVBD) to 69% late in MI (6.5 h after GVBD). In contrast, CDK1-inhibited oocytes reached only 31% stable attachments at 4.5 h, similar to control oocytes at 2.5 h, and 48% by 6.5 h (Fig. 18 C-E). At 11 h, just before anaphase I, CDK1-inhibited oocytes still had fewer stable attachments than controls at 6.5 h (Fig. 18 F), suggesting that full CDK1 activity is required to stabilize attachments. In addition, the number of lateral K-MT interactions was consistently higher in oocytes treated with CDK1 inhibitor (Fig. 18 C-E). These results indicate that in oocytes with lower CDK1 activity, kinetochores are more likely to interact with microtubules laterally as in earlier stages of spindle formation, and stable end-on binding is delayed.

If the gradual increase in CDK1 activity acts as a timing mechanism to control K-MT interactions, we predict that a more rapid increase would lead to faster K-MT binding. To increase CDK1 activity, we over-expressed cyclin B in oocytes by microinjecting cRNA encoding cyclin B-GFP. We chose this approach because the gradual increase in cyclin B abundance during meiosis I mirrors CDK1 activity levels (Hampl and Eppig, 1995), suggesting that cyclin B limits CDK1 activity. The *in vitro* histone-H1 kinase assay shows that CDK1 activity increases more rapidly in oocytes over-expressing cyclin B compared to control oocytes (Fig. 21 B and Fig. 19 A). In

addition, maximal CDK1 activity is higher in oocytes over-expressing cyclin B. We were unable to find a level of cyclin B over-expression that would result in a similar rapid increase in histone-H1 kinase activity without also increasing the maximal kinase activity. The premature increase in CDK1 activity stabilizes K-MT attachments, with 75% of kinetochores binding cold-stable microtubules at 4.5 h after GVBD (early metaphase I) – a level similar to control oocytes at late metaphase I (6.5 h after GVBD) (Fig. 19 B-D). Consistent with early attachment stabilization, MAD2 disappears from kinetochores by 4.5 h after GVBD in oocytes injected with cyclin B cRNA (Fig. 23 A, B) (Lane et al., 2012; Wassmann et al., 2003; Waters et al., 1998). Moreover, prematurely increasing CDK1 activity resulted in stable attachment of nearly all kinetochores at 6.5 h (Fig. 19 B, D). We achieved a similar increase in H1-kinase activity (Fig. 21 C, D) and attachment stabilization by co-injecting a lower amount of cRNA encoding cyclin B together with cRNA encoding CDK1, neither of which on their own increased either H1-kinase activity or attachment stabilization. These results show that we can manipulate K-MT attachments by either reducing or prematurely increasing CDK1 activity.

As potential downstream CDK1 effectors that might contribute to stabilizing K-MTs, we considered TPX2 and HURP, both of which accumulate on kinetochore fibers during progression through MI (Breuer et al., 2010; Brunet et al., 2008; Koffa et al., 2006; Ma et al., 2011; Silljé et al., 2006; Wong and Fang, 2006). A premature increase in CDK1 activity led to HURP enrichment on kinetochore fibers earlier than in control oocytes (Fig. 23 D), whereas TPX2 localization was not strongly affected (Fig. 23 C).

CDK1 activity may directly regulate HURP binding to K-MTs, or the difference in localization may reflect the higher number of stable K-MTs available for HURP to bind.

It may be beneficial for oocytes to delay K-MT stabilization until late in MI to minimize improper attachments in the context of a multipolar spindle. We predicted that early attachment stabilization due to a premature increase in CDK1 activity would result in increased incidence of lagging chromosomes at anaphase I as a result of incorrect attachments. We injected oocytes with cRNAs encoding cyclin B to increase CDK1 activity and histone H2B-mCherry to label chromosomes. Levels of cyclin B over-expression that prematurely increase CDK1 activity also arrest oocytes at MI as previously described (Ledan et al., 2001), likely because high cyclin B levels overwhelm the proteosomal degradation machinery. To allow cyclin B degradation, we blocked translation at 6.5 hrs, when spindle formation is complete in both control and cyclin B over-expressing oocytes, using the translation inhibitor cycloheximide. Under these conditions, anaphase I occurs with normal timing at 7-10 h after GVBD. We counted lagging chromosomes during anaphase I by live imaging of H2B-mCherry. Anaphases with lagging chromosomes were frequent in oocytes co-injected with cyclin B (63%) compared to control oocytes (12%) (Fig. 20 A, B), consistent with premature stabilization of incorrect attachments early in metaphase I.

DISCUSSION

We address the question of how the timing of K-MT attachment is regulated during meiosis I in oocytes. We are able to manipulate the timing of K-MT attachments by altering meiotic CDK1 activity: partial CDK1 inhibition delays attachments, and a premature increase in kinase activity stabilizes attachments early and leads to lagging chromosomes at anaphase I. We conclude that the slow increase in CDK1 activity in meiosis I acts as a timing mechanism to delay stabilization of attachments and prevent segregation errors.

Preventing K-MT stabilization early in MI, in the presence of multipolar spindle intermediates and multiple MTOCs around the chromosomes, serves as a strategy to promote the formation of correctly bi-oriented attachments late in MI (Fig. 20 C). Other mechanisms also increase the likelihood of correct bi-orientation. For example, positioning chromosomes at the spindle equator during prometaphase, through lateral interactions between kinetochores and microtubules, promotes kinetochore capture by MTs emanating from opposite spindle poles (Cai et al., 2009; Kapoor et al., 2006; Kitajima et al., 2011; Magidson et al., 2011). This initial chromosome positioning, together with the CDK1-dependent K-MT attachment delay described here, optimizes bi-orientation when stable end-on attachments do form.

Mechanisms that ensure formation of correct attachments are especially important during meiosis I, which is notoriously prone to chromosome segregation errors (Hassold and Hunt, 2009). The spindle assembly checkpoint (SAC) should prevent these errors by

delaying anaphase until all chromosomes achieve bi-orientation. Although the SAC is functional in meiosis I (Hached et al., 2011; Homer et al., 2005; Li et al., 2009; McGuinness et al., 2009; Niault et al., 2007; Wei et al., 2010), it is silenced late in metaphase I despite the presence of multiple misaligned chromosomes because these chromosomes do make stable attachments (Gui and Homer, 2012; Kolano et al., 2012; Lane et al., 2012). Our findings suggest that meiosis I is error-prone because the SAC is silenced when attachments – whether correct or not – are stabilized by high CDK1 activity late in MI.

In addition to CDK1 activity, other factors may contribute to the timing of attachment stabilization in oocytes. We show here that tension and Aurora B/C kinases contribute to regulation of attachments in MI, and a decrease in Aurora kinase activity or an increase in phosphatase activity may regulate attachment timing. Another potential regulator is the APC/C activator CDH1, as attachments are stabilized early in an oocyte-specific CDH1 knockout (Holt et al., 2012).

The downstream effectors for regulation of K-MT attachments by CDK1 are unknown. As a master-regulator of meiosis progression, CDK1 phosphorylates many substrates that play a role in K-MT interactions. For example, CDK1 phosphorylation of the chromosome passenger complex regulates Aurora B localization to centromeres (Tsukahara et al., 2010). Phosphorylation by CDK1 is also required for proper function of MAP-4, a MT-associated protein important for MT stability (Aizawa et al., 1991), and MT plus-end tracking proteins Clip-170 (Yang et al., 2009) and CLASP2 (Maia et al., 2012). In addition, CDK1 phosphorylates known regulators of K-MT interactions such

as BubR1 and Mps1 (Jaspersen and Winey, 2004; Morin et al., 2012; Wong and Fang, 2007), and BubR1 phosphorylation recruits B56-PP2A phosphatase to kinetochores, which may stabilize attachments by counteracting Aurora B activity (Kruse et al., 2013). An important goal for future work is to determine which CDK1 targets regulate the timing of K-MT attachments in oocytes.

MATERIALS AND METHODS

Oocyte collection, culture, and microinjection

CF-1 mice (Harlan) were used for all experiments described here. Prior to oocyte collection 6 to 12 week-old female mice were hormonally primed with eCG. GV-intact oocytes were collected and micro-injected in bicarbonate-free minimal essential medium with polyvinylpyrrolidone and Hepes (MEM-PVP) and cultured in Chatot-Ziomek-Bavister (CZB) medium in an atmosphere of 5% CO_2 in air at 37 °C. Meiotic resumption was inhibited by addition of 2.5μM milrinone (Sigma Aldrich), or 10 μM RO-3306 (EMD Millipore) in cyclin B-GFP over-expression experiments. Milrinone or RO-3306 were subsequently washed out to allow meiotic resumption. All animal experiments were approved by the institutional animal use and care committee and were consistent with the National Institutes of Health (NIH) guidelines. The Aurora B/C inhibitor ZM447439 was used at 20 μM and the CDK1 inhibitor RO-3306 at 0.5 or 2 μM.

Oocytes were micro-injected in MEM-PVP medium with a Narishige micromanipulator and a Medical Systems Corp. picoinjector; each oocyte was injected

with 10 pL. The microinjected oocytes were then incubated for 1 hr at 37°C in a humidified atmosphere of 5% CO, in air.

The following cRNA was used for microinjection - H2B-mCherry (human histone H2B coding sequence with mCherry tag at the C-terminus), GFP, or cyclin B-GFP at 700ng/μL (human cyclin B1 cRNA was generated by amplifying *Ccnb1* lacking the first 270 bp, with a GFP tag at the C-terminus) generated previously (Schindler and Schultz, 2009). In Fig. 19 C and D, cyclin B over-expression results were combined with data obtained from co-injection of cRNA encoding CDK1-mCherry with a low level of cRNA encoding cyclin B-GFP (200ng/μL). The CDK1-mCherry plasmid was generated by inserting the mouse *CDC2* into the C-terminal mCherry-pIVT plasmid described previously (Igarashi et al., 2007), and cRNA was synthesized using the TranscriptAid T7 High Yield Transcription Kit (Thermo Fisher Scientific). To destroy cohesion at metaphase I, cRNA encoding AA-separase mutant (constructed by mutating both CDK1 phosphorylation sites, S1121A and T1342A, in a full-length mouse separase (Espl1) cDNA clone (Source BioScience) using the Quikchange Multi Site-Directed Mutagenesis kit, generated previously (Chiang et al., 2011) and securin morpholino (MO) were micro-injected into GV-intact oocytes. Following micro-injection oocytes were incubated for 16-18 hours to allow protein expression.

Cold-stable microtubule assay and immunocytochemistry

To depolymerize unstable microtubules, oocytes were placed in ice-cold MEM-PVP medium for 10 min, followed by fixation and immunocytochemistry. Oocytes were fixed in freshly prepared 2% paraformaldehyde with 0.1% Triton-X100 for 30 min at

room temperature, then placed in blocking solution (PBS containing 0.3% BSA and 0.01% Tween-20) overnight, then permeabilized in PBS with 0.3% bovine serum albumin (BSA) and 0.1% Triton X-100 for 15 min, then washed in blocking solution prior to antibody staining. Human CREST autoimmune serum (1:40 dilution, Immunovision, Springdale, AZ) and rabbit beta-tubulin (9F3) monoclonal antibody conjugated to Alexa Fluor-488 (1:75 dilution, Cell Signaling Technologies) were used to label centromeres and MTs, respectively. After a 1 h incubation with primary antibodies, cells were washed 3 times, 15 min each wash. The CREST primary antibody was detected using an Alexa Fluor 594-conjugated goat anti-human secondary antibody (Invitrogen, Carlsbad, CA). Cells were again washed and mounted in Vectashield with Bisbenzimide Hoechst 33342 (Sigma Aldrich) to visualize chromosomes.

Confocal images were collected as Z-stacks at 0.3 μm intervals to visualize the entire meiotic spindle at room temperature using a spinning disc confocal microscope (DMI4000 B; Leica) equipped with a 100X 1.4 NA oil-immersion objective, an XY piezo Z stage (Applied Scientific Instrumentation), a spinning disk confocal scanner (Yokogawa), an electron multiplier charge-coupled device camera (Hamamatsu Photonics, ImageEM C9100-13), and an LMM5 laser merge module with 488 and 593 nm diode lasers (Spectral Applied Research) controlled by Metamorph (MDS Analytical Technologies) software. The Subtract Background tool of ImageJ (NIH) with 20 pixel radius was used for image presentation. To classify kinetochore attachments, the CREST channel was used to select a centromere while blind to MTs, then its attachment status

was scored around the same Z-plane using the merged 2-color confocal stack of CREST and microtubule images.

MAD2, HURP, and TPX2 were stained using the immunocytochemistry protocol described above. The rabbit polyclonal antibody raised against human MAD2 (Kops et al., 2005), a gift from Dr. Beth Weaver, was used at 1:200 dilution. To quantify MAD2 levels at kinetochores, MAD2 intensity was measured only where it co-localized with CREST and normalized by the CREST signal intensity for every cell. The rabbit immune serum raised against the human TPX2 (Brunet et al., 2008), a gift from Dr. Oliver Gruss, was used at 1:500 dilution. The rabbit polyclonal antibody raised against mouse HURP (Santa Cruz Biotechnologies) was used at 1:200 dilution.

Histone-H1 kinase assay

Oocytes were collected and cultured as described above for the amount of time indicated then immediately frozen in kinase lysis buffer. The histone-H1 kinase reaction was initiated by the addition of 5 µl of kinase buffer (24 mM p-nitrophenyl phosphate, 90 mM β- glycerophosphate, 24 mM MgCl2, 24 mM EGTA, 0.2 mM EDTA, 4.6 mM sodium orthovanadate, 4 mM NaF, 1.6 mM dithiothreitol, 60 µg/ml aprotinin, 60 µg/ml leupeptin, 2 mg/ml polyvinyl alcohol, 2.2 µM protein kinase A inhibitor peptide (Sigma), 40 mM 3-(n- morpholino) propanesulfonic acid (MOPS), pH 7.2, 0.6 mM ATP, 2 mg/ml histone (type III-S, Sigma)) with 500 µCi/ml [γ-32P]ATP (3000 Ci/mmol; Amersham). To determine the background level of phosphorylation for histone-H1, 5 µl of double kinase lysis buffer was added instead of oocyte lysate. The reaction was conducted for 30 minutes at 30°C and terminated by the addition of 10 µl double-strength concentrated

SDS-PAGE sample buffer and boiling for 3 minutes. Following SDS-PAGE, the 15% gel was fixed in 10% acetic acid/30% methanol, dried and exposed to a phosphorimager screen for 16 to 24 hours. Gel images were detected on a Typhoon 9410 PhosphoImager (GE Healthcare) and band intensities were quantified using ImageJ software (NIH). CDK1 activity was assessed by the phosphorylation status of histone-H1 based on the phosphoimager gel results. Control lanes (lysis buffer with no lysate) were used for background subtraction. Representative experiments are shown and were repeated with similar results.

Live DIC and confocal imaging

To measure the timing of meiotic progression following partial CDK1 inhibition, oocytes were washed out of milrinone into CZB medium containing DMSO (1:1000) or 0.5 or 2 μM RO-3306 to allow GVBD but partially inhibit CDK1 activity. The oocytes were then placed in the same medium in a glass bottom dish coated with protamine sulfate (Sigma Aldrich) as previously described (Bornslaeger et al., 1986), which allows oocytes to attach to the glass. Differential interference contrast (DIC) images were acquired using a microscope (DMI6000 B; Leica) equipped with a 40X 1.25 NA oil-immersion objective, a charge-coupled device camera (Photometrics QuantEM, 512 SC) controlled by Metamorph (MDS Analytical Technologies) software, and a stage top incubator (ZILCS; Tokai Hit) heated at 37 ^{o}C with 5%CO_2. Oocytes were imaged by DIC from GVBD until anaphase I every 12 min as Z-stacks at 5 μm intervals to monitor time to GVBD, chromosome alignment, and polar body extrusion. Chromosome

alignment was defined as the first time when no misaligned chromosomes were apparent by DIC in any of the Z-planes.

To follow anaphase I progression live, oocytes were injected with cRNA encoding H2B-mCherry and cyclin B to increase CDK1 activity and label chromosomes, then incubated for 16-18 h to allow protein expression in 10 μM RO-3306. Because CDK1 activity was increased in these oocytes due to cyclin B over-expression, a CDK1 inhibitor was used to prevent spontaneous GVBD. At 6.5 h after GVBD, oocytes were placed in 10 μM cycloheximide to inhibit further cyclin B protein expression and allow anaphase I to progress normally. Oocytes were then placed in protamine sulfate-coated dishes into a heated environmental chamber (Incubator BL, Pecon GmBH) with a stage top incubator (DM IRB+IRE2) to maintain 5% CO_2 in air and 37^{o}C. Confocal images of H2B-mCherry were acquired every 3 min using the spinning disc confocal microscope described above with 63X 1.4 NA glycerol-immersion objective. Images were acquired as Z-stacks at 1μm intervals capturing all the chromosomes.

Figure 16

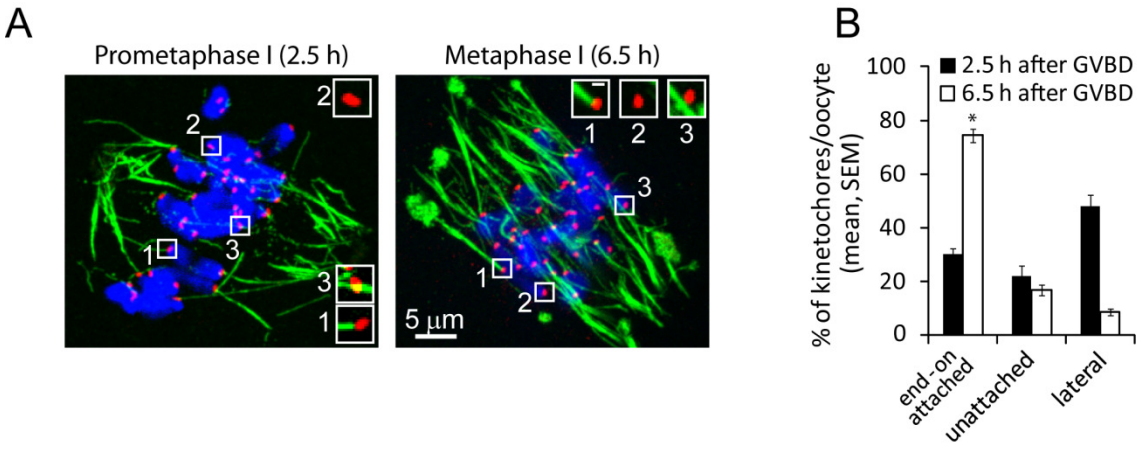

Figure 16. Stable K-MT attachment is delayed until late in Metaphase I. Oocytes were cultured for 2.5 h after GVBD to Prometaphase I or 6.5 h to Metaphase I, then analyzed for cold-stable microtubules. Images (A) are projections of confocal Z series showing microtubules (green), kinetochores (CREST, red), and DNA (blue). Individual kinetochores were classified as end-on attached (1), unattached (2) or lateral (3); insets are optical sections showing examples of each (scale bar 0.5 µm). The percent of kinetochores in each category was averaged over multiple cells ($n \geq 17$, 15 kinetochores per cell) at each time point (B, * $p<0.001$).

Figure 17

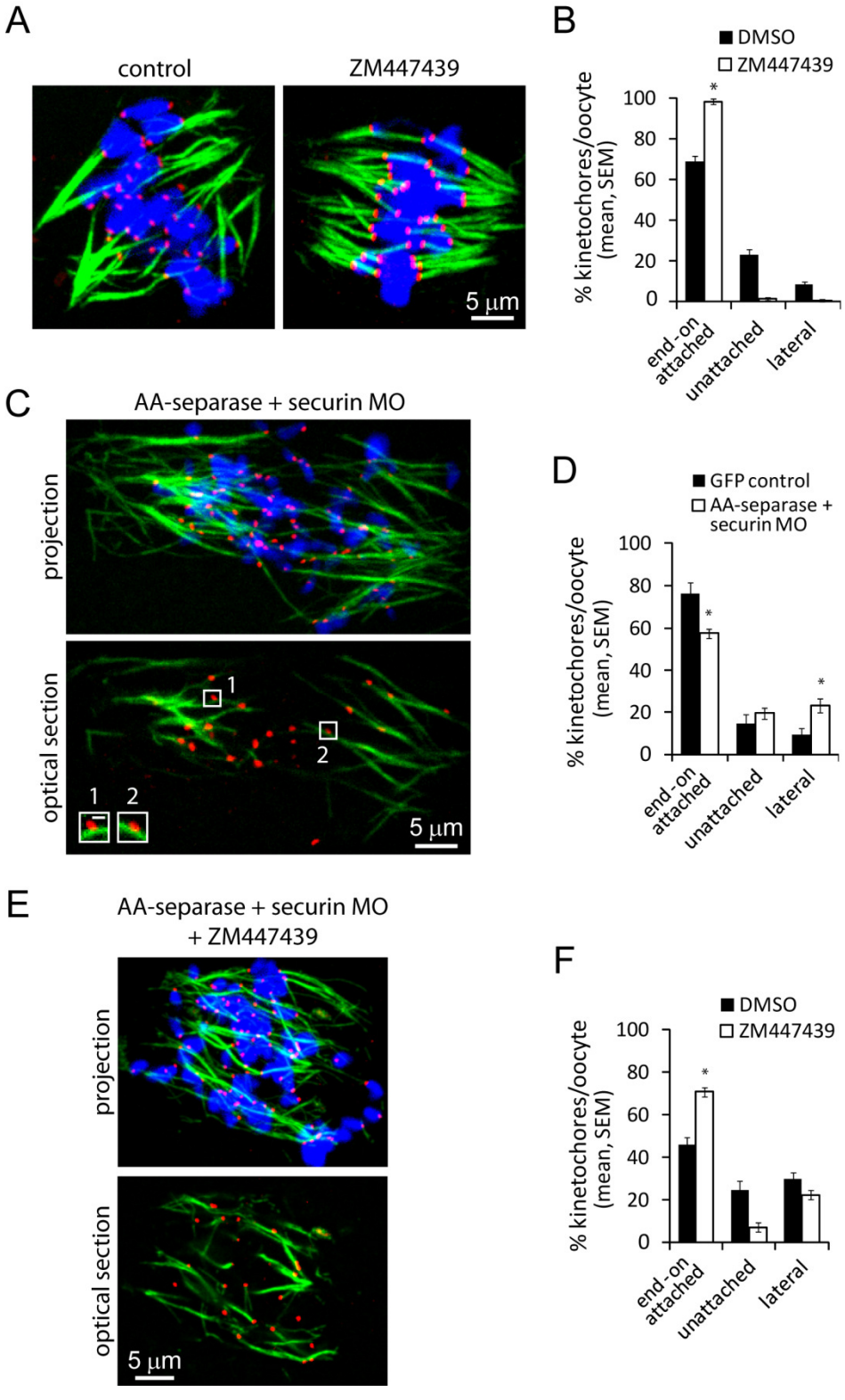
A
control
ZM447439
5 μm
B
DMSO
ZM447439
% kinetochores/oocyte (mean, SEM)
100
80
60
40
20
0
*
end-on attached
unattached
lateral
C
AA-separase + securin MO
projection
optical section
1
2
1
2
5 μm
D
GFP control
AA-separase + securin MO
% kinetochores/oocyte (mean, SEM)
100
80
60
40
20
0
*
*
end-on attached
unattached
lateral
E
AA-separase + securin MO + ZM447439
projection
optical section
5 μm
F
DMSO
ZM447439
% kinetochores/oocyte (mean, SEM)
100
80
60
40
20
0
*
end-on attached
unattached
lateral

Figure 17. Aurora B/C kinase activity and tension regulate K-MT attachments during meiosis I. (A, B) Oocytes were cultured for 5.5 h after GVBD, then treated with Aurora B/C inhibitor ZM447439 or DMSO (control) for 1 hour prior to analysis of cold-stable MTs. (C, D) Oocytes injected with AA-separase cRNA together with securin MO, or GFP cRNA as a control, were matured for 6.5 h after GVBD, then analyzed for cold-stable MTs. (E, F) Oocytes injected with AA-separase cRNA and securin MO were cultured for 5.5 h after GVBD, then treated with ZM447439 (or DMSO) for 1 h prior to analyzing cold-stable MTs. Only oocytes with complete chromatid separation were analyzed, indicating loss of cohesion. Images (A, C, E) are projections of confocal Z series showing microtubules (green), kinetochores (CREST, red), and DNA (blue). Insets (C) are optical sections showing lateral interactions, scale bar 0.5 μm. Percentages of end-on attached, unattached and lateral kinetochores were averaged over multiple cells ($n \geq 13$, ≥ 15 kinetochores per cell, * $p<0.001$).

Figure 18

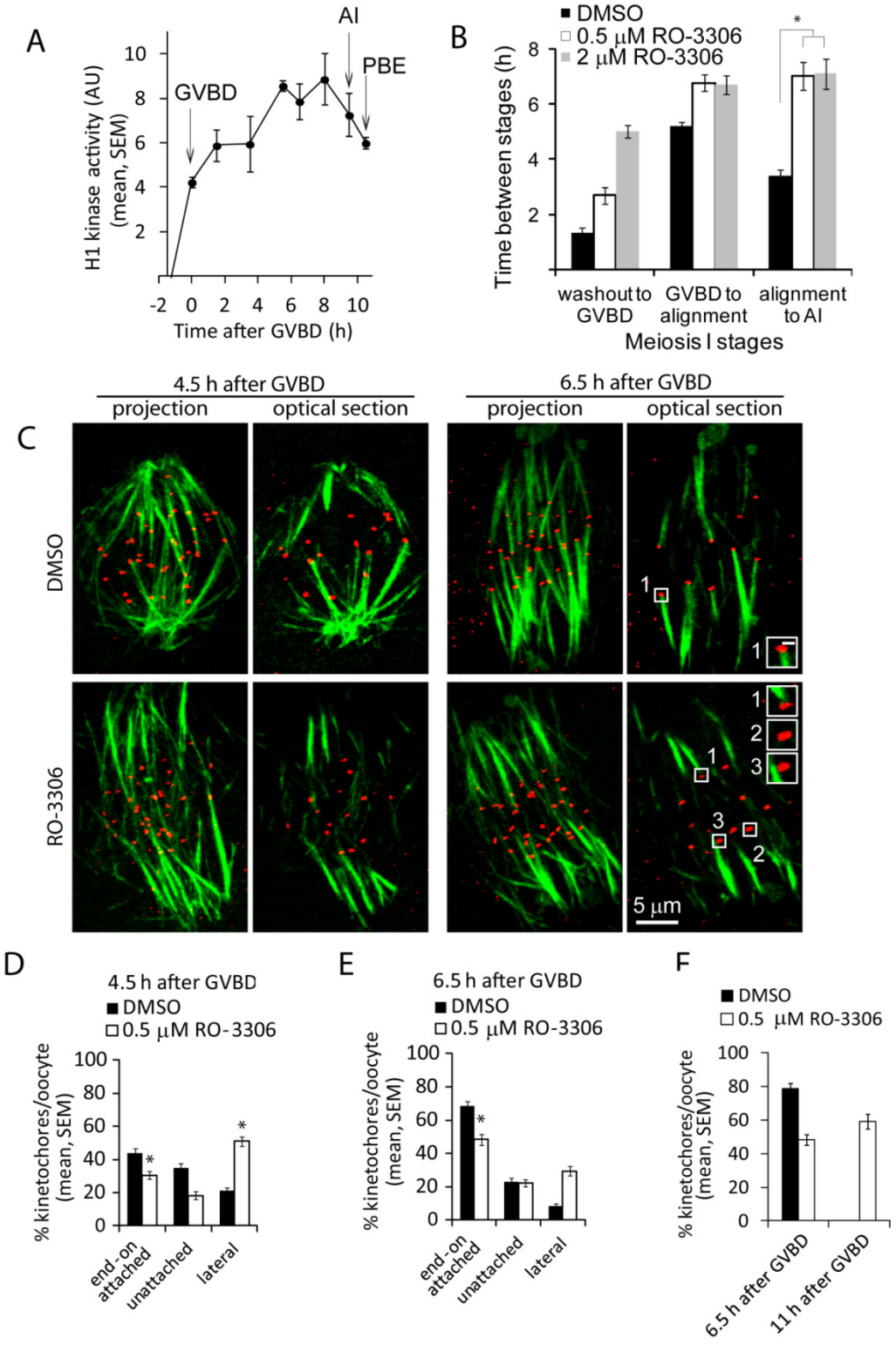
A
AI
PBE
GVBD
H1 kinase activity (AU) (mean, SEM)
Time after GVBD (h)
B
DMSO
0.5 μM RO-3306
2 μM RO-3306
Time between stages (h)
washout to GVBD
GVBD to alignment
alignment to AI
Meiosis I stages
C
4.5 h after GVBD
6.5 h after GVBD
projection
optical section
DMSO
RO-3306
5 μm
D
4.5 h after GVBD
DMSO
0.5 μM RO-3306
% kinetochores/oocyte (mean, SEM)
end-on attached
unattached
lateral
E
6.5 h after GVBD
DMSO
0.5 μM RO-3306
% kinetochores/oocyte (mean, SEM)
end-on attached
unattached
lateral
F
DMSO
0.5 μM RO-3306
% kinetochores/oocyte (mean, SEM)
6.5 h after GVBD
11 h after GVBD

Figure 18. Partial CDK1 inhibition slows stabilization of attachments. (A) Histone-H1 kinase activity was measured in oocytes at the indicated time points relative to GVBD. Each data point represents H1 phosphorylation averaged over 3 lysates, each with 3 oocytes. Arrows indicate time of GVBD, anaphase I (AI), and first polar body extrusion (PBE). (B) Oocytes were matured with low concentrations of CDK1 inhibitor RO-3306 (0.5 and 2 μM) or DMSO (control). Meiosis I progression from GV to AI was followed live by DIC microscopy. Times from milrinone washout to GVBD, GVBD to chromosome alignment, and alignment to anaphase I were averaged over multiple cells ($n \geq 18$). (C-F) Oocytes were cultured with 0.5 μM RO-3306 or DMSO for 4.5, 6.5, or 11 h after GVBD, then analyzed for cold stable MTs. Images (C) are projections of confocal Z series or optical sections showing microtubules (green) and kinetochores (CREST, red). Insets show individual kinetochores classified as attached (1), unattached (2) or lateral (3), scale bar 0.5 μm. Percentages of each attachment state were averaged over multiple cells ($n \geq 23$, 15 kinetochores per cell, $*p<0.001$) at each time point.

Figure 19

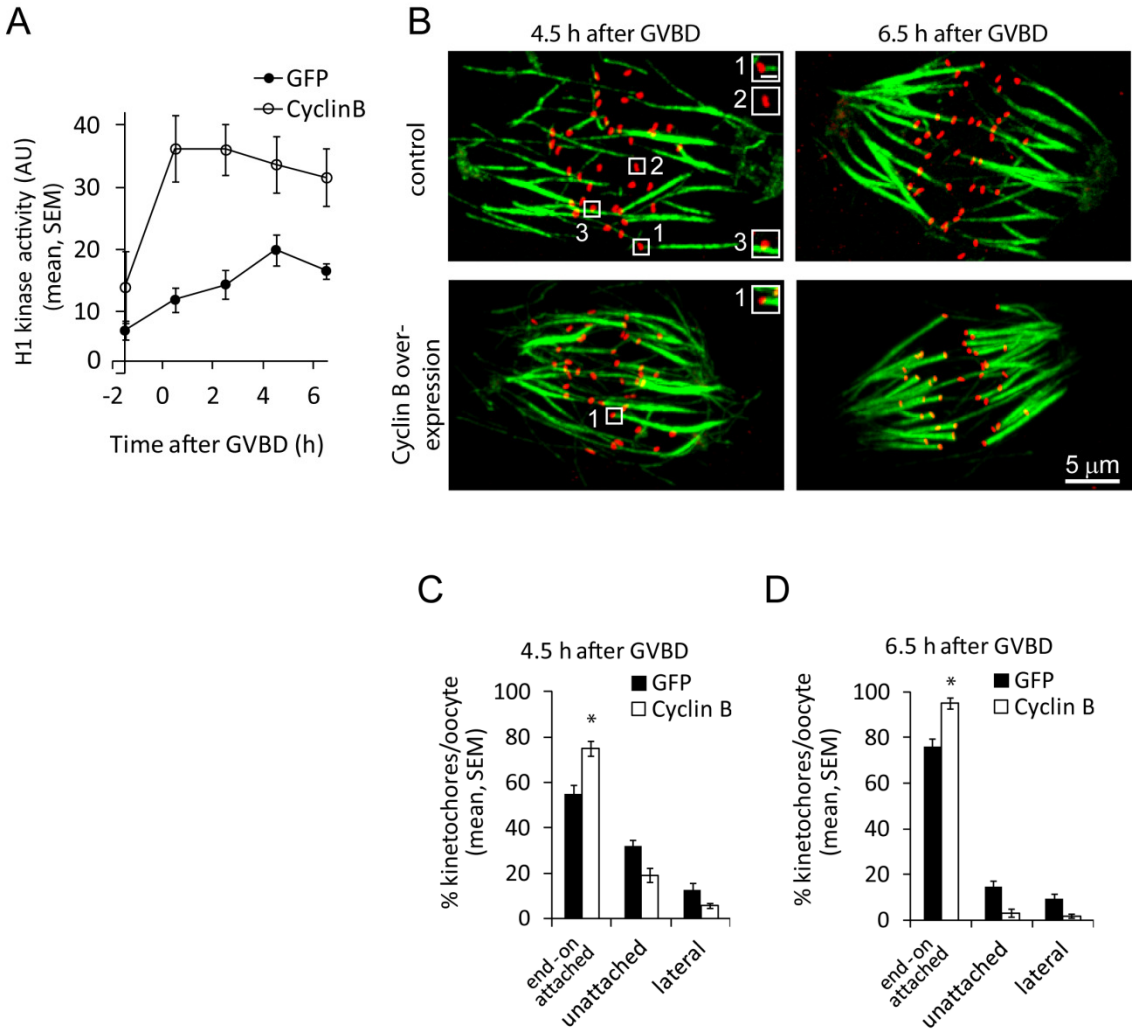
A
GFP
CyclinB
H1 kinase activity (AU)
(mean, SEM)
40
30
20
10
0
-2
0
2
4
6
Time after GVBD (h)
B
4.5 h after GVBD
6.5 h after GVBD
control
Cyclin B over-
expression
1
2
3
5 μm
C
4.5 h after GVBD
% kinetochores/oocyte
(mean, SEM)
GFP
Cyclin B
100
80
60
40
20
0
*
end-on
attached
unattached
lateral
D
6.5 h after GVBD
% kinetochores/oocyte
(mean, SEM)
GFP
Cyclin B
100
80
60
40
20
0
*
end-on
attached
unattached
lateral

Figure 19. Prematurely increasing CDK1 activity stabilizes K-MT attachments. (A, B) Oocytes injected with GFP cRNA or cyclin B-GFP cRNA (700 ng/μL) were analyzed for histone-H1 kinase activity (A) or cold-stable MTs (B) at the indicated time points. H1 kinase activity (A) was averaged over 3 lysates, each with 1 oocyte. Images (B) are projections of confocal Z series showing microtubules (green) and kinetochores (CREST, red). Insets show individual kinetochores classified as attached (1), unattached (2) or lateral (3), scale bar 0.5 μm. Injecting lower levels of cyclin B-GFP cRNA (200 ng/μL) together with CDK1 cRNA gave similar results in both the H1 kinase and cold-stable MT assays. (C, D) Percentages of each attachment state were averaged over multiple cells ($n \geq 22$, 15 kinetochores per cell, $*p<0.001$) at each time point. Results of the cold-stable MT assay were combined for oocytes injected with cyclin B-GFP cRNA (700 ng/μL) or CDK1 cRNA together with lower levels cyclin B-GFP cRNA (200ng/μL).

Figure 20

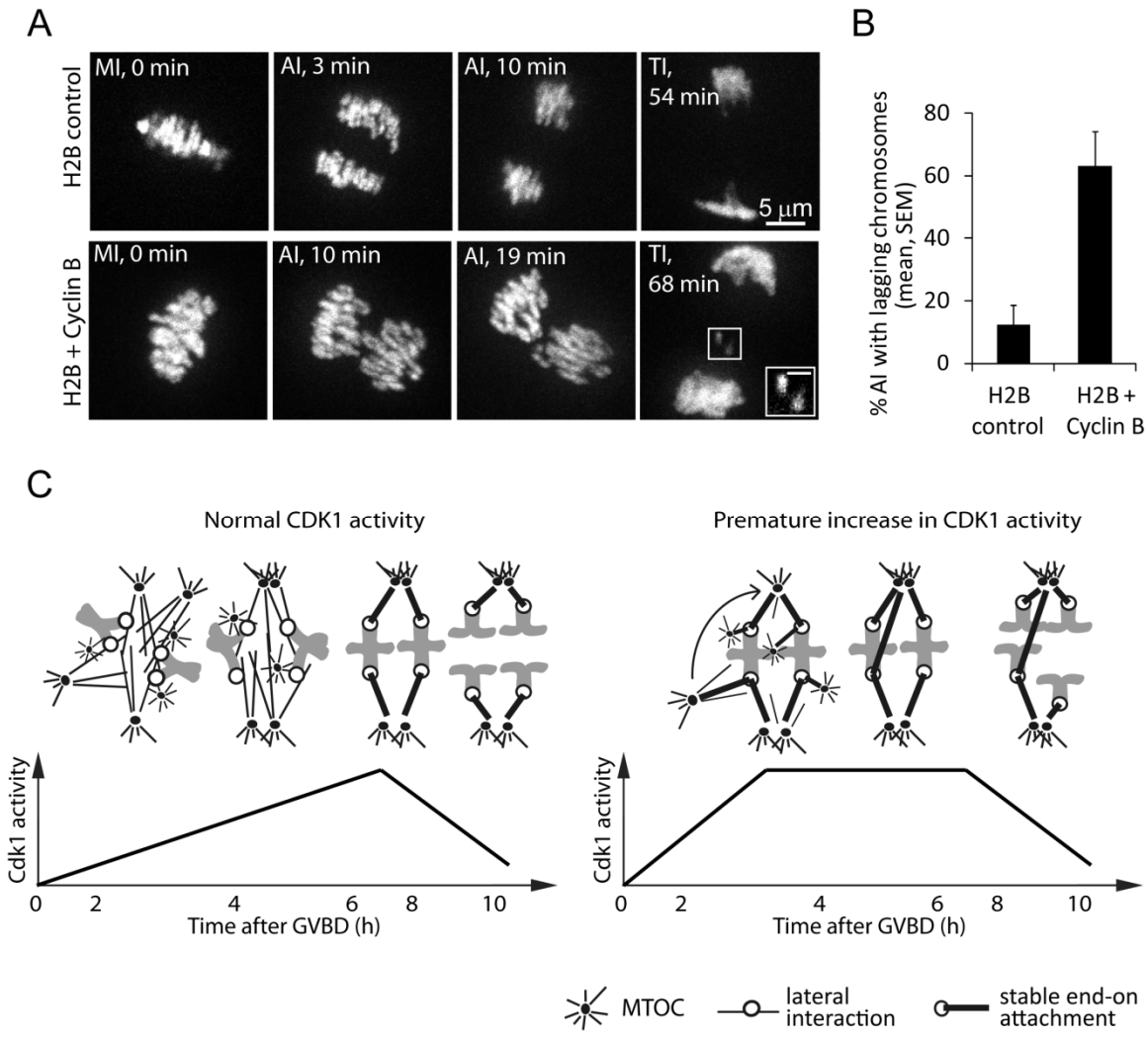
A
H2B control
MI, 0 min
AI, 3 min
AI, 10 min
TI, 54 min
5 μm
H2B + Cyclin B
MI, 0 min
AI, 10 min
AI, 19 min
TI, 68 min
B
% AI with lagging chromosomes (mean, SEM)
80
60
40
20
0
H2B control
H2B + Cyclin B
C
Normal CDK1 activity
Premature increase in CDK1 activity
Cdk1 activity
0
2
4
6
8
10
Time after GVBD (h)
MTOC
lateral interaction
stable end-on attachment

Figure 20. Prematurely increasing CDK1 activity leads to lagging chromosomes at Anaphase I. (A, B) Oocytes microinjected with H2B-mCherry cRNA, with or without cyclin B-GFP cRNA, were cultured for 6.5 h after GVBD, incubated with 10 μM cycloheximide to allow normal anaphase I progression, and imaged live from MI through telophase I (TI). Images (A) are maximal intensity projections of confocal Z-series showing all the chromosomes (time stamps relative to anaphase onset). Inset shows lagging chromosomes at anaphase (brightness increased for clarity, scale bar 2 μm). The percentage of anaphases with lagging chromosomes was averaged over three independent experiments ($n \geq 5$ cells per experiment, $*p<0.001$). (C) Model schematic depicts the timing of K-MT stabilization when CDK1 activity rises normally (left panel) vs. prematurely (right panel) during MI. Normally, kinetochores interact with MTs laterally to achieve chromosome congression, and attachments are stabilized ~7 h after GVBD when CDK1 activity is maximal (left). If K-MT attachments are stabilized too early, in the presence of multipolar spindle intermediates and multiple MTOCs close to the chromosomes, incorrect attachments can lead to lagging chromosomes at AI (right).

Figure 21

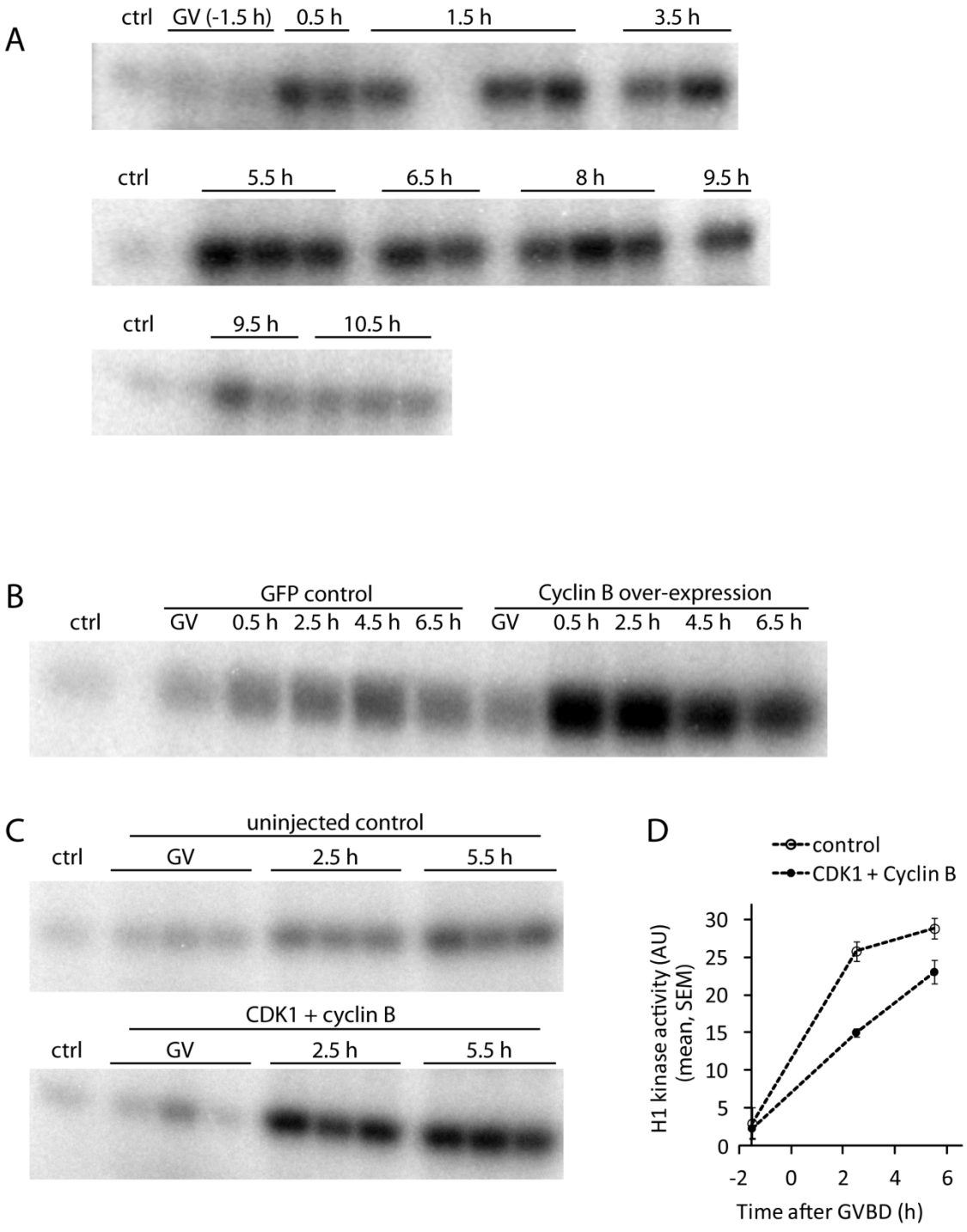
A
ctrl
GV (-1.5 h)
0.5 h
1.5 h
3.5 h
ctrl
5.5 h
6.5 h
8 h
9.5 h
ctrl
9.5 h
10.5 h
B
GFP control
Cyclin B over-expression
ctrl
GV
0.5 h
2.5 h
4.5 h
6.5 h
GV
0.5 h
2.5 h
4.5 h
6.5 h
C
uninjected control
ctrl
GV
2.5 h
5.5 h
CDK1 + cyclin B
ctrl
GV
2.5 h
5.5 h
D
control
CDK1 + Cyclin B
H1 kinase activity (AU)
(mean, SEM)
30
25
20
15
10
5
0
-2
0
2
4
6
Time after GVBD (h)

Figure 21. Histone H1-kinase assay gels. Histone-H1 kinase assay was performed at the indicated timepoints relative to GVBD. (A) Each lane represents histone-H1 phosphorylation in a lysate from 3 oocytes. Control lanes contained lysis buffer only with no oocytes. For quantitation, intensities of the three bands at each timepoint were averaged after subtracting the control intensity (Fig. 18 A). (B-D) Oocytes were injected with either a high concentration of cyclin B-GFP cRNA (700 ng/μL) or a low concentration of cyclin B-GFP cRNA (200 ng/μL) together with CDK1 cRNA. Time points are relative to GVBD. Each lane represents a lysate from a single oocyte; control lanes contained lysis buffer only with no oocytes. (B) Representative gel showing histone-H1 phosphorylation in oocytes injected with GFP or cyclin B-GFP cRNA (700 ng/μL). Values obtained from three such gels were averaged, after subtracting the control, to quantify the average histone-H1 kinase activity at each time point (single oocyte per lane, n = 3 for every data point). (C, D) Results of a histone-H1 kinase assay performed in uninjected control oocytes or oocytes co-injected with CDK1 cRNA and a low level of cyclin B cRNA (200 ng/μL). Values were averaged over the three lanes

Figure 22

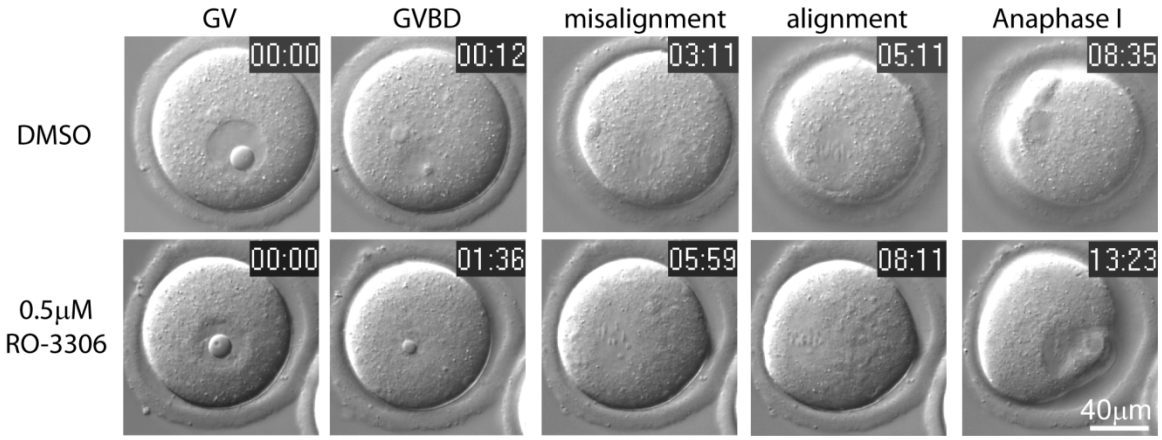

Figure 22. Representative DIC images of meiosis I progression in control and CDK1-inhibited oocytes. DIC microscopy was used to follow oocyte maturation at 12 min intervals and assess the timing of GVBD, chromosome alignment, and anaphase I. Representative images of oocytes maturing from GV to anaphase I in DMSO or CDK1 inhibitor RO-3306 are representative of the meiotic hallmarks observed. Time of GVBD was indicated by disappearance of the germinal vesicle, chromosome alignment was scored as the first time when no misaligned chromosomes were apparent, and the first instance of chromosome separation was defined as anaphase I. Time stamps indicate the time elapsed from the start of imaging after milrinone washout, but before GVBD. The quantitative results are shown in Fig. 18 B.

Figure 23

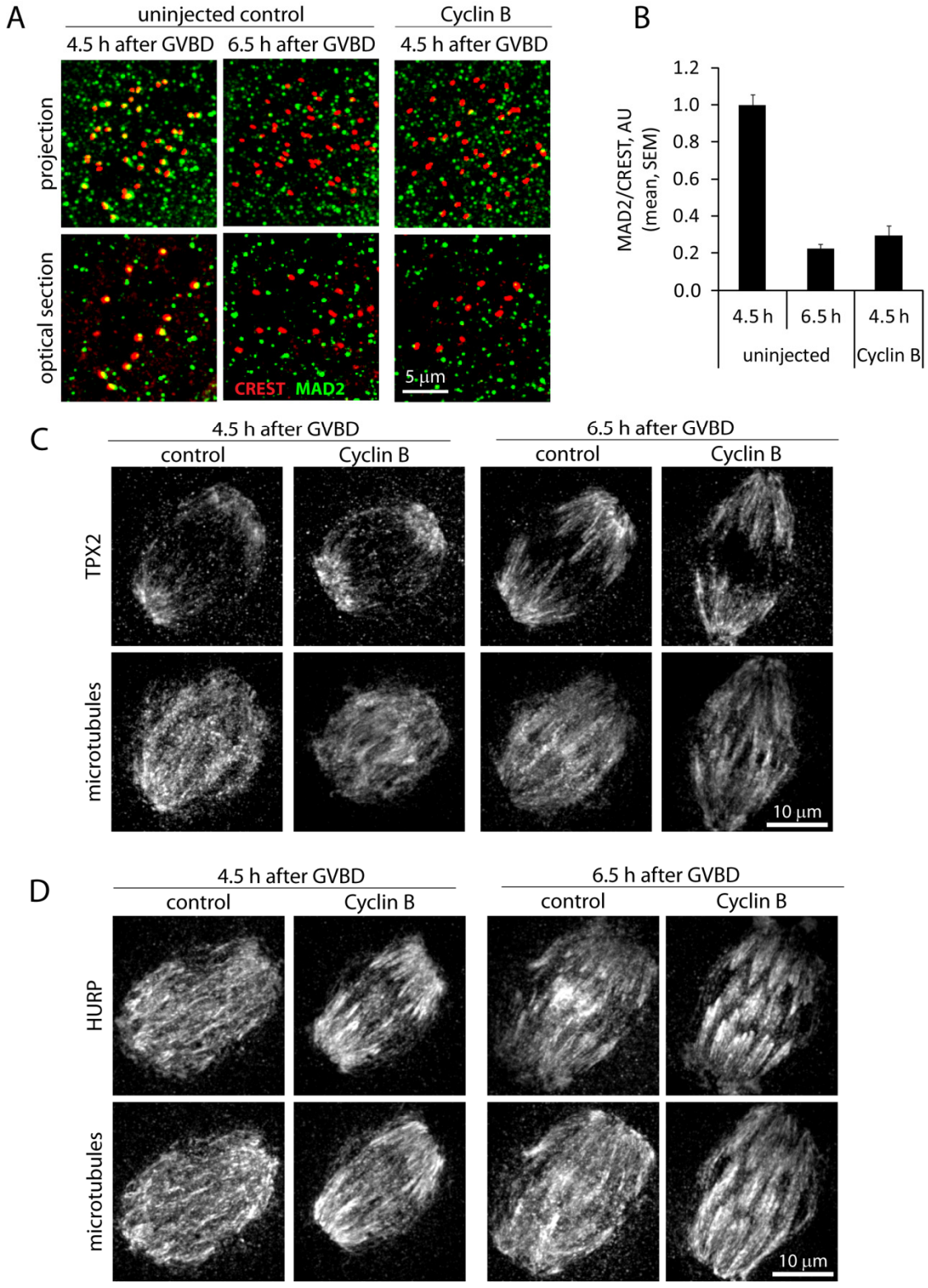
A
uninjected control
Cyclin B
4.5 h after GVBD
6.5 h after GVBD
4.5 h after GVBD
projection
optical section
CREST MAD2
5 μm
B
MAD2/CREST, AU (mean, SEM)
1.2
1.0
0.8
0.6
0.4
0.2
0.0
4.5 h
6.5 h
4.5 h
uninjected
Cyclin B
C
4.5 h after GVBD
6.5 h after GVBD
control
Cyclin B
control
Cyclin B
TPX2
microtubules
10 μm
D
4.5 h after GVBD
6.5 h after GVBD
control
Cyclin B
control
Cyclin B
HURP
microtubules
10 μm

Figure 23. Localization of MAD2, HURP and TPX2 proteins in control and cyclin B cRNA-injected oocytes. At 4.5 or 6.5 h after GVBD, oocytes were fixed and stained for MAD2 and CREST (A), TPX2 and tubulin (C), or HURP and tubulin (D). (A) Top panels are projections of confocal Z series showing MAD2 (green) and CREST (red); bottom panels are optical sections. (B) The ratio of MAD2/CREST intensity was quantified at centromeres identified by CREST signal, averaged over multiple cells, and normalized to the Mad2/CREST ratio at 4.5 h in control oocytes ($n \geq 10$). (C, E) Images are projections of confocal Z series of TPX2 or HURP, together with spindle microtubules. ≥10 cells were imaged in each group, and representative images are shown.

CHAPTER 4

Conclusions and Future Directions

The purpose of this dissertation is to describe the meiosis-specific adaptations of Aurora B kinase and CDK1 – two major regulators of mitosis. These mitotic kinases have taken on a number of functions to help cells cope with the unique requirements of meiosis, namely the acentrosomal spindles and regulation of homologous chromosome cohesion. Some of these adaptations, which were described previously, are summarized in Chapter 1 of this dissertation. Chapters 2 and 3 contain my contributions to this field. The work described here was performed in mouse oocytes and preimplantation embryos and serves as a model for all known mammalian oocyte systems. Our understanding of the oocyte meiosis is especially crucial, because abnormal meiosis progression may produce an aneuploid egg, which can give rise to an abnormal pregnancy.

AURKC compensates for loss of AURKB protein in oocytes and embryos

To investigate the requirement for AURKC expression in germ cells, the AURKC knock-out mouse model was used. This was necessary, because sequence and functional similarities between AURKB and AURKC rendered inhibitor studies inconclusive, as most Aurora kinase inhibitors are likely to affect both homologs (Gautschi et al., 2008; Lane et al., 2010; Shuda et al., 2009; Swain et al., 2008; Vogt et al., 2008). The AURKC knock-out mice were subfertile, suggesting that the presence of AURKC is important. Indeed, the effect of missing AURKC on meiosis progression was detrimental, with knock-out oocytes having more misaligned chromosomes and delayed anaphase I progression. However, somewhat surprisingly, no effect of AURKC knock-out on egg ploidy was observed. After fertilization, the effect of AURKC knock-out on early embry development was more pronounced. Fewer and fewer embryos reached developmental

stages between 2-cell and blastocyst, likely because of defects such as cytokinesis failure, which are characteristic of AURKB deletion/inhibition.

The fact that AURKC knock-out phenotypes became more pronounced between meiosis and embryogenesis, prompted the investigation of degradation kinetics of AURKs in meiosis. As a result, AURKB was found to be degraded more rapidly than AURKC, which led to the conclusion that progressive loss of AURKB during meiosis necessitates the translational recruitment of its homolog AURKC to compensate for it. This was confirmed by the finding that both AURKB and AURKC could restore the knock-out phenotypes to wild-type levels, and is in agreement with previous studies (Fernández-Miranda et al., 2011; Sasai et al., 2004; Slattery et al., 2009). The reason behind the differences in destruction dynamics of these AURKs remains to be found. While the role of the destruction sequences present in the N-terminus of AURKB, but not AURKC (D-box and KEN-box), was tested, they were not found to have an effect on AURKB degradation dynamics. Therefore, this difference in degradation between the two AURKs remains to be investigated.

Also of interest is the localization of AURKC during meiosis in oocytes. AURKB is mostly found at centromeres during metaphase of mitosis and meiosis. However, AURKC localizes all over chromosomes during meiosis I. What dictates this localization and whether it has a functional significance is unknown. However, because the role of AURKs in meiotic cohesion regulation has been demonstrated in several organisms (Chapter 1), it would be interesting to test if AURKC plays a similar role in mammalian meiosis. It is possible that AURKC co-localization with bivalent arm

cohesins points to its involvement in their protection at metaphase I or cleavage at anaphase I.

CDK1 acts as a molecular clock that times K-MT attachments in meiosis I

While others have speculated that the slow increase in meiotic CDK1 activity may act as a timer for stabilization of K-MT attachments, this work for the first time demonstrates this. By modulating CDK1 activity via partial inhibition or premature activation, I was able to manipulate attachment timing. In addition to showing that high CDK1 activity is required for K-MT stabilization, this work also offers an insight into why attachments are delayed until late in metaphase I of meiosis. I observe that precocious attachment stabilization results in a drastic increase in lagging chromosomes at anaphase I. Given that acentrosomal spindle formation and bipolarity establishment is a prolonged process, which goes through several multipolar intermediates, I propose that it is beneficial to the oocyte to delay attachments until the spindle is truly bipolar and mistakes in biorientation can be avoided.

This result is also in line with our understanding of how the SAC functions in oocytes. The checkpoint is functional in meiosis I, because oocytes are able to arrest at metaphase I in response to SAC protein knock down and gross spindle perturbations like the use of microtubule poisons (Hached et al., 2011; Homer et al., 2005; Li et al., 2009; McGuinness et al., 2009; Wei et al., 2010). However, recent reports have shown that the checkpoint is unable to respond to single non-bioriented chromosomes, as it does in mitosis (Gui and Homer, 2012; Lane et al., 2012). Our results suggest that this is not

because of permissiveness of the meiotic SAC, but rather due to high CDK1 activity late in metaphase I, which somehow overrides checkpoint signaling to stabilize attachments regardless of their correctness. The role of CDK1 activity on attachment timing as well as its downstream targets remain to be investigated in other systems.

BIBLIOGRAPHY

Abe, Y., Okumura, E., Hosoya, T., Hirota, T. and Kishimoto, T. (2010). A single starfish Aurora kinase performs the combined functions of Aurora-A and Aurora-B in human cells. *Journal of cell science* **123**, 3978–88.

Adams, R. R., Maiato, H., Earnshaw, W. C. and Carmena, M. (2001). Essential roles of Drosophila inner centromere protein (INCENP) and aurora B in histone H3 phosphorylation, metaphase chromosome alignment, kinetochore disjunction, and chromosome segregation. *The Journal of cell biology* **153**, 865–80.

Aizawa, h, Kamijo, M., Ohba, M., Mori, A., Okuhara, K., Kawasaki, H., Murofushi, J., Suzuki, K. and Yasuda, H. (1991). Microtubule destabilization by cdcZ/Hl Histone kinase: Phosphorylation of a "Pro-rich region" in the microtubule-binding domain of MAP-4. *Biochemical and Biophysical Research Communications* **179**, 1620–1626.

Anger, M., Stein, P. and Schultz, R. M. (2005). CDC6 requirement for spindle formation during maturation of mouse oocytes. *Biology of reproduction* **72**, 188–94.

Avo Santos, M., Van de Werken, C., De Vries, M., Jahr, H., Vromans, M. J. M., Laven, J. S. E., Fauser, B. C., Kops, G. J., Lens, S. M. and Baart, E. B. (2011). A role for Aurora C in the chromosomal passenger complex during human preimplantation embryo development. *Human reproduction* **26**, 1868–81.

Baldini, E., Arlot-Bonnemains, Y., Sorrenti, S., Mian, C., Pelizzo, M. R., De Antoni, E., Palermo, S., Morrone, S., Barollo, S., Nesca, A., et al. (2011). Aurora kinases are expressed in medullary thyroid carcinoma (MTC) and their inhibition suppresses in vitro growth and tumorigenicity of the MTC derived cell line TT. *BMC cancer* **11**, 411.

Ben Khelifa, M., Zouari, R., Harbuz, R., Halouani, L., Arnoult, C., Lunardi, J. and Ray, P. F. (2011). A new AURKC mutation causing macrozoospermia: implications for human spermatogenesis and clinical diagnosis. *Molecular human reproduction* **17**, 762–8.

Bernard, P., Maure, J. F. and Javerzat, J. P. (2001). Fission yeast Bub1 is essential in setting up the meiotic pattern of chromosome segregation. *Nature cell biology* **3**, 522–6.

Blangy, a, Lane, H. a, d'Hérin, P., Harper, M., Kress, M. and Nigg, E. a (1995). Phosphorylation by p34cdc2 regulates spindle association of human Eg5, a kinesin-related motor essential for bipolar spindle formation in vivo. *Cell* **83**, 1159–69.

Bornslaeger, E. a, Mattei, P. and Schultz, R. M. (1986). Involvement of cAMP-dependent protein kinase and protein phosphorylation in regulation of mouse oocyte maturation. *Developmental biology* **114**, 453–62.

Breuer, M., Kolano, A., Kwon, M., Li, C.-C., Tsai, T.-F., Pellman, D., Brunet, S. and Verlhac, M.-H. (2010). HURP permits MTOC sorting for robust meiotic spindle bipolarity, similar to extra centrosome clustering in cancer cells. *The Journal of cell biology* **191**, 1251–60.

Brunet, S., Maria, A. S., Guillaud, P., Dujardin, D., Kubiak, J. Z. and Maro, B. (1999). Kinetochore fibers are not involved in the formation of the first meiotic spindle in mouse oocytes, but control the exit from the first meiotic M phase. *The Journal of Cell Biology* **146**, 1–12.

Brunet, S., Dumont, J., Lee, K. W., Kinoshita, K., Hikal, P., Gruss, O. J., Maro, B. and Verlhac, M.-H. (2008). Meiotic regulation of TPX2 protein levels governs cell cycle progression in mouse oocytes. *PloS one* **3**, e3338.

Cahu, J., Olichon, A., Hentrich, C., Schek, H., Drinjakovic, J., Zhang, C., Doherty-Kirby, A., Lajoie, G. and Surrey, T. (2008). Phosphorylation by Cdk1 increases the binding of Eg5 to microtubules in vitro and in Xenopus egg extract spindles. *PloS one* **3**, e3936.

Cai, S., O'Connell, C. B., Khodjakov, A. and Walczak, C. E. (2009). Chromosome congression in the absence of kinetochore fibres. *Nature cell biology* **11**, 832–8.

Carmena, M., Wheelock, M., Funabiki, H. and Earnshaw, W. C. (2012). The chromosomal passenger complex (CPC): from easy rider to the godfather of mitosis. *Nature reviews. Molecular cell biology* **13**, 789–803.

Chatot, C. L., Ziomek, C. A., Bavister, B. D., Lewis, J. L. and Torres, I. (1989). An improved culture medium supports development of random-bred 1-cell mouse embryos in vitro. *Journal of reproduction and fertility* **86**, 679–88.

Chen, J., Melton, C., Suh, N., Oh, J. S., Horner, K., Xie, F., Sette, C., Blelloch, R. and Conti, M. (2011). Genome-wide analysis of translation reveals a critical role for deleted in azoospermia-like (Dazl) at the oocyte-to-zygote transition. *Genes & development* **25**, 755–66.

Chiang, T., Duncan, F. and Schindler, K. (2010a). Evidence that weakened centromere cohesion is a leading cause of age-related aneuploidy in oocytes. *Current Biology* **20**, 1522–1528.

Chiang, T., Duncan, F. E., Schindler, K., Schultz, R. M. and Lampson, M. a (2010b). Evidence that weakened centromere cohesion is a leading cause of age-related aneuploidy in oocytes. *Current biology : CB* **20**, 1522–8.

Chiang, T., Schultz, R. M. and Lampson, M. a (2011). Age-dependent susceptibility of chromosome cohesion to premature separase activation in mouse oocytes. *Biology of reproduction* **85**, 1279–83.

Choi, T., Aoki, F., Mori, M. and Yamashita, M. (1991). Activation of p34cdc2 protein kinase activity in meiotic and mitotic cell cycles in mouse oocytes and embryos. *Development* **795**, 789–795.

Ciosk, R., Zachariae, W., Michaelis, C., Shevchenko, a, Mann, M. and Nasmyth, K. (1998). An ESP1/PDS1 complex regulates loss of sister chromatid cohesion at the metaphase to anaphase transition in yeast. *Cell* **93**, 1067–76.

Clift, D. and Marston, A. L. (2011). The role of shugoshin in meiotic chromosome segregation. *Cytogenetic and genome research* **133**, 234–42.

Colombié, N., Cullen, C. F., Brittle, A. L., Jang, J. K., Earnshaw, W. C., Carmena, M., McKim, K. and Ohkura, H. (2008). Dual roles of Incenp crucial to the assembly of the acentrosomal metaphase spindle in female meiosis. *Development (Cambridge, England)* **135**, 3239–46.

Downs, S. M. (1990). Protein synthesis inhibitors prevent both spontaneous and hormone-dependent maturation of isolated mouse oocytes. *Molecular reproduction and development* **27**, 235–43.

Dumont, J. and Desai, A. (2012). Acentrosomal spindle assembly and chromosome segregation during oocyte meiosis. *Trends in cell biology* **22**, 241–9.

Dumont, J., Oegema, K. and Desai, A. (2010). A kinetochore-independent mechanism drives anaphase chromosome separation during acentrosomal meiosis. *Nature Cell Biology* **12**, 894–901.

Duncan, F. E., Chiang, T., Schultz, R. M. and Lampson, M. a (2009). Evidence that a defective spindle assembly checkpoint is not the primary cause of maternal age-associated aneuploidy in mouse eggs. *Biology of reproduction* **81**, 768–76.

Ellefson, M. L. and McNally, F. J. (2011). CDK-1 inhibits meiotic spindle shortening and dynein-dependent spindle rotation in C. elegans. *The Journal of cell biology* **193**, 1229–44.

Fabritius, A. S., Ellefson, M. L. and McNally, F. J. (2011). Nuclear and spindle positioning during oocyte meiosis. *Current opinion in cell biology* **23**, 78–84.

Fernández-Miranda, G., Trakala, M., Martín, J., Escobar, B., González, A., Ghyselinck, N. B., Ortega, S., Cañamero, M., Pérez De Castro, I. and Malumbres, M. (2011). Genetic disruption of aurora B uncovers an essential role for aurora C during early mammalian development. *Development* **138**, 2661–2672.

Gadea, B. B. and Ruderman, J. V (2005). Aurora kinase inhibitor ZM447439 blocks chromosome-induced spindle assembly, the completion of chromosome condensation, and the establishment of the spindle integrity checkpoint in Xenopus egg extracts. *Molecular biology of the cell* **16**, 1305–18.

Ganem, N. J., Godinho, S. a and Pellman, D. (2009). A mechanism linking extra centrosomes to chromosomal instability. *Nature* **460**, 278–82.

Gassmann, R., Carvalho, A., Henzing, A. J., Ruchaud, S., Hudson, D. F., Honda, R., Nigg, E. A., Gerloff, D. L. and Earnshaw, W. C. (2004). Borealin: a novel chromosomal passenger required for stability of the bipolar mitotic spindle. *The Journal of cell biology* **166**, 179–91.

Gautschi, O., Heighway, J., Mack, P. C., Purnell, P. R., Lara, P. N. and Gandara, D. R. (2008). Aurora kinases as anticancer drug targets. *Clinical cancer research : an official journal of the American Association for Cancer Research* **14**, 1639–48.

Gavet, O. and Pines, J. (2010). Progressive activation of CyclinB1-Cdk1 coordinates entry to mitosis. *Developmental Cell* **18**, 533–543.

Gavin, A. (1994). Histone H1 kinase activity, germinal vesicle breakdown and M phase entry in mouse oocytes. *Journal of cell science* **283**, 275–283.

Giet, R. and Glover, D. M. (2001). Drosophila aurora B kinase is required for histone H3 phosphorylation and condensin recruitment during chromosome condensation and to organize the central spindle during cytokinesis. *The Journal of cell biology* **152**, 669–82.

Gillies, S. C., Lane, F. M., Paik, W., Pyrtel, K., Wallace, N. T. and Gilliland, W. D. (2013). Nondisjunctional segregations in Drosophila female meiosis I are preceded by homolog malorientation at metaphase arrest. *Genetics* **193**, 443–51.

Gilliland, W. D., Hughes, S. E., Cotitta, J. L., Takeo, S., Xiang, Y. and Hawley, R. S. (2007). The multiple roles of mps1 in Drosophila female meiosis. *PLoS genetics* **3**, e113.

Golbus, M. S. and Stein, M. P. (1976). Qualitative patterns of protein synthesis in the mouse oocyte. *The Journal of experimental zoology* **198**, 337–42.

Gopalan, G., Chan, C. S. and Donovan, P. J. (1997). A novel mammalian, mitotic spindle-associated kinase is related to yeast and fly chromosome segregation regulators. *The Journal of cell biology* **138**, 643–56.

Gui, L. and Homer, H. (2012). Spindle assembly checkpoint signalling is uncoupled from chromosomal position in mouse oocytes. *Development* **139**, 1941–6.

Hached, K., Xie, S., Buffin, E. and Cladière, D. (2011). Mps1 at kinetochores is essential for female mouse meiosis I. *Development* **138**, 2261–2271.

Hampl, A. and Eppig, J. (1995). Translational regulation of the gradual increase in histone H1 kinase activity in maturing mouse oocytes. *Molecular reproduction and development* **40**, 9–15.

Hassold, T. and Hunt, P. (2009). Maternal age and chromosomally abnormal pregnancies: what we know and what we wish we knew. *Current opinion in pediatrics* **21**, 703–8.

Hauf, S., Cole, R. W., LaTerra, S., Zimmer, C., Schnapp, G., Walter, R., Heckel, A., Van Meel, J., Rieder, C. L. and Peters, J.-M. (2003). The small molecule Hesperadin reveals a role for Aurora B in correcting kinetochore-microtubule attachment and in maintaining the spindle assembly checkpoint. *The Journal of cell biology* **161**, 281–94.

Hoar, K., Chakravarty, A., Rabino, C., Wysong, D., Bowman, D., Roy, N. and Ecsedy, J. A. (2007). MLN8054, a small-molecule inhibitor of Aurora A, causes spindle pole and chromosome congression defects leading to aneuploidy. *Molecular and cellular biology* **27**, 4513–25.

Holt, J. E., Lane, S. I. R., Jennings, P., García-Higuera, I., Moreno, S. and Jones, K. T. (2012). APC(FZR1) prevents nondisjunction in mouse oocytes by controlling meiotic spindle assembly timing. *Molecular biology of the cell* **23**, 3970–81.

Homer, H. a, McDougall, A., Levasseur, M., Murdoch, A. P. and Herbert, M. (2005). Mad2 is required for inhibiting securin and cyclin B degradation following spindle depolymerisation in meiosis I mouse oocytes. *Reproduction* **130**, 829–843.

Hu, H. M., Chuang, C. K., Lee, M. J., Tseng, T. C. and Tang, T. K. (2000). Genomic organization, expression, and chromosome localization of a third aurora-related kinase gene, Aie1. *DNA and cell biology* **19**, 679–88.

Huang, X. and Hatcher, R. (2005). Securin and separase phosphorylation act redundantly to maintain sister chromatid cohesion in mammalian cells. *Molecular biology of the cell* **16**, 4725–4732.

Igarashi, H., Knott, J. G., Schultz, R. M. and Williams, C. J. (2007). Alterations of PLCbeta1 in mouse eggs change calcium oscillatory behavior following fertilization. *Developmental biology* **312**, 321–30.

Jaspersen, S. L. and Winey, M. (2004). The budding yeast spindle pole body: structure, duplication, and function. *Annual review of cell and developmental biology* **20**, 1–28.

Kaitna, S., Pasierbek, P., Jantsch, M., Loidl, J. and Glotzer, M. (2002). The aurora B kinase AIR-2 regulates kinetochores during mitosis and is required for separation of homologous Chromosomes during meiosis. *Current biology : CB* **12**, 798–812.

Kapoor, T. M., Lampson, M. a, Hergert, P., Cameron, L., Cimini, D., Salmon, E. D., McEwen, B. F. and Khodjakov, A. (2006). Chromosomes can congress to the metaphase plate before biorientation. *Science* **311**, 388–391.

Kimmins, S., Crosio, C., Kotaja, N., Hirayama, J., Monaco, L., Höög, C., Van Duin, M., Gossen, J. a and Sassone-Corsi, P. (2007). Differential functions of the Aurora-B and Aurora-C kinases in mammalian spermatogenesis. *Molecular endocrinology* **21**, 726–39.

Kishimoto, T. (2011). A primer on meiotic resumption in starfish oocytes: the proposed signaling pathway triggered by maturation-inducing hormone. *Molecular reproduction and development* **78**, 704–7.

Kitajima, T. S., Kawashima, S. A. and Watanabe, Y. (2004). The conserved kinetochore protein shugoshin protects centromeric cohesion during meiosis. *Nature* **427**, 510–7.

Kitajima, T. S., Hauf, S., Ohsugi, M., Yamamoto, T. and Watanabe, Y. (2005). Human Bub1 defines the persistent cohesion site along the mitotic chromosome by affecting Shugoshin localization. *Current biology : CB* **15**, 353–9.

Kitajima, T. S., Ohsugi, M. and Ellenberg, J. (2011). Complete kinetochore tracking reveals error-prone homologous chromosome biorientation in Mammalian oocytes. *Cell* **146**, 568–581.

Koffa, M. D., Casanova, C. M., Santarella, R., Köcher, T., Wilm, M. and Mattaj, I. W. (2006). HURP is part of a Ran-dependent complex involved in spindle formation. *Current biology : CB* **16**, 743–54.

Kolano, Brunet, Silk, Cleveland and Verlhac (2012). Error-prone mammalian female meiosis from silencing the spindle assembly checkpoint without normal interkinetochore tension. *Proceedings of the National Academy of Sciences* **109**, E1858–E1867.

Kops, G. J. P. L., Kim, Y., Weaver, B. a a, Mao, Y., McLeod, I., Yates, J. R., Tagaya, M. and Cleveland, D. W. (2005). ZW10 links mitotic checkpoint signaling to the structural kinetochore. *The Journal of cell biology* **169**, 49–60.

Kotani, T., Yoshida, N., Mita, K. and Yamashita, M. (2001). Requirement of cyclin B2, but not cyclin B1, for bipolar spindle formation in frog (Rana japonica) oocytes. *Molecular reproduction and development* **59**, 199–208.

Kruse, T., Zhang, G., Larsen, M. S. Y., Lischetti, T., Streicher, W., Kragh Nielsen, T., Bjørn, S. P. and Nilsson, J. (2013). Direct binding between BubR1 and B56-PP2A phosphatase complexes regulate mitotic progression. *Journal of cell science* **126**, 1086–92.

Lampson, M. a and Cheeseman, I. M. (2011). Sensing centromere tension: Aurora B and the regulation of kinetochore function. *Trends in cell biology* **21**, 133–40.

Lane, S. I. R., Chang, H.-Y., Jennings, P. C. and Jones, K. T. (2010). The Aurora kinase inhibitor ZM447439 accelerates first meiosis in mouse oocytes by overriding the spindle assembly checkpoint. *Reproduction (Cambridge, England)* **140**, 521–30.

Lane, S., Yun, Y. and Jones, K. (2012). Timing of anaphase-promoting complex activation in mouse oocytes is predicted by microtubule-kinetochore attachment but not by bivalent alignment or tension. *Development* **139**, 1947–1955.

Ledan, E., Polanski, Z., Terret, M. E. and Maro, B. (2001). Meiotic maturation of the mouse oocyte requires an equilibrium between cyclin B synthesis and degradation. *Developmental biology* **232**, 400–13.

Li, M., Li, S., Yuan, J., Wang, Z.-B., Sun, S.-C., Schatten, H. and Sun, Q.-Y. (2009). Bub3 is a spindle assembly checkpoint protein regulating chromosome segregation during mouse oocyte meiosis. *PloS one* **4**, e7701.

Lim, H. H., Zhang, T. and Surana, U. (2009). Regulation of centrosome separation in yeast and vertebrates: common threads. *Trends in cell biology* **19**, 325–33.

Ma, P. and Schultz, R. M. (2008). Histone deacetylase 1 (HDAC1) regulates histone acetylation, development, and gene expression in preimplantation mouse embryos. *Developmental biology* **319**, 110–20.

Ma, N., Titus, J., Gable, A., Ross, J. L. and Wadsworth, P. (2011). TPX2 regulates the localization and activity of Eg5 in the mammalian mitotic spindle. *The Journal of cell biology* **195**, 87–98.

Maciejowski, J., George, K. a, Terret, M.-E., Zhang, C., Shokat, K. M. and Jallepalli, P. V (2010). Mps1 directs the assembly of Cdc20 inhibitory complexes during interphase and mitosis to control M phase timing and spindle checkpoint signaling. *The Journal of Cell Biology* **190**, 89–100.

Magidson, V., O'Connell, C. B., Lončarek, J., Paul, R., Mogilner, A. and Khodjakov, A. (2011). The spatial arrangement of chromosomes during prometaphase facilitates spindle assembly. *Cell* **146**, 555–67.

Maia, A. R. R., Garcia, Z., Kabeche, L., Barisic, M., Maffini, S., Macedo-Ribeiro, S., Cheeseman, I. M., Compton, D. a, Kaverina, I. and Maiato, H. (2012). Cdk1 and Plk1 mediate a CLASP2 phospho-switch that stabilizes kinetochore–microtubule attachments. *The Journal of Cell Biology* **199**, 285–301.

Malmanche, N., Owen, S., Gegick, S., Steffensen, S., Tomkiel, J. E. and Sunkel, C. E. (2007). Drosophila BubR1 is essential for meiotic sister-chromatid cohesion and maintenance of synaptonemal complex. *Current biology : CB* **17**, 1489–97.

Marumoto, T., Honda, S., Hara, T., Nitta, M., Hirota, T., Kohmura, E. and Saya, H. (2003). Aurora-A kinase maintains the fidelity of early and late mitotic events in HeLa cells. *The Journal of biological chemistry* **278**, 51786–95.

Maton, G., Thibier, C., Castro, A., Lorca, T., Prigent, C. and Jessus, C. (2003). Cdc2-cyclin B triggers H3 kinase activation of Aurora-A in Xenopus oocytes. *The Journal of biological chemistry* **278**, 21439–49.

McGuinness, B. E., Anger, M., Kouznetsova, A., Gil-Bernabé, A. M., Helmhart, W., Kudo, N. R., Wuensche, A., Taylor, S., Hoog, C., Novak, B., et al. (2009). Regulation of APC/C activity in oocytes by a Bub1-dependent spindle assembly checkpoint. *Current biology : CB* **19**, 369–80.

Melters, D. P., Paliulis, L. V, Korf, I. F. and Chan, S. W. L. (2012). Holocentric chromosomes: convergent evolution, meiotic adaptations, and genomic analysis. *Chromosome research : an international journal on the molecular, supramolecular and evolutionary aspects of chromosome biology* **20**, 579–93.

Meraldi, P. and Nigg, E. a (2002). The centrosome cycle. *FEBS letters* **521**, 9–13.

Meyer, R. E., Kim, S., Obeso, D., Straight, P. D., Winey, M. and Dawson, D. S. (2013). Mps1 and Ipl1/Aurora B Act Sequentially to Correctly Orient Chromosomes on the Meiotic Spindle of Budding Yeast. *Science (New York, N.Y.)* **339**, 1071–4.

Mori, D., Yano, Y., Toyo-oka, K., Yoshida, N., Yamada, M., Muramatsu, M., Zhang, D., Saya, H., Toyoshima, Y. Y., Kinoshita, K., et al. (2007). NDEL1 phosphorylation by Aurora-A kinase is essential for centrosomal maturation, separation, and TACC3 recruitment. *Molecular and cellular biology* **27**, 352–67.

Morin, V., Prieto, S., Melines, S., Hem, S., Rossignol, M., Lorca, T., Espeut, J., Morin, N. and Abrieu, A. (2012). CDK-Dependent Potentiation of MPS1 Kinase Activity Is Essential to the Mitotic Checkpoint. *Current Biology* **22**, 289–95.

Murai, S., Stein, P., Buffone, M. G., Yamashita, S. and Schultz, R. M. (2010). Recruitment of Orc6l, a dormant maternal mRNA in mouse oocytes, is essential for DNA replication in 1-cell embryos. *Developmental biology* **341**, 205–12.

Musacchio, A. and Salmon, E. D. (2007). The spindle-assembly checkpoint in space and time. *Nature reviews. Molecular cell biology* **8**, 379–93.

Nguyen, H. G., Chinnappan, D., Urano, T. and Ravid, K. (2005). Mechanism of Aurora-B degradation and its dependency on intact KEN and A-boxes: identification of an aneuploidy-promoting property. *Molecular and cellular biology* **25**, 4977–92.

Niault, T., Hached, K., Sotillo, R., Sorger, P. K., Maro, B., Benezra, R. and Wassmann, K. (2007). Changing Mad2 levels affects chromosome segregation and spindle assembly checkpoint control in female mouse meiosis I. *PloS one* **2**, e1165.

Nicklas, R. B. (1997). How cells get the right chromosomes. *Science* **275**, 632–7.

Oegema, K. and Hyman, A. A. (2006). Cell division. *WormBook : the online review of C. elegans biology* 1–40.

Oh, J. S., Susor, A. and Conti, M. (2011). Protein tyrosine kinase Wee1B is essential for metaphase II exit in mouse oocytes. *Science (New York, N.Y.)* **332**, 462–5.

Ohi, R., Sapra, T., Howard, J. and Mitchison, T. J. (2004). Differentiation of cytoplasmic and meiotic spindle assembly MCAK functions by Aurora B-dependent phosphorylation. *Molecular biology of the cell* **15**, 2895–906.

Okano-Uchida, T., Okumura, E., Iwashita, M., Yoshida, H., Tachibana, K. and Kishimoto, T. (2003). Distinct regulators for Plk1 activation in starfish meiotic and early embryonic cycles. *The EMBO journal* **22**, 5633–42.

Oliveira, R. a and Nasmyth, K. (2010). Getting through anaphase: splitting the sisters and beyond. *Biochemical Society transactions* **38**, 1639–44.

Pan, H., Ma, P., Zhu, W. and Schultz, R. M. (2008). Age-associated increase in aneuploidy and changes in gene expression in mouse eggs. *Developmental biology* **316**, 397–407.

Pearson, N. J., Cullen, C. F., Dzhindzhev, N. S. and Ohkura, H. (2005). A pre-anaphase role for a Cks/Suc1 in acentrosomal spindle formation of Drosophila female meiosis. *EMBO reports* **6**, 1058–63.

Petronczki, M., Lénárt, P. and Peters, J.-M. (2008). Polo on the Rise-from Mitotic Entry to Cytokinesis with Plk1. *Developmental cell* **14**, 646–59.

Polanski, Z., Ledan, E. and Brunet, S. (1998). Cyclin synthesis controls the progression of meiotic maturation in mouse oocytes. *Development* **125**, 4989–4997.

Price, D. M., Kanyo, R., Steinberg, N., Chik, C. L. and Ho, A. K. (2009). Nocturnal activation of aurora C in rat pineal gland: its role in the norepinephrine-induced phosphorylation of histone H3 and gene expression. *Endocrinology* **150**, 2334–41.

Remeseiro, S. and Losada, A. (2013). Cohesin, a chromatin engagement ring. *Current opinion in cell biology* **25**, 63–71.

Resnick, T. D., Satinover, D. L., MacIsaac, F., Stukenberg, P. T., Earnshaw, W. C., Orr-Weaver, T. L. and Carmena, M. (2006). INCENP and Aurora B promote meiotic sister chromatid cohesion through localization of the Shugoshin MEI-S332 in Drosophila. *Developmental cell* **11**, 57–68.

Richter, J. D. (2007). CPEB: a life in translation. *Trends in biochemical sciences* **32**, 279–85.

Riedel, C. G., Katis, V. L., Katou, Y., Mori, S., Itoh, T., Helmhart, W., Gálová, M., Petronczki, M., Gregan, J., Cetin, B., et al. (2006). Protein phosphatase 2A protects centromeric sister chromatid cohesion during meiosis I. *Nature* **441**, 53–61.

Rieder, C. L. (1981). The structure of the cold-stable kinetochore fiber in metaphase PtK1 cells. *Chromosoma* **84**, 145–58.

Rogers, E., Bishop, J. D., Waddle, J. A., Schumacher, J. M. and Lin, R. (2002). The aurora kinase AIR-2 functions in the release of chromosome cohesion in Caenorhabditis elegans meiosis. *The Journal of cell biology* **157**, 219–29.

Ruchaud, S., Carmena, M. and Earnshaw, W. C. (2007). Chromosomal passengers: conducting cell division. *Nature reviews. Molecular cell biology* **8**, 798–812.

Sampath, S. C., Ohi, R., Leismann, O., Salic, A., Pozniakovski, A. and Funabiki, H. (2004). The chromosomal passenger complex is required for chromatin-induced microtubule stabilization and spindle assembly. *Cell* **118**, 187–202.

Sasai, K., Katayama, H., Stenoien, D. L., Fujii, S., Honda, R., Kimura, M., Okano, Y., Tatsuka, M., Suzuki, F., Nigg, E. A., et al. (2004). Aurora-C kinase is a novel chromosomal passenger protein that can complement Aurora-B kinase function in mitotic cells. *Cell motility and the cytoskeleton* **59**, 249–63.

Satyanarayana, A. and Kaldis, P. (2009). Mammalian cell-cycle regulation: several Cdks, numerous cyclins and diverse compensatory mechanisms. *Oncogene* **28**, 2925–39.

Schindler, K. and Schultz, R. M. (2009). CDC14B acts through FZR1 (CDH1) to prevent meiotic maturation of mouse oocytes. *Biology of Reproduction* **80**, 795–803.

Schindler, K., Davydenko, O., Fram, B., Lampson, M. A. and Schultz, R. M. (2012). Maternally recruited Aurora C kinase is more stable than Aurora B to support mouse oocyte maturation and early development. *Proceedings of the National Academy of Sciences of the United States of America* **109**, E2215–22.

Schuh, M. and Ellenberg, J. (2007). Self-organization of MTOCs replaces centrosome function during acentrosomal spindle assembly in live mouse oocytes. *Cell* **130**, 484–98.

Schvarzstein, M., Wignall, S. M. and Villeneuve, A. M. (2010). Coordinating cohesion, co-orientation, and congression during meiosis: lessons from holocentric chromosomes. *Genes & development* **24**, 219–28.

Severson, A. F., Hamill, D. R., Carter, J. C., Schumacher, J. and Bowerman, B. (2000). The aurora-related kinase AIR-2 recruits ZEN-4/CeMKLP1 to the mitotic spindle at metaphase and is required for cytokinesis. *Current biology : CB* **10**, 1162–71.

Shao, H., Ma, C., Zhang, X., Li, R., Miller, A. L., Bement, W. M. and Liu, X. J. (2012). Aurora B regulates spindle bipolarity in meiosis in vertebrate oocytes. *Cell cycle (Georgetown, Tex.)* **11**, 2672–80.

Sharif, B., Na, J., Lykke-Hartmann, K., McLaughlin, S. H., Laue, E., Glover, D. M. and Zernicka-Goetz, M. (2010). The chromosome passenger complex is required

for fidelity of chromosome transmission and cytokinesis in meiosis of mouse oocytes. *Journal of cell science* **123**, 4292–300.

Shuda, K., Schindler, K., Ma, J., Schultz, R. M. and Donovan, P. J. (2009). Aurora kinase B modulates chromosome alignment in mouse oocytes. *Molecular Reproduction and Development* **76**, 1094–1105.

Silkworth, W. T., Nardi, I. K., Scholl, L. M. and Cimini, D. (2009). Multipolar spindle pole coalescence is a major source of kinetochore mis-attachment and chromosome mis-segregation in cancer cells. *PloS one* **4**, e6564.

Silljé, H. H. W., Nagel, S., Körner, R. and Nigg, E. a (2006). HURP is a Ran-importin beta-regulated protein that stabilizes kinetochore microtubules in the vicinity of chromosomes. *Current biology : CB* **16**, 731–42.

Slattery, S. D., Mancini, M. A., Brinkley, B. R. and Hall, R. M. (2009). Aurora-C kinase supports mitotic progression in the absence of Aurora-B. *Cell cycle (Georgetown, Tex.)* **8**, 2984–94.

Stein, P. and Schindler, K. (2011). Mouse oocyte microinjection, maturation and ploidy assessment. *Journal of visualized experiments : JoVE*.

Stemmann, O., Zou, H., Gerber, S. a, Gygi, S. P. and Kirschner, M. W. (2001). Dual inhibition of sister chromatid separation at metaphase. *Cell* **107**, 715–26.

Stewart, S. and Fang, G. (2005). Destruction box-dependent degradation of aurora B is mediated by the anaphase-promoting complex/cyclosome and Cdh1. *Cancer research* **65**, 8730–5.

Swain, J. E., Ding, J., Wu, J. and Smith, G. D. (2008). Regulation of spindle and chromatin dynamics during early and late stages of oocyte maturation by aurora kinases. *Molecular Human Reproduction* **14**, 291–299.

Tang, Z., Sun, Y., Harley, S. E., Zou, H. and Yu, H. (2004). Human Bub1 protects centromeric sister-chromatid cohesion through Shugoshin during mitosis. *Proceedings of the National Academy of Sciences of the United States of America* **101**, 18012–7.

Terada, Y., Uetake, Y. and Kuriyama, R. (2003). Interaction of Aurora-A and centrosomin at the microtubule-nucleating site in Drosophila and mammalian cells. *The Journal of cell biology* **162**, 757–63.

Thompson, S. L. and Compton, D. a (2008). Examining the link between chromosomal instability and aneuploidy in human cells. *The Journal of cell biology* **180**, 665–72.

Tsafriri, A., Chun, S. Y., Zhang, R., Hsueh, A. J. and Conti, M. (1996). Oocyte maturation involves compartmentalization and opposing changes of cAMP levels in follicular somatic and germ cells: studies using selective phosphodiesterase inhibitors. *Developmental biology* **178**, 393–402.

Tseng, T. C., Chen, S. H., Hsu, Y. P. and Tang, T. K. (1998). Protein kinase profile of sperm and eggs: cloning and characterization of two novel testis-specific protein kinases (AIE1, AIE2) related to yeast and fly chromosome segregation regulators. *DNA and cell biology* **17**, 823–33.

Tsukahara, T., Tanno, Y. and Watanabe, Y. (2010). Phosphorylation of the CPC by Cdk1 promotes chromosome bi-orientation. *Nature* **467**, 719–23.

Voet, M. Van Der, Lorson, M. A., Srinivasan, D. G., Bennett, K. L. and Heuvel, S. Van Den (2009). C . elegans mitotic cyclins have distinct as well as overlapping functions in chromosome segregation. 4091–4102.

Vogt, E., Kirsch-Volders, M., Parry, J. and Eichenlaub-Ritter, U. (2008). Spindle formation, chromosome segregation and the spindle checkpoint in mammalian oocytes and susceptibility to meiotic error. *Mutation Research* **651**, 14–29.

Vogt, E., Kipp, A. and Eichenlaub-Ritter, U. (2009). Aurora kinase B, epigenetic state of centromeric heterochromatin and chiasma resolution in oocytes. *Reproductive biomedicine online* **19**,.

Wadsworth, P. and Khodjakov, A. (2004). E pluribus unum: towards a universal mechanism for spindle assembly. *Trends in cell biology* **14**, 413–9.

Walczak, C. E., Vernos, I., Mitchison, T. J., Karsenti, E. and Heald, R. (1998). A model for the proposed roles of different microtubule-based motor proteins in establishing spindle bipolarity. *Current biology : CB* **8**, 903–13.

Wassmann, K., Niault, T. and Maro, B. (2003). Metaphase I arrest upon activation of the Mad2-dependent spindle checkpoint in mouse oocytes. *Current Biology* **13**, 1596–1608.

Waters, J. C., Chen, R. H., Murray, a W. and Salmon, E. D. (1998). Localization of Mad2 to kinetochores depends on microtubule attachment, not tension. *The Journal of cell biology* **141**, 1181–91.

Wei, L., Liang, X.-W., Zhang, Q.-H., Li, M., Yuan, J., Li, S., Sun, S.-C., Ouyang, Y.-C., Schatten, H. and Sun, Q.-Y. (2010). BubR1 is a spindle assembly checkpoint protein regulating meiotic cell cycle progression of mouse oocyte. *Cell cycle* **9**, 1112–1121.

Winston, N. J., Biologie, D. De, Paris, U. and Paris, F.- (1997). Stability of cyclin B protein during meiotic maturation and the first mitotic cell division in mouse oocytes. *Biology of the cell* 211–219.

Wong, J. and Fang, G. (2006). HURP controls spindle dynamics to promote proper interkinetochore tension and efficient kinetochore capture. *The Journal of cell biology* **173**, 879–91.

Wong, O. K. and Fang, G. (2007). Cdk1 phosphorylation of BubR1 controls spindle checkpoint arrest and Plk1-mediated formation of the 3F3/2 epitope. *The Journal of cell biology* **179**, 611–7.

Xu, Z., Williams, C. J., Kopf, G. S. and Schultz, R. M. (2003). Maturation-associated increase in IP3 receptor type 1: role in conferring increased IP3 sensitivity and Ca2+ oscillatory behavior in mouse eggs. *Developmental biology* **254**, 163–71.

Yabe, T., Ge, X., Lindeman, R., Nair, S., Runke, G., Mullins, M. C. and Pelegri, F. (2009). The maternal-effect gene cellular island encodes aurora B kinase and is essential for furrow formation in the early zebrafish embryo. *PLoS genetics* **5**, e1000518.

Yan, X., Wu, Y., Li, Q., Cao, L., Liu, X., Saiyin, H. and Yu, L. (2005a). Cloning and characterization of a novel human Aurora C splicing variant. *Biochemical and biophysical research communications* **328**, 353–61.

Yan, X., Cao, L., Li, Q., Wu, Y., Zhang, H., Saiyin, H., Liu, X., Zhang, X., Shi, Q. and Yu, L. (2005b). Aurora C is directly associated with Survivin and required for cytokinesis. *Genes to cells devoted to molecular cellular mechanisms* **10**, 617–626.

Yanai, A., Arama, E., Kilfin, G. and Motro, B. (1997). ayk1, a novel mammalian gene related to Drosophila aurora centrosome separation kinase, is specifically expressed during meiosis. *Oncogene* **14**, 2943–50.

Yang, X., Li, H., Liu, X. S., Deng, A. and Liu, X. (2009). Cdc2-mediated phosphorylation of CLIP-170 is essential for its inhibition of centrosome reduplication. *The Journal of biological chemistry* **284**, 28775–82.

Yang, K., Li, S., Chang, C., Tang, C. C., Lin, Y., Lee, S. and Tang, T. K. (2010). Aurora-C Kinase Deficiency Causes Cytokinesis Failure in Meiosis I and Production of Large Polyploid Oocytes in Mice. *Molecular biology of the cell* **21**, 2371–2383.

Yu, H.-G. and Koshland, D. (2007). The Aurora kinase Ipl1 maintains the centromeric localization of PP2A to protect cohesin during meiosis. *The Journal of cell biology* **176**, 911–8.